EFFECTS OF LIFESTYLE AND PHYLOGENY ON THE VERTEBRATE VISUAL SYSTEM

Jasper E. Hunt

Nuffield Department of Clinical Neurosciences
and
Lincoln College

University of Oxford



A thesis presented for the degree of
Doctor of Philosophy

Word Count: 28,484

August, 2025

ACKNOWLEDGEMENTS

It is my pleasure to record here a debt of gratitude to the many persons who have assisted me through the development and completion of this project.

I have especial reason to be thankful to my faculty supervisors, Professors Rogier B. Mars and Zoltán Molnár. I am grateful to Rogier for his encouragement and advice on matters both scientific and professional – a generosity which has at times felt in excess of my deserts. I am grateful to Zoltán for supporting my interest in questions of evolution and development for years, to say nothing of his infectious optimism. In kindness and capability, I could not have asked for a better supervisory team.

To all of my research colleagues, both current and former, I would like to extend my warmest thanks. Attending conferences together and exchanging cat pictures over Zoom, the fond memories are too many to count. It is thanks to you that I have been able to conduct experiments to the best of my abilities and explore the beauty of our natural world through scientific investigation.

To my family, I cannot say enough. Thank you for offering your open arms every time I needed an embrace. I especially wish to commemorate my uncle, Dr. James R. “Rick” Jones III, who passed away in the summer of 2023. Although I wish he could have witnessed the completion of my DPhil, I shall nonetheless always remember him as my kind and loving uncle with an unrivalled enthusiasm for academic scholarship, including in his own field of archaeology.

Finally, I would like to thank Professor Kara G. Pratt and the late Professor Susanna L. Goodin of the University of Wyoming for their unwavering friendship and support. It is in Kara’s laboratory that I first became a neuroscientist and discovered a boundless curiosity about the biological world. It was under the wing of Susanna’s wisdom that I found the fortitude to continue, even when things were not easy. To all of these people, it is my joy to acknowledge a gratitude most tremendous in scale.

ABSTRACT

The visual system enables a wide variety of animals across the vertebrate lineage to interact with their environments, presenting a prime opportunity to examine how ecological pressures have shaped animals' behaviours and developmental strategies. This thesis seeks to advance scientific understanding of the evolution and diversity of vertebrate visual systems. The present work is comprised of two parts in service of this aim.

Part one revisits prior reports on spontaneous retinal waves, a kind of spontaneous activity in the developing retina. Considering the ecological contexts in which different animals develop and the taxonomic relationships between the species in which retinal waves have been studied, particularly zebrafish and *Xenopus* frogs, a novel account of the evolution of retinal waves is advanced.

Part two develops a data-driven approach for identifying and analysing white matter fibre bundles in understudied brains. The technique, based on a non-negative matrix factorisation (NMF) dimensionality reduction algorithm, is appropriate for cross-species comparisons, even at low sample sizes. This approach is used to reconstruct the anterior ventral stream connections across four species of primates: the rhesus macaque, the black-capped squirrel monkey, the ring-tailed lemur, and the Senegal bushbaby. The prefrontal cortical innervation of the strepsirrhine ventral stream is determined to be more restricted to the orbitofrontal cortex than in anthropoids. This finding is used to draw inferences about ventral stream evolution across primates. An additional analysis characterises the extent of cross-species variability compared to that from individual differences and methodological considerations, providing an important validation of previous cross-species comparisons in white matter connectivity.

In sum, this thesis advances our knowledge about the evolution of visual systems across the vertebrate lineage. The tools and approaches advanced here will support future comparative neuroscience research, particularly the characterisation of white matter connectivity in previously understudied species.

TABLE OF CONTENTS

Acknowledgements i
Abstract ii
Table of Contents iii
List of Tables vi
List of figures vii
List of abbreviations viii

1. Introduction: Vertebrate vision and the evolution of sensory systems 1
Declarations 3
1. Why study vision? 5
1.1. A long-standing human fascination 5
1.2. A natural history of vision 7
2. Why compare species? 10
2.1. History of the comparative approach 10
2.2. The benefits of comparative neuroscience 13
2.3. Challenges for comparative neuroscience 22
3. Primate visual evolution 24
4. Thesis outline 30
References 31

2. Neuroethology and retinal waves 49
Declarations 51
Abstract 53
1. Introduction: Behaviour, evolution, and development 55
2. Retinal waves: A neuroethological perspective 51
2.1. How widespread are retinal waves? 58
2.2. The ethological role of retinal waves 61
2.3. Retinal waves in the broader context of development 63
2.4. Revisiting retinal waves in frogs 69
2.5. The origin of retinal waves 72
3. Concluding remarks 74
3.1. The roads paved by behaviour 75
3.2. The future of behaviour 76
References 78

3. Development of a data-driven approach to investigate white matter connectivity in lesser-studied brains 89
Declarations 91
Abstract 93
1. Introduction: How do we compare unusual brains? 95
2. Methods 97
2.1. Data sources 97
2.2. Data acquisition and preprocessing 99
2.3. Data-driven tractography 100

2.4. Atlas-based tractography and statistical comparison 102
3. Results 103
3.1. NMF output recapitulates known white matter tracts in human and macaque, at small sample sizes 104
3.2. NMF output effectively reconstructs different tracts at different component numbers 109
4. Discussion 110
References 115

4. An anthropoid/strepsirrhine divergence in ventral visual stream connectivity 123
Declarations 125
Abstract 127
1. Introduction: The visual primate brain 129
2. Methods 133
2.1. Data sources 133
2.2. Data acquisition and preprocessing 133
2.3. Data-driven tractography 134
2.4. Tractography comparison 136
2.5. Component selection 137
2.6. Statistical analysis of innervation patterns 140
3. Results 141
3.1. NMF performs similarly with one brain and three brains 142
3.2. Anterior temporal-frontal and occipitotemporal-frontal connections can be reliably reconstructed across primate species 145
3.3. Prefrontal innervation of the anterior temporal-frontal connections is more restricted to the orbitofrontal cortex in the lemur 148
3.4. Cross-species differences explain far more variance in anterior temporal-frontal connectivity than within-species differences or algorithmic parameters 150
3.5. The lemur's occipitotemporal-frontal connections' prefrontal innervation is more restricted to orbitofrontal cortex 151
4. Discussion 153
References 157

5. Data-driven analysis of prefrontal-innervating ventral stream connections in *Galago senegalensis* 167
Declarations 169
Abstract 171
1. Introduction: The strepsirrhine lineage 173
2. Methods 175
2.1. Data sources 175
2.2. Data acquisition and preprocessing 175
2.3. Data-driven tractography 176
2.4. Component selection 177
2.5. Statistical analysis of orbitofrontal innervation 179
3. Results 180

3.1. NMF identifies occipitotemporal-frontal connections in the galago, but does not distinguish between ventral stream connections at low component numbers 181
3.2. At higher component numbers, NMF reliably reconstructs and differentiates ventral stream connections in the galago 183
3.3. The galago's ventral visual stream's prefrontal innervation patterns are most similar to those in lemur 185
4. Discussion 187
References 191

6. General discussion 199
Declarations 201
1. Summary of findings 203
1.1. Neuroethology and retinal waves 203
1.2. Developing a data-driven approach to study white matter connections across species 204
1.3. An anthropoid/strepsirrhine divergence in ventral visual stream connectivity 204
1.4. Ventral stream connectivity in the galago 205
2. Future work: methodological considerations 205
2.1. Granularity of analysis 205
2.2. Model selection 207
3. Neuroanatomical findings: implications for an evolutionary framework 208
3.1. White matter expansion in the anthropoid lineage 208
3.2. Implications for the ancestral state 211
4. Conclusions 214
References 215

LIST OF TABLES

Table 2.1. Summary of retinal wave studies 60
Table 3.1. Best-matching NMF components per tract, human 108
Table 3.2. Best-matching NMF components per tract, macaque 110

LIST OF FIGURES

Figure 1.1. The muffin pan illusion 6
Figure 1.2. Belon's early modern comparative anatomy 12
Figure 1.3. Benefits of comparative neuroscience 14
Figure 1.4. Simplified primate cladogram 26
Figure 2.1. Cladogram depicting the study of spontaneous retinal waves 59
Figure 2.2. Temporal-to-nasal patterned retinal activity 62
Figure 2.3. Development of the *Xenopus* visual system 68
Figure 3.1. NMF validation procedure and methods overview 98
Figure 3.2. Quantitative comparison between NMF outputs and atlas-derived tracts 105
Figure 3.3. Visual anatomical characteristics of NMF-derived tracts in macaque 106
Figure 4.1. Study overview 132
Figure 4.2. Performance of NMF decomposition in macaque with three brains 144
Figure 4.3. Reconstruction of anterior temporal-frontal and occipitotemporal-frontal connections 146
Figure 4.4. Lemur shows the highest orbitofrontal bias in both sets of connections 149
Figure 5.1. Merging of anterior temporal-frontal and occipitotemporal-frontal connections at 50- and 60-component levels 182
Figure 5.2. NMF-based reconstruction of ventral stream connections in the galago 184
Figure 5.3. Density of prefrontal and orbitofrontal cortical innervation, across all species 187
Figure 6.1. Simplified primate cladogram with annotations 209

LIST OF ABBREVIATIONS

7T	7-Tesla
ANOVA	Analysis of variance
CaMKII	Calmodulin-dependent protein kinase II
D.F.	Degrees of freedom
DW-SEMS	Diffusion-weighted spin-echo multi-slice sequence
FSL	FMRIB Software Library
ILF	Inferior longitudinal fasciculus
IPL	Inner plexiform layer
IQR	Inter-quartile range
K	Number of components
MMORF	MultiMOdal Registration Framework
Mr Cat	Magnetic resonance Comparative anatomy toolbox
MRI	Magnetic resonance imaging
n	Sample size
NMF	Non-negative matrix factorisation
NNDSVD	Non-negative double singular value decomposition
NOIB	Non-orbitofrontal innervation bias
OB	Olfactory bulbs
OFC	Orbitofrontal cortex
OR	Optic radiation
PBS	Phosphate-buffer saline
PFC	Prefrontal cortex
PKC	Protein kinase C
RGC	Retinal ganglion cell
STR	Superior thalamic radiation
TE	Echo time
TR	Repetition time
VLPFC	Ventrolateral prefrontal cortex
XTRACT	Cross-species tractography toolbox

Chapter 1

Introduction: Vertebrate vision and the evolution of sensory systems.

Declarations

Contribution statement

JEH drafted all of the text and produced all figures which appear in this chapter. ZM and RBM assisted in editing the manuscript and designing figures.

Acknowledgements

JEH is funded by a Wellcome Trust Doctoral Studentship in Neuroscience (222368/Z/21/Z). RBM is supported by the Biotechnology and Biological Sciences Research Council UK (BB/N019814/1) and the Medical Research Council UK (MR/Y010698/1). The funders had no role in the design or writing of this report, nor in the collection, analysis, and interpretation of data.

1. Why study vision?

1.1. A long-standing human fascination

Humans have occupied themselves with the particularities of vision since antiquity. In the 4th century BCE, Aristotle provided a written account of an optical illusion, since dubbed the "waterfall illusion". In his treatise *On Dreams* (Beare, 1984 translation), Aristotle writes:

> And also when persons turn away from looking at objects in motion, e.g. rivers, and especially those which flow very rapidly, they find that the visual stimulations still present themselves, for the things really at rest are then seen moving…

Of course, Aristotle was surely not the first human to take an interest in visual perception and optical illusions. Donald Hoffman (1998) identifies a bracelet, carved circa 22,000 BCE from mammoth ivory, which uses zig-zag patterns to create illusory contours. That is, the bracelet contains empty spaces which appear to continue the lines and shapes which are absent between the carvings.

In the thousands of years since these early examples, our fascination with vision has not waned. The annals of the Royal Society of London (Birch, 1756, p. 349) include the tale of a new microscope, presented to the Society in 1668, which led to the surprising observation that a coin's engraving could appear depressed to some viewers and embossed to others, under magnification. This phenomenon was investigated further by David Rittenhouse in the 18th century, who generated what has subsequently been dubbed the "muffin pan" illusion (Ings, 2008). This illusion, presented in Figure 1.1, is a subject of ongoing research today (e.g., Proulx, 2014).

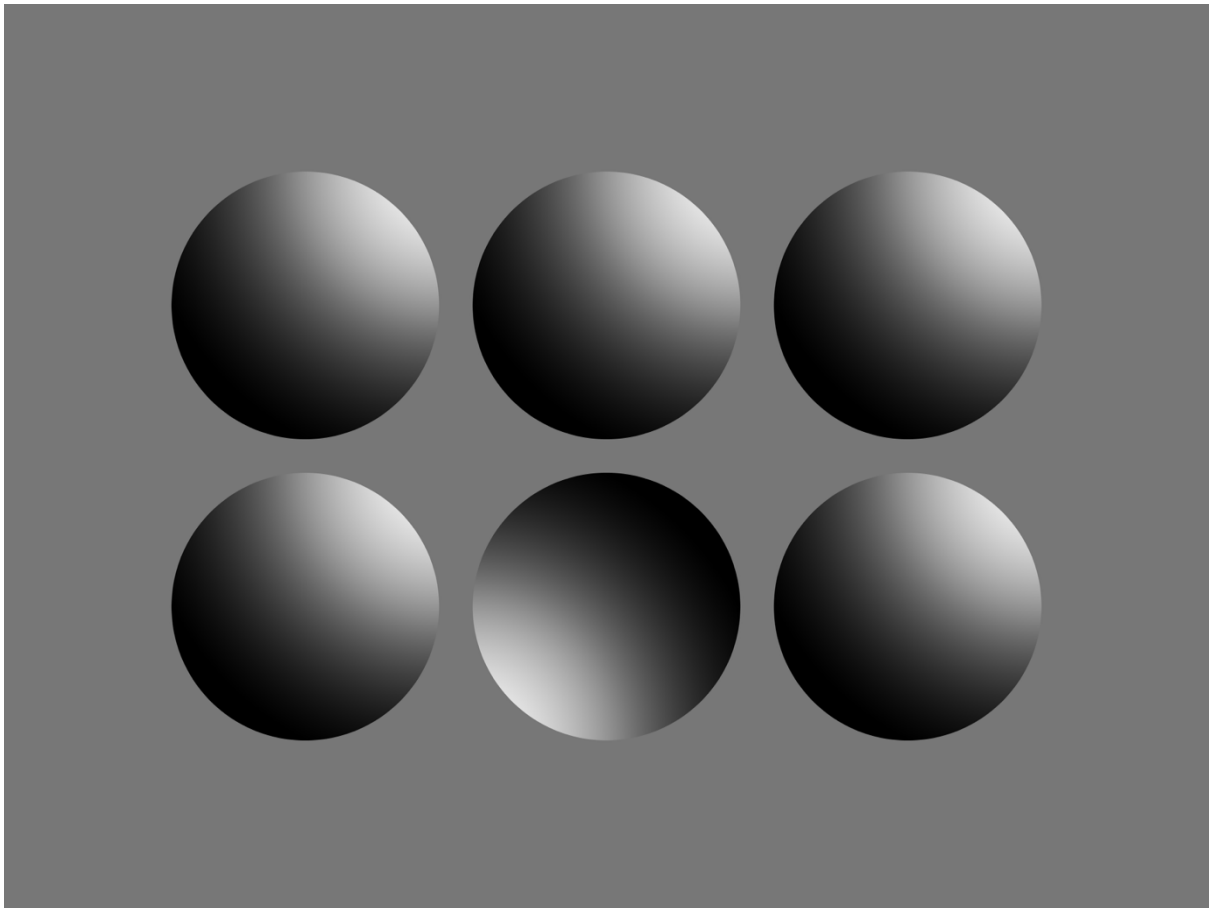


Figure 1.1. The muffin pan illusion. *Whether the bottom-centre circle is depressed or embossed depends on which way you view it. If this page is rotated 180-degrees, the circles will change from depressed to embossed and vice-versa.*

Despite our longstanding fascination with vision, it is but one sense of many. Although there is a tradition of claiming that vision is the most "developed" (Hutmacher, 2019) or most "noble" (Jay, 2011) of the senses in humans, a powerful argument can be made that vision is neither more important nor more "developed" than the other senses. The work of Paul Bach-y-Rita on sensory substitution (e.g., Bach-y-Rita, 1967; Bach-y-Rita et al., 2005) demonstrates that visual information can be recapitulated by other sensory modalities. Bach-y-Rita's camera-guided devices harnessed patients' neural plasticity and translated visible light into tactile information. Using these devices, patients could perceive and respond to visual

stimuli even in the absence of a functioning visual system. These studies are but one example demonstrating the commensurability between sensory modalities. Other examples abound. Reading tends to be a visual task, but this is what philosophers might describe as a contingent state of affairs – that is, it need not be that way by necessity. The existence of Braille as a non-visual writing system is evidence enough of this claim.

Nonetheless, the visual system continues to be the subject of exceptional interest for both researchers and the general public. Hutmacher (2019) found in the period of 2008 through mid-2019 that over 75% of psychological studies on sensory memory were focused on visual memory as opposed to other sensory modalities, while Howes (2010) describes an erasure of the non-visual senses in qualitative research, including ethnographic studies. Enoch and colleagues (2019) found in a cross-sectional survey of UK adults that participants valued sight over all other senses, while Scott et al. (2016) found that US adults describe the loss of eyesight as worse than losing one's memory, speech, hearing, or a limb. Although the modern perspectives presented here inordinately represent attitudes expressed in the Western, English-language corpus, it seems inescapable that contemporary writers frequently elevate vision above the other senses.

1.2. A natural history of vision

Some would say that our fascination with the visual system could be forgiven, as primates are an overwhelmingly visual order compared to other mammals. There is good reason to be sympathetic to this claim. The last common ancestor to primates is thought to have been adapted for a life in the fine branches of trees, using a leaping-

grasping form of locomotion and engaging frontally-directed eyes to guide visual foraging (Cartmill, 1992; Fleagle, 2013; Kaas et al., 2021). This ancestral state has been elaborated upon in extant primates. Eocene fossils indicate that early primates, both nocturnal and diurnal, possessed a small foramen; that is to say, the opening for the optic nerve at the back of the orbit (i.e., the foramen) is relatively narrow in these early primates (Martin, 2004). In contrast, extant primates show a clear demarcation between nocturnality and diurnality in foramen size (Kay & Kirk, 2000), suggesting different visual adaptations between early primates and modern primates. This has led to the conclusion that early primates depended less on vision than their modern, extant relatives (Kaas, 2012). In this way, the evolutionary history of primates seems to describe a visually-oriented lineage that came to rely further on vision with successive adaptations.

Yet vision is expensive – and not just for primates. Turning more broadly from primates to vertebrates in general, a provocative study by Moran and colleagues (2015) gives a glimpse into how expensive visual systems can be, by studying *Astyanax mexicanus*, the Mexican tetra fish. The Mexican tetra has diversified into different ecological niches including both river and cave environments, multiple times across its evolutionary history. Intriguingly, the surface ecotype found in rivers has well-developed eyes and optic tecta (homologous to the mammalian superior colliculus), while the most divergent cave ecotype in Pachón is completely eyeless and has substantially reduced optic tecta (approximately 50% smaller in adults; Rodrigues, 2013). By calculating the energetic requirements of these different ecotypes of Mexican tetra, Moran and colleagues (2015) identify that vision-related

costs account for 5% to 15% of the resting metabolism of an 8.5-gram fish and a 1-gram fish, respectively.

The energetic expense of vision may be relatively high, especially for small vertebrates – yet despite this, vision is widespread. In all eyes described to date, vision is enabled by opsins, light-sensitive proteins found in photoreceptor cells. Yet opsins are much older than eyes, evolutionarily. Phylogenetic modelling suggests that at least nine opsins were present in the last common ancestor to all nephrozoan animals (Ramirez et al., 2016) – the lineage which includes all animals except xenacoelomorphs (small, bilateral, marine, worm-like invertebrates), placozoans (a kind of small, flat marine invertebrate, approximately one mm across), comb jellies, jellyfishes, corals, and sponges (Parry & Pisani, 2016). While opsins are used for both visual and non-visual light sensation, understanding the evolutionary history of opsins is key to understanding how eyes and vision evolved across multiple branches of the animal kingdom. Nephrozoans have been incredibly successful, representing most of the diversity of animals on this planet, and current evidence suggests that light-sensitivity was present even in the earliest nephrozoans. The cost of light sensitivity seems to have been one worth bearing for our ancestors – and the evolutionary innovation of opsins enabled the eyes which came afterwards. In the scheme of animal evolutionary history, light and vision seem to have been present at several notable inflection points, making vision a subject ripe for evolutionary study.

To understand the diversity and evolution of visual systems, it is necessary to look at the development of visual systems. This is because evolution is the evolution of development (García-Moreno & Molnár, 2020; Molnár, 2021). Specifically, evolution must act on the developing organism, because adult animals do not

transform into other adult animals. As such, to properly understand how visual systems have evolved, we must study the development of visual systems across species. Indeed, I examine cross-species differences in visual system development in Chapter 2 of this thesis. However, access to high-quality data across multiple developmental time points is lacking. As such, in Chapters 3 through 5, I consider cross-species differences in adult organisms to draw inferences about the evolution of vision systems. Because evolution is the evolution of development, it should be understood that any evolutionary differences identified therein almost certainly arise from developmental processes.

It is not lost on me that I am putting the cart before the horse, in a sense, when I describe the importance of comparing developmental trajectories before having discussed the importance of comparative neuroscience at all. Thus, I would like to now make a foray into the motivation for studies of comparative neuroscience *in genere*.

2. Why compare species?

2.1. History of the comparative approach

The relationship between humans and other primates is both fraught and rich. Alfred Wallace's careful documentation and description of New World monkeys' geographic distributions in 1852 (Wallace, 2009b) preceded his 1855 insight that "[e]very species has come into existence coincident both in space and time with a pre-existing closely allied species" (Wallace, 2009a) and his 1858 description of survival by fitness. Wallace communicated his findings to Darwin, and their work was read

together to the Linnean Society that year (Wallace, 2009c). It was only by considering geographic distributions and comparative anatomy, among other factors, that Wallace was able to make sense of the relationships between species and pen these precursors to the theory of evolution by natural selection (Costa, 2023; Shostak, 2024).

This was not the first time the comparative approach had yielded insights into the field which would become evolutionary biology. In 1735, Carl Linneas classified humans in a taxonomic group with other primates, and in the 1830s, the first fossils of extinct primates were discovered (Fleagle, 2000). The former event set the stage for the consideration of primates to understand humans, while the latter event presented the first pre-evolutionary evidence that primates existed before the present time and that there were primates in the fossil record which were not known to be alive in the present. Of course, it was only by comparison of skeletal anatomy that the fossilised remains were identified to belong to a primate species – and an as-yet unidentified species, at that.

Comparative studies are not limited to the primate lineage. Wallace wrote of birds in his 1858 essay (2009c), and before him, early modern European naturalists such as Pierre Belon (Gudger, 1934) provided detailed comparative accounts of avian anatomy (Figure 1.2) which laid the groundwork for contemporary ornithology.

Comparative studies have not only provided historical value, but continue to benefit scientific enquiry today. For example, within neuroscience, it has only been by comparing the expression and function of the speech-related transcription factor FoxP2 in songbirds and humans that insights have been drawn about the conserved role of this protein in speech generation (Brainard & Doupe, 2013; Burkett et al., 2018; Haesler et al., 2007; Konopka & Roberts, 2016; Schulz et al., 2010; Xiao et al.,

2021 and more), with implications for research into both human speech pathology and convergent evolution. Cross-species descriptions of the craniofacial alterations and changes in prosocial behaviour which occur during domestication have given rise to the human self-domestication hypothesis and a rich literature surrounding it (Cieri et al., 2014; Geiger et al., 2017; Theofanopoulou et al., 2017; Torres-Pérez et al., 2023; Wrangham, 2019; Zanella et al., 2019 and more). Comparing the motor

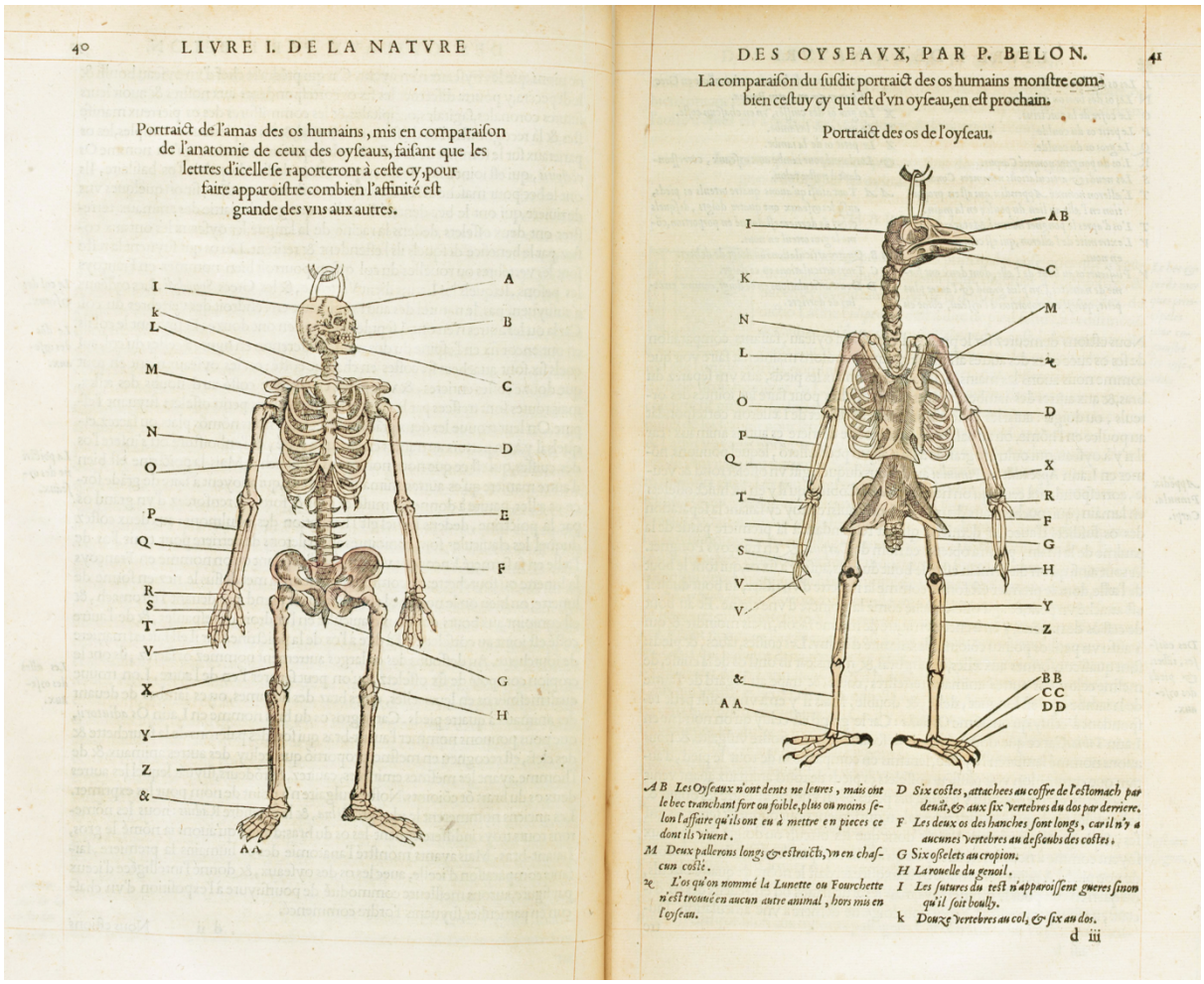


Figure 1.2. Belon's early modern comparative anatomy. *Illustrations of human and avian skeletons by Pierre Belon (1555), from* L'Histoire de la Nature des Oyseaux *(trans. "Natural History of Birds"). The text contains detailed descriptions and illustrations of more than 150 birds, categorised by habitat and behaviour.*

cortical representations of the larynx across primates has given rise to the dual larynx motor networks hypothesis, yielding insights into the origins of human speech and language (Belyk et al., 2021; Eichert et al., 2020; Hickok et al., 2023). These are but a few examples to illustrate the richness of contemporary comparative neuroscience. But beyond the specific benefits and insights gleaned from each of these "case studies", what can be said about the benefits of modern comparative neuroscience more generally?

2.2. The benefits of comparative neuroscience

I am far from the first to espouse the virtues of comparative neuroscience (Bullock, 1984; and many more) and I certainly will not be the last. Comparative neuroscience findings have impacted numerous fields and the area continues to hold importance for a variety of subjects of enquiry, some of which I have outlined below. These subjects are outlined in Figure 1.3 and in the paragraphs which follow.

Translational research

A great many neuroscientific studies are aimed at curing diseases, and the research funding landscape reflects and likely drives this reality. For instance, the US-based National Institutes of Health dedicated over $6.5 billion USD to mental health and neurological disease research in 2019 alone (Ballreich et al., 2021). Within this funding landscape, the vast majority of preclinical studies are done using rodents to model disease states and test potential therapies.

Historical reports suggest that in the 1980s, approximately 85 percent of the

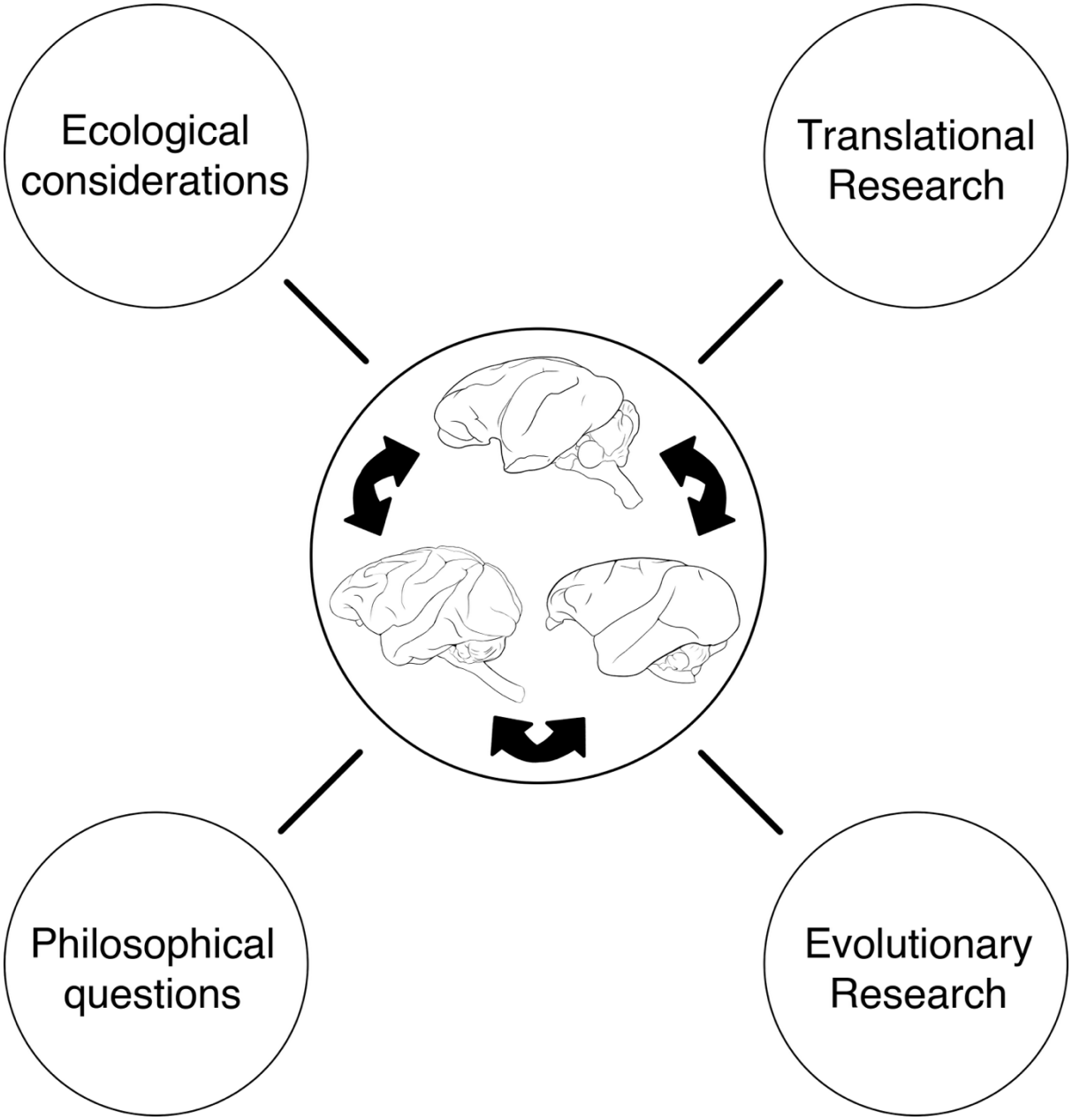


Figure 1.3. Benefits of comparative neuroscience. *Comparing brains (centre) yields benefits across several disparate domains (perimeter). The brains here, not drawn to scale, are those of a lemur (top-centre), squirrel monkey (bottom-right), and macaque (bottom-left).*

---

animals used in biomedical research in the United States were rats and mice (Institute of Medicine & National Research Council, 1988). A more recent analysis (Gattani et al., 2025) found that in PubMed-indexed publications from 2016 to 2021 which report the use of small laboratory animals, over 98% of studies used mice or rats,

sometimes in combination with *in vitro* methods. In the United Kingdom, the latest statistics on the use of animals for scientific procedures (Home Office, 2024) reflect a similar reality. Roughly 72% of scientific procedures conducted on animals for basic and translational/applied research were in mice and rats. Regarding procedures related to the creation and breeding of genetically altered animals – comprising 45% of all procedures – 87% of procedures were conducted on mice and rats, a proportion which reflects the trend towards modelling disease states in bespoke transgenic mouse lines.

The dominance of rats and mice as models in biomedical research is a relatively recent phenomenon, however. As the celebrated neurophysiologist Eve Marder explains:

> Not that long ago, neuroscience graduate students were expected to wander the woods, explore tide pools, take ocean voyages, or pore over tomes of zoological texts with wonderful old drawings in search of the perfect preparation with which to study an important problem… Today it is almost inconceivable that many neuroscientists would venture back to the ocean, river, field or forest in search of a new preparation.
>
> – Eve Marder, *Non-mammalian models for studying neural development and function (*2002)

The idea of going into the field – metaphorically or literally – to identify a new organism in which to study a neuroscience problem does seem antiquated, indeed. Developing a new model of a disease state is a daunting prospect. The sheer quantity of experimental and descriptive research characterising mouse and rat anatomy and physiology – including their nervous systems – makes these rodents an easy choice for modelling disease states and testing therapeutic interventions, to say nothing of the power of transgenic lines and other genetic tools available in rodents. Yet for decades,

researchers have questioned the validity of the most common animal models for modelling disease states and therapeutic interventions (e.g., Collins, 2011; Dawson & Tricklebank, 1995; Geerts, 2009; Insel, 2007; Keifer & Summers, 2016; Loewa et al., 2023).

It would be presumptuous to imagine I could solve the problem of translational failures in biomedical research in the Introduction to my thesis. However, I believe few would argue against the benefits to employing a wider diversity of organismal disease models. Indeed, traditional and non-standard models can be used in conjunction to inform each other (Watson & Platt, 2012). The benefits to establishing new disease models could be great, and many of the hurdles to using non-standard models are practical. As Marder (2002) adeptly recognises, these hurdles include the prohibitive amount of groundwork to establish a new model and the social conformism that influences scientists' decision-making, to name a couple.

The former of these two problems at least is within the purview of this thesis. To establish the suitability of a model, comparative neuroanatomical studies are key to identify similarities and differences between species. Bearing special mention is the recent work of Glud and colleagues (2024) in describing the anatomy and connectivity of the Göttingen minipig's subgenual cingulate area and comparing it to that in the human. This work was carried out with the aim of establishing the minipig as a model for evaluating deep brain stimulation to the subgenual gyrus as a potential treatment for depression. These kinds of studies can establish new model systems for preclinical research, but they are relatively rare, as they have traditionally been expensive and time-consuming to conduct.

Fortunately, as Mars and Palomero-Gallagher (2024) remark, “Neuroanatomy is entering the era of big data”. The development of new approaches to comparative neuroanatomy holds the potential to identify with greater throughput and precision the similarities and dissimilarities between a putative model and its target system, enabling researchers to make better decisions about how to model disease states. Several studies have begun applying such approaches to traditional rodent model systems (Balsters et al., 2020; Beauchamp et al., 2022; Huang et al., 2025; Jaroszynski et al., 2025), with the promise of improving translations between rodents and humans. However, significant challenges remain (see Section 2.3, “Challenges for comparative neuroscience”). This thesis, in part, seeks to develop methodologies to address these challenges.

Evolutionary research

The conduct of science has sometimes been compared to the “streetlight effect”, perhaps first in the 1960s (Kaplan, 1964), and several times again thereafter, including notably by the linguist Noam Chomsky (Barsky, 1998). The name of the effect is a reference to a popular joke, which goes roughly as follows:

> A police officer finds a drunk man frantically searching for something under the beam of a streetlight. When asked what he is looking for, the drunk replies, “My keys! I’ve dropped my keys.” The police officer joins in the search, but after several fruitless minutes, he asks, “Are you sure you lost your keys here?” The drunk says, “No, I dropped my keys over there in the park.” Exasperated, the officer asks, “Then why are you looking here?” The drunk replies, “Well, this is where the light is.”

In particular, I have had occasion to hear the science of evolutionary biology compared to the streetlight effect.

For an organism to appear in the fossil record, several things need to go right. During or after the organism's death, the remains must generally be rapidly buried in a low-oxygen environment to stop the decomposition process. In the most common form of fossilisation, the remains are then infiltrated by minerals, often through the groundwater, which then forms an internal cast of the organism. The fossil then must be preserved until it is unearthed through natural or anthropogenic processes. The confluence of these factors led early authors to speculate on why so few primate fossils had been found, as when Cautley and Falconer (1837) opined that primates were simply more adept at avoiding burial by floodwaters than other animals, and thus did not produce many fossils.

The many circumstances which must coincide for the formation of a fossil has been described as the streetlight in the metaphor. Evolutionary biologists may look where the streetlight is shining, but this approach provides only a brief glimpse into the evolutionary histories and geographic distributions of our ancestral relatives. For the evolutionary *neuro*biologist, the situation is even trickier, for soft tissues generally are not fossilised at all. Cranial endocasts may be used to estimate properties of brains, such as gyrification patterns and relative expansion of brain regions – and some of this work is described in Chapter 6 of this thesis – but other neuroanatomical properties such as white matter innervation patterns are completely absent from the fossil record, to our knowledge. Neurophysiological phenomena, such as distinctive patterns of spontaneous cellular activity in development (discussed further in Chapter 2 of this thesis), leave no fossilised traces either.

Fortunately, the study of evolution has tools beyond the fossil record at its disposal. Genetic techniques have frequently been used to produce phylogenetic trees;

this was the approach used in the study on the ancestral origin of opsins cited previously (Ramirez et al., 2016; see Section 1.2, “A natural history of vision”). Additionally, comparative neuroanatomy and neurophysiology can be used to infer a shared evolutionary history for a trait in the absence of fossil or genetic data – though care must be taken with this approach to consider the possibility of convergent evolution. For complex, emergent traits which are not preserved in the fossil record and do not have a clearly-identified genetic basis, this comparative approach is a primary tool of the evolutionary neurobiologist. The evolutionary motivations of the present work are discussed further in Section 3, “Primate visual evolution”.

Philosophical questions

“When neuroscientists become old, they try to solve the problem of consciousness”, quips Dick Passingham in his 2008 book, *What is Special About the Human Brain?*. Fortunately, I am not yet an old neuroscientist, so I do not have to tackle the problem of consciousness in this thesis. Though more seriously, it would be presumptuous of me to interpret the limited findings of the present work as yielding substantive insights into the innumerable debates surrounding consciousness. What can be said, though, is that the field of comparative neuroscience lays as strong a claim on the field of consciousness as any. Consciousness is entangled with many of the fundamental questions that comparative neuroscience seeks to address. How large is the gap between humans and our closest relatives? Does the human brain give rise to human consciousness – and if so, are these consciousness-making bits present in other species?

Most philosophers today identify as physicalists about the mind (Bourget & Chalmers, 2023; Yaden & Anderson, 2021). Although it would be challenging to define physicalism in a way that is acceptable to all philosophers, a rough sketch would say that physicalists deny the dualistic view that the mind exists distinctly from the body, as a non-physical entity. Taking this view, it seems that any physicalist must reckon with the work being done to compare different species' nervous systems if they are interested in the differences in mental phenomena between different animals. This claim could also be made towards views which assert the physical gives rise to the mental – even if one believes mental states cannot causally act on physical states (i.e., epiphenomenalism).

Comparative neuroscience also has implications for ethical and policy considerations. For instance, nociceptive pathways in the roundworm *C. elegans* share a genetic basis with human nociceptive pathways (Jordan & Glauser, 2023). Nociception is better known as the sensation of pain in humans, but stated more precisely, nociception is the transduction and transmission of signals about potentially harmful stimuli, which is associated with the subjective experience of pain in humans. This distinction between signal transduction and subjective experience matters, because thermal nociception robustly elicits distinct aversive responses in *C. elegans*, depending on where the heat is applied to the body (Mohammadi et al., 2013). Stated more simply, different painful stimuli elicit distinct pain-like responses in *C. elegans*. Yet *C. elegans* is not subject to legislative protections on animal experimentation in any jurisdiction to my knowledge, and the vast majority – or all – experiments involving *C. elegans* are performed without the administration of anaesthetic. Philosophically, this is unproblematic primarily because we assert that

C. elegans probably does not feel the subjective experience of pain. Indeed, *C. elegans* does not have a cerebral cortex, and the cerebral cortex has been consistently implicated in pain perception (Ong et al., 2019; Treede et al., 1999; Xie et al., 2009). However, for an animal with a cerebral cortex, it would require a strong scientific justification to perform painful experiments in the absence of all anaesthesia. This kind of conclusion can only be drawn on the basis of a comparative approach.

Ecological considerations

Finally, comparative neuroscience has the potential to guide wildlife conservation and management. Understanding the mechanistic underpinnings of individual naturalistic behaviours is key to predicting population-level trends (Blumstein & Berger-Tal, 2015; Blumstein & Fernández-Juricic, 2004) and mitigating the impact of anthropogenic activities (Dominoni et al., 2020). Limiting the effects of anthropogenic activities on vulnerable species has grown increasingly important, as natural areas are reduced by both urban and cropland expansion (van Vliet, 2019).

Comparative approaches allow for the identification of commonalities between species, with great potential to inform conservation efforts. It is not feasible to study the sensory biology of every animal which might be affected by human activities, let alone to synthesise this information to guide decision-making. Yet by incorporating both “vertical” and “horizontal” translations – comparisons of brain organisation across modalities or spatial scales, and comparisons of brain organisation across species, respectively – comparative neuroscience could allow for the rapid deployment of formal predictions about animals’ nervous systems even in the absence of direct observation in the species of interest (Mars et al., 2021). However, despite

the immense promise of these approaches, comparative neuroscience has traditionally been hampered by several challenges, outlined below.

2.3. Challenges for comparative neuroscience

Comparative neuroscience has traditionally relied on detailed tracer studies to identify regional connectivity across species. These studies, though commonly hailed as the gold standard, face substantial challenges. They require sacrifice of numerous animals per species, are expensive, and are time- and labour-intensive (Nectow & Nestler, 2020). In contrast, recent advances in neuroimaging allow high quality, whole brain data to be collected relatively cheaply either *in vivo* or from post-mortem brains that are not sacrificed specifically for scientific research (Prescott & Poirier, 2021; Thiebaut de Schotten et al., 2019). Case-in-point, none of the animals analysed in this study (Chapters 3-5) were sacrificed for this research. The brains whose data comprise the Digital Brain Zoo (Tendler et al., 2022) are overwhelmingly specimens from museum collections, zoos, and other research facilities, the animals of which were sacrificed or passed away for unrelated reasons, and whose brains may now benefit science. Particularly important for museum specimens, including the two thylacine brains in the Digital Brain Zoo, most neuroimaging techniques are non-invasive, which allows researchers to examine these brains in unprecedented detail without compromising the integrity of the specimens. There are still substantial challenges to studying these brains, though. Many of the species for which neuroimaging data are now available have been studied only sparsely, and ready-made processing tools are rarely available, affecting the study of both grey and white matter neuroanatomy.

A substantial portion of this thesis focuses on the study of white matter connectivity. Traditionally, brains have been described in terms of grey matter areal specialisations. In the post-phrenology era of cognitive science, the tradition of cortical functional localisation can find its roots in the debate between Friedrich Leopold Golz and Sir David Ferrier, who in 1881 described disparate cortical lesion experiments in carnivore and primate brains, and their effects on animal behaviour (Molnár, 2021). There is still value in ascribing functions to cortical areas, but it is increasingly appreciated that many complex functions arise from distributed networks of interconnected regions (Mars et al., 2018; Molnár, 2021; Passingham et al., 2002), with a variety of subcortical regions playing a critical role in the network architecture underlying these functions (Bell & Shine, 2016; Miller & Clark, 2018; Whiting & Barton, 2003). White matter connectivity can describe principles of brain organisation that are directly relevant for behavioural functions (Mars et al., 2018), yet there is a profound dearth of information on the evolution of white matter connectivity. This is in part because information about white matter connectivity is not preserved in fossils (discussed further in Section 3, “Primate visual evolution”), but also due to a lack of processing tools to characterise white matter connectivity in understudied brains.

The study of white matter connectivity via neuroimaging is primarily done through diffusion tensor imaging and fibre tractography. Diffusion tensor imaging is a structural MRI technique which provides a quantitative description of the directionality of water flow in a brain. Because water cannot flow through the fat of a myelin sheath, voxels which contain white matter (composed of myelinated axons) will generally show a mean diffusivity in the predominant direction of the axons contained within that voxel. Fibre tractography (or simply tractography) is the

process of reconstructing white matter tracts on the basis of diffusion tensor images. Standard tractography protocols are atlas-based, meaning they rely on a white matter atlas which specifies each tract's origin, course, and termination. Such an atlas generally includes "start", "stop", and "exclusion" masks (regions of interest) among other priors, the specification of which requires substantial foreknowledge of the brain under study. Such knowledge is increasingly available in human and macaque (Assimopoulos et al., 2024; Warrington et al., 2020), but by and large absent in other species. As such, to study less-known brains, it is necessary to take a data-driven approach which is agnostic to the brains being studied. Developing such an approach for comparative studies is one of the aims of this thesis.

Finally, another challenge of comparative neuroscience – regardless of methodology – is that sample sizes tend to be small. Particularly because comparative studies tend to be exploratory in nature, laboratory-based colonies are rarely available for the species which researchers wish to study. Thus, it is important for any methodology to have enough fidelity/precision that it can detect effects of the required size at low sample numbers. To that end, Chapters 3 and 4 of this thesis quantify the performance of the novel approach taken here, to determine its suitability at low sample sizes.

3. Primate visual evolution

A substantial portion of this thesis is dedicated to the study of how certain traits have evolved within the primate order. Specifically, I examine the evolution of the anterior ventral visual stream within the primates. One motivation for this is that

primates are an overwhelmingly visual order (see Section 1.2, “A natural history of vision”).

Beyond the general adaptations described previously, a particularly prominent aspect of primates’ visual heritage is the existence of two visual cortical pathways in the neocortex. Starting in the striate visual cortex, two canonical, anterior-posterior visual pathways process different aspects of visual information (Baizer et al., 1991; Goodale & Milner, 1992). The dorsal pathway to posterior parietal cortex processes visual information for visually guided actions (Rizzolatti & Matelli, 2003) while a ventral pathway to inferior temporal cortex was traditionally seen as important in object recognition or more generally the processing of object representations (Kravitz et al., 2013). However, underlying these gross anatomical similarities are myriad visual adaptations, specific to different lineages within the primates.

Primates are incredibly diverse order with over 500 recognised extant species (Fleagle & Seiffert, 2020). These species are divided into two suborders (Figure 1.4). According to one popular taxonomy, the one adopted here, the haplorhines consist of the anthropoids and tarsiers while the strepsirrhines consist of the lemurs and lorises. While tarsiers possess a fascinating visual system with high acuity under scotopic (i.e., very low light) conditions (Collins et al., 2005) and an early emergence of long- and medium-wavelength cones supporting trimochromatic vision despite a nocturnal heritage (Melin et al., 2013), the present work will focus on differences between strepsirrhines and anthropoids, omitting the tarsiers from analysis due to unavailability of neuroimaging data in tarsiers.

Nocturnality and diurnality are the two most prominent kinds of “diel activity pattern”. Diel activity pattern, the time of day in which an animal is active, is

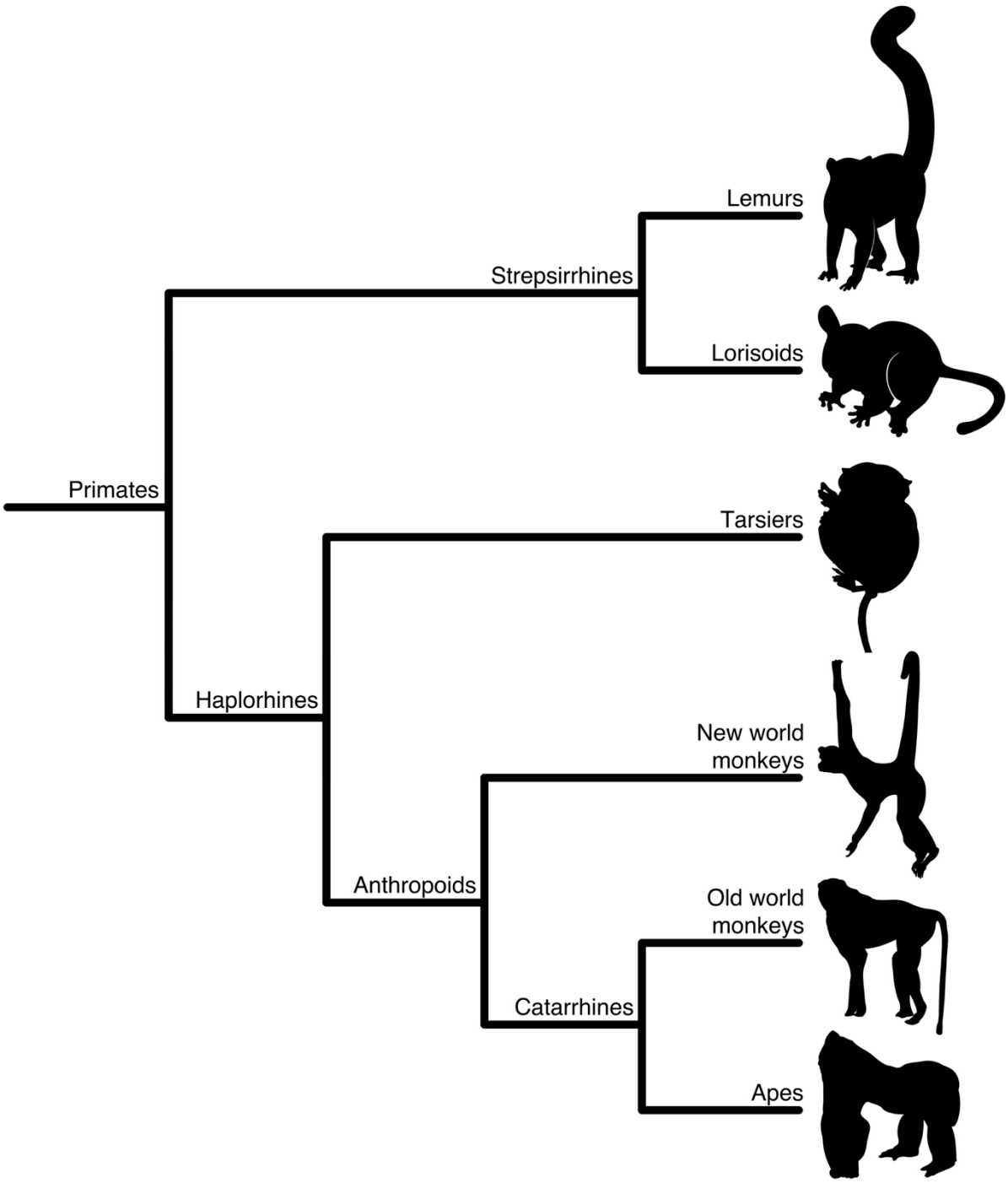


Figure 1.4. Simplified primate cladogram. *Primates are divided into haplorhines (lower branch) and strepsirrhines (upper branch). The haplorhines consist of anthropoids and tarsiers. The present work focuses on comparing anthropoids with strepsirrhines.*

---

associated with several differences in visual anatomy. For instance, nocturnal primates have a larger corneal diameter than diurnal primates (Kirk, 2006). The

diurnal-nocturnal division in foramen size described in previously (Section 1.2, “A natural history of vision”) is more pronounced in the anthropoids than the strepsirrhines (Kay & Kirk, 2000), consistent with the general sentiment that the anthropoids are more visually-oriented than the strepsirrhines. The lateral geniculate nucleus – the visual relay of the thalamus – contains more parvocellular neurons and has a greater relative volume in diurnal primates than their nocturnal counterparts (Barton, 1998).

However, within the primates, there is considerable variation in both diel activity pattern and visual adaptations. Perhaps the most well-studied of the strepsirrhines, the ring-tailed lemur (*Lemur catta*), has historically been regarded as strictly diurnal (Howarth et al., 1986; Jolly, 1966), though more recent reports (Donati et al., 2013; LaFleur et al., 2014; Parga, 2011) have suggested that ring-tailed lemurs may be cathemeral – showing activity during both daytime and nighttime. Indeed, this seems to be the growing consensus. Cox and Gaston (2024) classify the ring-tailed lemur as a facultative cathemeral species meaning it, like the mongoose lemur (Cox & Gaston, 2024; Curtis et al., 1999), is able to transition its behaviour from a diurnal pattern to a cathemeral one. Kirk (2006) reports that the corneal diameter of the ring-tailed lemur is intermediate, between those of nocturnal and diurnal strepsirrhines. This places further anatomical evidence behind the claim of cathemerality for the ring-tailed lemur. But in addition to cathemeral species like the ring-tailed lemur, some lemur species are believed to be almost completely diurnal (Bearder et al., 2006). This is in stark contrast to the lorisoids which are understood to all be strictly nocturnal (Nekaris & Bearder, 2011; Svensson et al.,

2018). Intriguingly, this diversity in strepsirrhines' diel activity patterns corresponds to some cross-species differences in sensory biology.

In most jawed vertebrates, olfaction depends on distinct olfactory systems, primarily the main olfactory system and the accessory olfactory system (Poncelet & Shimeld, 2020). Although there is overlap in the functions of the two systems, the accessory olfactory system is classically considered to be dedicated to the processing of scents from conspecifics, such as pheromones, while the main olfactory system processes other odorants. It is thought that strepsirrhines rely more on olfactory sensation than haplorhines, overall. Behavioural reports of olfactory-based foraging in strepsirrhines (e.g., Cunningham et al., 2021) converge with the anatomical and genetic evidence in this regard. Genetic studies using distinct methodologies have reliably found that haplorhines possess fewer functional olfactory receptor genes than strepsirrhines (Gilad et al., 2004, 2007; Matsui et al., 2010). Unlike strepsirrhines, some haplorhines are believed to have only a vestigial accessory olfactory system or to have lost the accessory olfactory system entirely (Eisthen, 1992; Poncelet & Shimeld, 2020). Additionally, all strepsirrhines have a rhinarium – a hairless surface around the nostril openings – which haplorhines lack (Smith et al., 2007). Furthermore, strepsirrhines possess relatively enlarged olfactory bulbs compared to haplorhines (Heritage, 2014). However, among strepsirrhines, there is a clear demarcation between two modes of olfactory sensory communication and diel activity pattern is coincident with this demarcation. Nocturnal strepsirrhines engage more prominently in urine marking, while diurnal and cathemeral strepsirrhines tend to engage in glandular scent marking (Drea et al., 2019; Schilling, 1980). Consistent with this, the urine of nocturnal strepsirrhines contains more volatile organic

compounds than that of diurnal and cathemeral strepsirrhines (Drea et al., 2019). While olfaction is important to myriad strepsirrhine species, different species produce olfactory cues in different ways, with an apparent demarcation along the same lines that divide the strepsirrhines' diel activity patterns. This demarcation between nocturnal, cathemeral, and diurnal strepsirrhines in *olfaction* prompts questions about whether and how the *visual* systems of strepsirrhines might differ from each other and from haplorhines'.

Even among nocturnal strepsirrhines, vision guides complex decision-making tasks. For instance, male *Galago moholi* primates – a kind of lorisoid – travel further on nights with greater moonlight illumination. Mysore slender lorises – another kind of lorisoid – prefer ants over more mobile prey during low-light conditions, an adaptation which may reduce the risk of encountering predators (Bearder et al., 2006). What is unknown is whether differences in diel activity pattern might be related to large-scale differences in the white matter substrates which support visual processing. This thesis studies the connectivity of the ventral visual stream in both a cathemeral and a nocturnal strepsirrhine, as well as two anthropoid species, to undertake a first exploration of this question.

While primates' grey matter evolution has been studied fairly extensively and benefits from the use of fossil evidence including cranial endocasts (see Section 2.2, "The benefits of comparative neuroscience" – subsection, "Evolutionary research"), there is less research on the evolution of white matter connectivity within the primates, owing in part to the dearth of fossil-based evidence and the lack of ready-made tools for the analysis of white matter connectivity. By addressing questions of white matter connectivity in a number of phylogenetically distant primates, this thesis

aims to address longstanding questions about the connectivity of visual processing regions within the primates.

4. Thesis outline

This thesis is comprised of two parts and six chapters – a total of four body chapters, excluding the general introduction and general discussion (i.e., Chapters 1 and 6). Both parts of this thesis consider the evolution of the visual system within the vertebrate lineage by making comparisons across species. The first part, comprising Chapter 2, develops a novel account of the evolution of a type of spontaneous activity in the development of the visual system known as retinal waves. By considering the lifestyles and phylogenetic relations between the species in which retinal waves have been observed, this work advances an account of the ancestral origin of retinal waves. The second part of this thesis, comprising Chapters 3 through 5, develops an approach for data-driven tractography in lesser-studied brains. This approach is applied to species from across the primate lineage, to draw insights about the evolution of the ventral visual stream within the primate order. In addition to the direct knowledge gained regarding primate visual evolution, it is my hope that this thesis shall have advanced methods which prove useful for the study of white matter connectivity across a variety of species.

References

Assimopoulos, S., Warrington, S., Bryant, K. L., Pszczolkowski, S., Jbabdi, S., Mars, R. B., & Sotiropoulos, S. N. (2024). Generalising XTRACT tractography protocols across common macaque brain templates. *Brain Structure and Function*. https://doi.org/10.1007/s00429-024-02760-0

Bach-y-Rita, P. (1967). Sensory plasticity: Applications to a vision substitution system. *Acta Neurologica Scandinavica*, *43*(4), 417–426. https://doi.org/10.1111/j.1600-0404.1967.tb05747.x

Bach-y-Rita, P., Danilov, Y., Tyler, M. E., & Grimm, R. J. (2005). Late human brain plasticity: Vestibular substitution with a tongue BrainPort human-machine interface. *Intellectica*, *40*(1), 115–122.

Baizer, J. S., Ungerleider, L. G., & Desimone, R. (1991). Organization of visual inputs to the inferior temporal and posterior parietal cortex in macaques. *Journal of Neuroscience*, *11*(1), 168–190. https://doi.org/10.1523/JNEUROSCI.11-01-00168.1991

Ballreich, J. M., Gross, C. P., Powe, N. R., & Anderson, G. F. (2021). Allocation of National Institutes of Health Funding by Disease Category in 2008 and 2019. *JAMA Network Open*, *4*(1), e2034890. https://doi.org/10.1001/jamanetworkopen.2020.34890

Balsters, J. H., Zerbi, V., Sallet, J., Wenderoth, N., & Mars, R. B. (2020). Primate homologs of mouse cortico-striatal circuits. *eLife*, *9*, e53680. https://doi.org/10.7554/eLife.53680

Barsky, R. F. (1998). *Noam Chomsky: A Life of Dissent*. MIT Press.

Barton, R. A. (1998). Visual specialization and brain evolution in primates. *Proceedings of the Royal Society of London. Series B: Biological Sciences*, *265*(1409), 1933–1937. https://doi.org/10.1098/rspb.1998.0523

Bearder, S. K., Nekaris, K. a. I., & Curtis, D. J. (2006). A Re-Evaluation of the Role of Vision in the Activity and Communication of Nocturnal Primates. *Folia Primatologica*, *77*(1–2), 50–71. https://doi.org/10.1159/000089695

Beare, J. I. (1984). On Dreams. In J. Barnes (Ed.), *Complete Works of Aristotle, Volume 1: The Revised Oxford Translation* (Vol. 2, pp. 729–735). Princeton University Press; JSTOR. https://doi.org/10.2307/j.ctt5vjv4w.21

Beauchamp, A., Yee, Y., Darwin, B. C., Raznahan, A., Mars, R. B., & Lerch, J. P. (2022). Whole-brain comparison of rodent and human brains using spatial transcriptomics. *eLife*, *11*, e79418. https://doi.org/10.7554/eLife.79418

Bell, P. T., & Shine, J. M. (2016). Subcortical contributions to large-scale network communication. *Neuroscience & Biobehavioral Reviews*, *71*, 313–322. https://doi.org/10.1016/j.neubiorev.2016.08.036

Belon, P. (with The Wellcome Library, L.). (1555). *L'histoire de la nature des oyseaux, avec leurs descriptions, et naïfs portraicts retirez du naturel / escrite en sept livres*. Prevotius, Benedictus. http://archive.org/details/hin-wel-all-00001828-001

Belyk, M., Eichert, N., & McGettigan, C. (2021). A dual larynx motor networks hypothesis. *Philosophical Transactions of the Royal Society B*, *376*(1840), 20200392.

Birch, T. (with Internet Archive). (1756). *The history of the Royal Society of London for improving of natural knowledge, from its first rise. ... By Thomas Birch, ... 1756:*

Vol 3. http://archive.org/details/bim_eighteenth-century_the-history-of-the-royal_birch-thomas_1756_3

Blumstein, D. T., & Berger-Tal, O. (2015). Understanding sensory mechanisms to develop effective conservation and management tools. *Current Opinion in Behavioral Sciences*, *6*, 13–18. https://doi.org/10.1016/j.cobeha.2015.06.008

Blumstein, D. T., & Fernández-Juricic, E. (2004). The Emergence of Conservation Behavior. *Conservation Biology*, *18*(5), 1175–1177. https://doi.org/10.1111/j.1523-1739.2004.00587.x

Bourget, D., & Chalmers, D. J. (2023). Philosophers on Philosophy: The 2020 PhilPapers Survey. *Philosophers' Imprint*, *23*(0), Article 0. https://doi.org/10.3998/phimp.2109

Brainard, M. S., & Doupe, A. J. (2013). Translating Birdsong: Songbirds as a Model for Basic and Applied Medical Research. *Annual Review of Neuroscience*, *36*(1), 489–517. https://doi.org/10.1146/annurev-neuro-060909-152826

Bullock, T. H. (1984). Comparative Neuroscience Holds Promise for Quiet Revolutions. *Science*, *225*(4661), 473–478. https://doi.org/10.1126/science.6740319

Burkett, Z. D., Day, N. F., Kimball, T. H., Aamodt, C. M., Heston, J. B., Hilliard, A. T., Xiao, X., & White, S. A. (2018). FoxP2 isoforms delineate spatiotemporal transcriptional networks for vocal learning in the zebra finch. *eLife*, *7*, e30649. https://doi.org/10.7554/eLife.30649

Cartmill, M. (1992). New views on primate origins. *Evolutionary Anthropology: Issues, News, and Reviews*, *1*(3), 105–111. https://doi.org/10.1002/evan.1360010308

Cautley, P. T., & Falconer, H. (1837). XXXIV.—Notice on the Remains of a Fossil Monkey from the Tertiary Strata of the Sewalik Hills in the North of Hindoostan. *Transactions of the Geological Society of London*, *5*(3), 499–504. https://doi.org/10.1144/transgslb.5.3.499

Cieri, R. L., Churchill, S. E., Franciscus, R. G., Tan, J., & Hare, B. (2014). Craniofacial feminization, social tolerance, and the origins of behavioral modernity. *Current Anthropology*, *55*(4), 419–443.

Collins, C. E., Hendrickson, A., & Kaas, J. H. (2005). Overview of the visual system of tarsius. *The Anatomical Record Part A: Discoveries in Molecular, Cellular, and Evolutionary Biology*, *287A*(1), 1013–1025. https://doi.org/10.1002/ar.a.20263

Collins, F. S. (2011). Reengineering Translational Science: The Time Is Right. *Science Translational Medicine*, *3*(90), 90cm17-90cm17. https://doi.org/10.1126/scitranslmed.3002747

Costa, J. T. (2023). *Radical by Nature: The Revolutionary Life of Alfred Russel Wallace*. Princeton University Press.

Cox, D. T. C., & Gaston, K. J. (2024). Cathemerality: A key temporal niche. *Biological Reviews*, *99*(2), 329–347. https://doi.org/10.1111/brv.13024

Cunningham, E. P., Edmonds, D., Stalter, L., & Janal, M. N. (2021). Ring-tailed lemurs (Lemur catta) use olfaction to locate distant fruit. *American Journal of Physical Anthropology*, *175*(1), 300–307. https://doi.org/10.1002/ajpa.24255

Curtis, D. J., Zaramody, A., & Martin, R. D. (1999). Cathemerality in the mongoose lemur, Eulemur mongoz. *American Journal of Primatology*, *47*(4), 279–298.

https://doi.org/10.1002/(SICI)1098-2345(1999)47:4%253C279::AID-AJP2%253E3.0.CO;2-U

Dawson, G. R., & Tricklebank, M. D. (1995). Use of the elevated plus maze in the search for novel anxiolytic agents. *Trends in Pharmacological Sciences*, *16*(2), 33–36. https://doi.org/10.1016/S0165-6147(00)88973-7

Dominoni, D. M., Halfwerk, W., Baird, E., Buxton, R. T., Fernández-Juricic, E., Fristrup, K. M., McKenna, M. F., Mennitt, D. J., Perkin, E. K., Seymoure, B. M., Stoner, D. C., Tennessen, J. B., Toth, C. A., Tyrrell, L. P., Wilson, A., Francis, C. D., Carter, N. H., & Barber, J. R. (2020). Why conservation biology can benefit from sensory ecology. *Nature Ecology & Evolution*, *4*(4), 502–511. https://doi.org/10.1038/s41559-020-1135-4

Donati, G., Santini, L., Razafindramanana, J., Boitani, L., & Borgognini-Tarli, S. (2013). (Un-)expected nocturnal activity in "Diurnal" Lemur catta supports cathemerality as one of the key adaptations of the lemurid radiation. *American Journal of Physical Anthropology*, *150*(1), 99–106. https://doi.org/10.1002/ajpa.22180

Drea, C. M., Goodwin, T. E., & delBarco-Trillo, J. (2019). P-Mail: The Information Highway of Nocturnal, but Not Diurnal or Cathemeral, Strepsirrhines. *Folia Primatologica*, *90*(5), 422–438. https://doi.org/10.1159/000495076

Eichert, N., Papp, D., Mars, R. B., & Watkins, K. E. (2020). Mapping Human Laryngeal Motor Cortex during Vocalization. *Cerebral Cortex*, *30*(12), 6254–6269. https://doi.org/10.1093/cercor/bhaa182

Eisthen, H. L. (1992). Phylogeny of the vomeronasal system and of receptor cell types in the olfactory and vomeronasal epithelia of vertebrates. *Microscopy Research and Technique*, *23*(1), 1–21. https://doi.org/10.1002/jemt.1070230102

Enoch, J., McDonald, L., Jones, L., Jones, P. R., & Crabb, D. P. (2019). Evaluating Whether Sight Is the Most Valued Sense. *JAMA Ophthalmology*, *137*(11), 1317–1320. https://doi.org/10.1001/jamaophthalmol.2019.3537

Fleagle, J. G. (2000). The century of the past: One hundred years in the study of primate evolution. *Evolutionary Anthropology: Issues, News, and Reviews*, *9*(2), 87–100. https://doi.org/10.1002/(SICI)1520-6505(2000)9:2%253C87::AID-EVAN3%253E3.0.CO;2-N

Fleagle, J. G. (2013). *Primate Adaptation and Evolution*. Academic Press.

Fleagle, J. G., & Seiffert, E. R. (2020). Chapter 20—The Phylogeny of Primates. In J. H. Kaas (Ed.), *Evolutionary Neuroscience (Second Edition)* (pp. 483–518). Academic Press. https://doi.org/10.1016/B978-0-12-820584-6.00020-9

García-Moreno, F., & Molnár, Z. (2020). Chapter 25—The impact of different modes of neuronal migration on brain evolution. In J. Rubenstein, P. Rakic, B. Chen, K. Y. Kwan, A. Kolodkin, & E. Anton (Eds), *Cellular Migration and Formation of Axons and Dendrites (Second Edition)* (pp. 555–576). Academic Press. https://doi.org/10.1016/B978-0-12-814407-7.00025-0

Gattani, A., Khurade, K., Tripathi, R., Seetharaman, R., & Jalgaonkar, S. (2025). A Comprehensive Analysis of Use of Small Laboratory Animals in Preclinical Research: A Five-Year Quantitative Descriptive Analysis. *Journal of Pharmacology and Pharmacotherapeutics*, *16*(2), 193–201. https://doi.org/10.1177/0976500X241299162

Geerts, H. (2009). Of Mice and Men. *CNS Drugs*, *23*(11), 915–926. https://doi.org/10.2165/11310890-000000000-00000

Geiger, M., Evin, A., Sánchez-Villagra, M. R., Gascho, D., Mainini, C., & Zollikofer, C. P. E. (2017). Neomorphosis and heterochrony of skull shape in dog domestication. *Scientific Reports*, *7*(1), 13443. https://doi.org/10.1038/s41598-017-12582-2

Gilad, Y., Wiebe, V., Przeworski, M., Lancet, D., & Pääbo, S. (2004). Loss of Olfactory Receptor Genes Coincides with the Acquisition of Full Trichromatic Vision in Primates. *PLOS Biology*, *2*(1), e5. https://doi.org/10.1371/journal.pbio.0020005

Gilad, Y., Wiebe, V., Przeworski, M., Lancet, D., & Pääbo, S. (2007). Correction: Loss of Olfactory Receptor Genes Coincides with the Acquisition of Full Trichromatic Vision in Primates. *PLOS Biology*, *5*(6), e148. https://doi.org/10.1371/journal.pbio.0050148

Glud, A. N., Zaer, H., Orlowski, D., Nielsen, M. S., Sørensen, J. C. H., & Bjarkam, C. R. (2024). Anatomy and connectivity of the Göttingen minipig subgenual cortex (Brodmann area 25 homologue). *Brain Structure and Function*, *229*(8), 1995–2010. https://doi.org/10.1007/s00429-024-02855-8

Goodale, M. A., & Milner, A. D. (1992). Separate visual pathways for perception and action. *Trends in Neurosciences*, *15*(1), 20–25. https://doi.org/10.1016/0166-2236(92)90344-8

Gudger, E. W. (1934). The Five Great Naturalists of the Sixteenth Century: Belon, Rondelet, Salviani, Gesner and Aldrovandi: A Chapter in the History of Ichthyology. *Isis*, *22*(1), 21–40. https://doi.org/10.1086/346870

Haesler, S., Rochefort, C., Georgi, B., Licznerski, P., Osten, P., & Scharff, C. (2007). Incomplete and Inaccurate Vocal Imitation after Knockdown of FoxP2 in Songbird Basal Ganglia Nucleus Area X. *PLOS Biology*, *5*(12), e321. https://doi.org/10.1371/journal.pbio.0050321

Heritage, S. (2014). Modeling Olfactory Bulb Evolution through Primate Phylogeny. *PLOS ONE*, *9*(11), e113904. https://doi.org/10.1371/journal.pone.0113904

Hickok, G., Venezia, J., & Teghipco, A. (2023). Beyond Broca: Neural architecture and evolution of a dual motor speech coordination system. *Brain*, *146*(5), 1775–1790. https://doi.org/10.1093/brain/awac454

Hoffman, D. D. (1998). *Visual Intelligence: How We Create what We See* (1st edn). W.W. Norton.

Home Office. (2024). *Statistics of scientific procedures on living animals, Great Britain: 2023* [Accredited official statistics]. United Kingdom of Great Britain and Northern Ireland. https://www.gov.uk/government/statistics/statistics-of-scientific-procedures-on-living-animals-great-britain-2023

Howarth, C. J., Wilson, J. M., Adamson, A. P., Wilson, M. E., & Boase, M. J. (1986). Population Ecology of the Ring-Tailed Lemur, Lemur catta, and the White Sifaka, Propithecus verreauxi verreauxi, at Berenty, Madagascar, 1981. *Folia Primatologica*, *47*(1), 39–48. https://doi.org/10.1159/000156262

Howes, D. (2010). *Sensual Relations: Engaging the Senses in Culture and Social Theory*. University of Michigan Press.

Huang, S., Zhang, T., Dong, C., Shi, Y., Peng, Y., Liu, X., Li, K., Wang, Q., He, Y., Xiao, F., Tian, X., Xian, J., Zhang, C., Wu, Q., Zou, Y., Li, L., Liu, B., Wang, X., & Li, A. (2025). *TransBrain: A computational framework for translating brain-*

wide phenotypes between humans and mice (p. 2025.01.27.635016). bioRxiv. https://doi.org/10.1101/2025.01.27.635016

Hutmacher, F. (2019). Why Is There So Much More Research on Vision Than on Any Other Sensory Modality? *Frontiers in Psychology*, *10*. https://doi.org/10.3389/fpsyg.2019.02246

Ings, S. (2008). *A Natural History of Seeing: The Art and Science of Vision*. W. W. Norton & Company.

Insel, T. R. (2007). From Animal Models to Model Animals. *Biological Psychiatry*, *62*(12), 1337–1339. https://doi.org/10.1016/j.biopsych.2007.10.001

Institute of Medicine, & National Research Council. (1988). *Use of Laboratory Animals in Biomedical and Behavioral Research*. The National Academies Press. https://doi.org/10.17226/1098

Jaroszynski, C., Amer, M., Beauchamp, A., Lerch, J. P., Sotiropoulos, S. N., & Mars, R. B. (2025). *Translating brain anatomy and neurodegenerative disease from mouse to human through latent gene expression space* (p. 2025.03.31.646307). bioRxiv. https://doi.org/10.1101/2025.03.31.646307

Jay, M. (2011). In the Realm of the Senses: An Introduction. *The American Historical Review*, *116*(2), 307–315.

Jolly, A. (with Internet Archive). (1966). *Lemur behavior: A Madagascar field study*. University of Chicago Press. http://archive.org/details/lemurbehaviormad0000joll_c5k6

Jordan, A., & Glauser, D. A. (2023). Distinct clusters of human pain gene orthologs in Caenorhabditis elegans regulate thermo-nociceptive sensitivity and plasticity. *Genetics*, *224*(1), iyad047. https://doi.org/10.1093/genetics/iyad047

Kaas, J. H. (2012). Chapter 5—The evolution of neocortex in primates. In M. A. Hofman & D. Falk (Eds), *Progress in Brain Research* (Vol. 195, pp. 91–102). Elsevier. https://doi.org/10.1016/B978-0-444-53860-4.00005-2

Kaas, J. H., Qi, H.-X., & Stepniewska, I. (2021). Escaping the nocturnal bottleneck, and the evolution of the dorsal and ventral streams of visual processing in primates. *Philosophical Transactions of the Royal Society B: Biological Sciences*, *377*(1844), 20210293. https://doi.org/10.1098/rstb.2021.0293

Kaplan, A. (1964). *The conduct of inquiry*. Transaction Publishers.

Kay, R. F., & Kirk, E. C. (2000). Osteological evidence for the evolution of activity pattern and visual acuity in primates. *American Journal of Physical Anthropology*, *113*(2), 235–262. https://doi.org/10.1002/1096-8644(200010)113:2%253C235::AID-AJPA7%253E3.0.CO;2-9

Keifer, J., & Summers, C. H. (2016). Putting the "Biology" Back into "Neurobiology": The Strength of Diversity in Animal Model Systems for Neuroscience Research. *Frontiers in Systems Neuroscience*, *10*. https://doi.org/10.3389/fnsys.2016.00069

Kirk, E. C. (2006). Eye Morphology in Cathemeral Lemurids and Other Mammals. *Folia Primatologica*, *77*(1–2), 27–49. https://doi.org/10.1159/000089694

Konopka, G., & Roberts, T. F. (2016). Animal Models of Speech and Vocal Communication Deficits Associated With Psychiatric Disorders. *Biological Psychiatry*, *79*(1), 53–61. https://doi.org/10.1016/j.biopsych.2015.07.001

Kravitz, D. J., Saleem, K. S., Baker, C. I., Ungerleider, L. G., & Mishkin, M. (2013). The ventral visual pathway: An expanded neural framework for the processing

of object quality. *Trends in Cognitive Sciences*, *17*(1), 26–49. https://doi.org/10.1016/j.tics.2012.10.011

LaFleur, M., Sauther, M., Cuozzo, F., Yamashita, N., Jacky Youssouf, I. A., & Bender, R. (2014). Cathemerality in wild ring-tailed lemurs (Lemur catta) in the spiny forest of Tsimanampetsotsa National Park: Camera trap data and preliminary behavioral observations. *Primates*, *55*(2), 207–217. https://doi.org/10.1007/s10329-013-0391-1

Loewa, A., Feng, J. J., & Hedtrich, S. (2023). Human disease models in drug development. *Nature Reviews Bioengineering*, *1*(8), 545–559. https://doi.org/10.1038/s44222-023-00063-3

Marder, E. (2002). Non-mammalian models for studying neural development and function. *Nature*, *417*(6886), 318–321. https://doi.org/10.1038/417318a

Mars, R. B., Jbabdi, S., & Rushworth, M. F. S. (2021). A Common Space Approach to Comparative Neuroscience. *Annual Review of Neuroscience*, *44*(1), 69–86. https://doi.org/10.1146/annurev-neuro-100220-025942

Mars, R. B., & Palomero-Gallagher, N. (2024). Towards multi-modal, multi-species brain atlases: Part two. *Brain Structure and Function*, *229*(8), 1769–1772. https://doi.org/10.1007/s00429-024-02858-5

Mars, R. B., Passingham, R. E., & Jbabdi, S. (2018). Connectivity Fingerprints: From Areal Descriptions to Abstract Spaces. *Trends in Cognitive Sciences*, *22*(11), 1026–1037. https://doi.org/10.1016/j.tics.2018.08.009

Martin, R. D. (2004). Chinese lantern for early primates. *Nature*, *427*(6969), 22–23. https://doi.org/10.1038/427022a

Matsui, A., Go, Y., & Niimura, Y. (2010). Degeneration of Olfactory Receptor Gene Repertories in Primates: No Direct Link to Full Trichromatic Vision. *Molecular Biology and Evolution*, *27*(5), 1192–1200. https://doi.org/10.1093/molbev/msq003

Melin, A. D., Matsushita, Y., Moritz, G. L., Dominy, N. J., & Kawamura, S. (2013). Inferred L/M cone opsin polymorphism of ancestral tarsiers sheds dim light on the origin of anthropoid primates. *Proceedings of the Royal Society B: Biological Sciences*, *280*(1759), 20130189. https://doi.org/10.1098/rspb.2013.0189

Miller, M., & Clark, A. (2018). Happily entangled: Prediction, emotion, and the embodied mind. *Synthese*, *195*(6), 2559–2575. https://doi.org/10.1007/s11229-017-1399-7

Mohammadi, A., Byrne Rodgers, J., Kotera, I., & Ryu, W. S. (2013). Behavioral response of Caenorhabditis elegansto localized thermal stimuli. *BMC Neuroscience*, *14*(1), 66. https://doi.org/10.1186/1471-2202-14-66

Molnár, Z. (2021). Zoltán Molnár: The developing brain. In T. L. Horváth, J. Hirsch, & Z. Molnár (Eds), *Body, Brain, Behavior: Three Views and a Conversation* (1st edn, pp. 1–66). Academic Press. https://doi.org/10.1016/B978-0-12-818093-8.00005-7

Moran, D., Softley, R., & Warrant, E. J. (2015). The energetic cost of vision and the evolution of eyeless Mexican cavefish. *Science Advances*, *1*(8), e1500363. https://doi.org/10.1126/sciadv.1500363

Nectow, A. R., & Nestler, E. J. (2020). Viral tools for neuroscience. *Nature Reviews Neuroscience*, *21*(12), 669–681. https://doi.org/10.1038/s41583-020-00382-z

Nekaris, A., & Bearder, S. K. (2011). The Lorisiform Primates of Asia and Mainland Africa. In *Primates in Perspective* (2nd edn, pp. 34–54). Oxford University Press.

Ong, W.-Y., Stohler, C. S., & Herr, D. R. (2019). Role of the Prefrontal Cortex in Pain Processing. *Molecular Neurobiology*, *56*(2), 1137–1166. https://doi.org/10.1007/s12035-018-1130-9

Parga, J. A. (2011). Nocturnal ranging by a diurnal primate: Are ring-tailed lemurs (Lemur catta) cathemeral? *Primates*, *52*(3), 201–205. https://doi.org/10.1007/s10329-011-0257-3

Parry, L., & Pisani, D. (2016). Cambrian Explosion: A Molecular Paleobiological Overview. In R. M. Kliman (Ed.), *Encyclopedia of Evolutionary Biology* (pp. 246–253). Academic Press. https://doi.org/10.1016/B978-0-12-800049-6.00271-7

Passingham, R. E. (2008). *What is special about the human brain?* Oxford university press.

Passingham, R. E., Stephan, K. E., & Kötter, R. (2002). The anatomical basis of functional localization in the cortex. *Nature Reviews Neuroscience*, *3*(8), 606–616. https://doi.org/10.1038/nrn893

Poncelet, G., & Shimeld, S. M. (2020). The evolutionary origins of the vertebrate olfactory system. *Open Biology*, *10*(12), 200330. https://doi.org/10.1098/rsob.200330

Prescott, M. J., & Poirier, C. (2021). The role of MRI in applying the 3Rs to non-human primate neuroscience. *NeuroImage*, *225*, 117521. https://doi.org/10.1016/j.neuroimage.2020.117521

Proulx, M. J. (2014). The perception of shape from shading in a new light. *PeerJ*, *2*, e363. https://doi.org/10.7717/peerj.363

Ramirez, M. D., Pairett, A. N., Pankey, M. S., Serb, J. M., Speiser, D. I., Swafford, A. J., & Oakley, T. H. (2016). The Last Common Ancestor of Most Bilaterian Animals Possessed at Least Nine Opsins. *Genome Biology and Evolution*, *8*(12), 3640–3652. https://doi.org/10.1093/gbe/evw248

Rizzolatti, G., & Matelli, M. (2003). Two different streams form the dorsal visual system: Anatomy and functions. *Experimental Brain Research*, *153*(2), 146–157. https://doi.org/10.1007/s00221-003-1588-0

Rodrigues, F. R. (2013). *Comparison of Brain and Cranial Nerve Morphology Between Eyed Surface Fish and Blind Cave Fish of Species Astyanax Mexicanus* [M.Sc., Universidade de Lisboa (Portugal)]. https://www.proquest.com/docview/2724236737/abstract/A45F2F70DD7B495FPQ/1

Schilling, A. (1980). The possible role of urine in territoriality of some nocturnal prosimians. *Symposia of the Zoological Society of London*, *45*, 165–193.

Schulz, S. B., Haesler, S., Scharff, C., & Rochefort, C. (2010). Knockdown of FoxP2 alters spine density in Area X of the zebra finch. *Genes, Brain and Behavior*, *9*(7), 732–740. https://doi.org/10.1111/j.1601-183X.2010.00607.x

Scott, A. W., Bressler, N. M., Ffolkes, S., Wittenborn, J. S., & Jorkasky, J. (2016). Public Attitudes About Eye and Vision Health. *JAMA Ophthalmology*, *134*(10), 1111–1118. https://doi.org/10.1001/jamaophthalmol.2016.2627

Shostak, S. (2024). 'The First Darwinian'. *The European Legacy*, *29*(3–4), 399–405. https://doi.org/10.1080/10848770.2023.2275888

Smith, T. D., Rossie, J. B., & Bhatnagar, K. P. (2007). Evolution of the nose and nasal skeleton in primates. *Evolutionary Anthropology: Issues, News, and Reviews*, *16*(4), 132–146. https://doi.org/10.1002/evan.20143

Svensson, M. S., Nekaris, K. a. i., Bearder, S. K., Bettridge, C. M., Butynski, T. M., Cheyne, S. M., Das, N., de Jong, Y. A., Luhrs, A. M., Luncz, L. V., Maddock, S. T., Perkin, A., Pimley, E., Poindexter, S. A., Reinhardt, K. D., Spaan, D., Stark, D. J., Starr, C. R., & Nijman, V. (2018). Sleep patterns, daytime predation, and the evolution of diurnal sleep site selection in lorisiforms. *American Journal of Physical Anthropology*, *166*(3), 563–577. https://doi.org/10.1002/ajpa.23450

Tendler, B. C., Hanayik, T., Ansorge, O., Bangerter-Christensen, S., Berns, G. S., Bertelsen, M. F., Bryant, K. L., Foxley, S., van den Heuvel, M. P., Howard, A. F., Huszar, I. N., Khrapitchev, A. A., Leonte, A., Manger, P. R., Menke, R. A., Mollink, J., Mortimer, D., Pallebage-Gamarallage, M., Roumazeilles, L., … Miller, K. L. (2022). The Digital Brain Bank, an open access platform for post-mortem imaging datasets. *eLife*, *11*, e73153. https://doi.org/10.7554/eLife.73153

Theofanopoulou, C., Gastaldon, S., O'Rourke, T., Samuels, B. D., Messner, A., Martins, P. T., Delogu, F., Alamri, S., & Boeckx, C. (2017). Self-domestication in Homo sapiens: Insights from comparative genomics. *PLOS ONE*, *12*(10), e0185306. https://doi.org/10.1371/journal.pone.0185306

Thiebaut de Schotten, M., Croxson, P. L., & Mars, R. B. (2019). Large-scale comparative neuroimaging: Where are we and what do we need? *Cortex*, *118*, 188–202. https://doi.org/10.1016/j.cortex.2018.11.028

Torres-Pérez, J. V., Anagianni, S., Mech, A. M., Havelange, W., García-González, J., Fraser, S. E., Vallortigara, G., & Brennan, C. H. (2023). Baz1b loss-of-function in zebrafish produces phenotypic alterations consistent with the domestication syndrome. *iScience*, *26*(1). https://doi.org/10.1016/j.isci.2022.105704

Treede, R.-D., Kenshalo, D. R., Gracely, R. H., & Jones, A. K. P. (1999). The cortical representation of pain. *PAIN*, *79*(2), 105–111. https://doi.org/10.1016/S0304-3959(98)00184-5

van Vliet, J. (2019). Direct and indirect loss of natural area from urban expansion. *Nature Sustainability*, *2*(8), 755–763. https://doi.org/10.1038/s41893-019-0340-0

Wallace, A. R. (2009a). On the Law Which Has Regulated the Introduction of New Species (1855). *Alfred Russel Wallace Classic Writings*. https://digitalcommons.wku.edu/dlps_fac_arw/2

Wallace, A. R. (2009b). On the Monkeys of the Amazon (1852). *Alfred Russel Wallace Classic Writings*, *3*. https://digitalcommons.wku.edu/dlps_fac_arw/3

Wallace, A. R. (2009c). On the Tendency of Varieties to Depart Indefinitely From the Original Type (1858). *Alfred Russel Wallace Classic Writings*. https://digitalcommons.wku.edu/dlps_fac_arw/1

Warrington, S., Bryant, K. L., Khrapitchev, A. A., Sallet, J., Charquero-Ballester, M., Douaud, G., Jbabdi, S., Mars, R. B., & Sotiropoulos, S. N. (2020). XTRACT - Standardised protocols for automated tractography in the human and macaque brain. *NeuroImage*, *217*, 116923. https://doi.org/10.1016/j.neuroimage.2020.116923

Watson, K. K., & Platt, M. L. (2012). Of mice and monkeys: Using non-human primate models to bridge mouse- and human-based investigations of autism spectrum disorders. *Journal of Neurodevelopmental Disorders*, *4*(1), 21. https://doi.org/10.1186/1866-1955-4-21

Whiting, B. A., & Barton, R. A. (2003). The evolution of the cortico-cerebellar complex in primates: Anatomical connections predict patterns of correlated evolution. *Journal of Human Evolution*, *44*(1), 3–10. https://doi.org/10.1016/S0047-2484(02)00162-8

Wrangham, R. W. (2019). Hypotheses for the evolution of reduced reactive aggression in the context of human self-domestication. *Frontiers in Psychology*, *10*, 1914.

Xiao, L., Merullo, D. P., Koch, T. M. I., Cao, M., Co, M., Kulkarni, A., Konopka, G., & Roberts, T. F. (2021). Expression of FoxP2 in the basal ganglia regulates vocal motor sequences in the adult songbird. *Nature Communications*, *12*(1), 2617. https://doi.org/10.1038/s41467-021-22918-2

Xie, Y., Huo, F., & Tang, J. (2009). Cerebral cortex modulation of pain. *Acta Pharmacologica Sinica*, *30*(1), 31–41. https://doi.org/10.1038/aps.2008.14

Yaden, D. B., & Anderson, D. E. (2021). The psychology of philosophy: Associating philosophical views with psychological traits in professional philosophers. *Philosophical Psychology*, *34*(5), 721–755. https://doi.org/10.1080/09515089.2021.1915972

Zanella, M., Vitriolo, A., Andirko, A., Martins, P. T., Sturm, S., O'Rourke, T., Laugsch, M., Malerba, N., Skaros, A., Trattaro, S., Germain, P.-L., Mihailovic, M., Merla, G., Rada-Iglesias, A., Boeckx, C., & Testa, G. (2019). Dosage analysis of the

7q11.23 Williams region identifies BAZ1B as a major human gene patterning the modern human face and underlying self-domestication. *Science Advances*, *5*(12), eaaw7908. https://doi.org/10.1126/sciadv.aaw7908

Chapter 2

Neuroethology and retinal waves.

Declarations

Publication history

Parts of this chapter have previously been published in the following manuscript, distributed under the terms of the Creative Commons Attribution-NonCommercial 4.0 International (CC BY-NC 4.0) license.

Hunt, J. E., Pratt, K. G., & Molnár, Z. (2024). Ocular Necessities: A Neuroethological Perspective on Vertebrate Visual Development. *Brain Behavior and Evolution*, *99*(2), 96-108. doi:10.1159/000536035

Contribution statement

JEH drafted all of the text and produced tables and figures which appear in this chapter. Mr. Erick Fernandez de Arteaga contributed to the production of Figure 2. KGP and ZM assisted in editing the manuscript and designing figures.

Acknowledgements

JEH would like to thank the attendees of the 2nd Meeting on Spontaneous Activity in Brain Development for their invaluable feedback on an earlier version of this work. We are indebted to Mr. Caio César Santos Santana for helpful comments on Figure 1 and Mr. Erick Fernandez de Arteaga for the production of Figure 2. We would additionally like to thank Mr. John R. Bruno, Dr. Uwemedimo G. Udoh, and members of the Cognitive Neuroecology Lab for valuable discussions which contributed to the drafting of this chapter.

Abstract

By examining species-specific innate behaviours, neuroethologists have characterised unique neural strategies and specializations from throughout the animal kingdom. Simultaneously, the field of evolutionary developmental biology (informally, “evo-devo”) seeks to make inferences about animals’ evolutionary histories through careful comparison of developmental processes between species, because evolution is the evolution of development. Yet despite the shared focus on cross-species comparisons, there is surprisingly little cross-talk between these two fields.

To bridge that gap, this chapter applies a neuroethological lens to the study of retinal waves, a form of spontaneous activity in visual development. First, literature on retinal waves is synthesised to describe the phylogenetic distribution of the phenomenon. Then, the current leading theory of the evolutionary origin of retinal waves is critically evaluated. A novel theory accounting for the evolution of spontaneous retinal waves is then proposed.

We find that ethological considerations explain some cross-species differences in the dynamics of retinal waves. In zebrafish, retinal waves may be more important for the development of the retina itself, rather than the retinofugal projections. Based on the species in which retinal waves have been described and the phylogenetic position of zebrafish, it is highly likely that retinal waves are preset in *Xenopus laevis* and play a role in the early development of the retina.

1. Introduction: Behaviour, evolution, and development

A major and longstanding mission for the field of neuroscience is the linking of nervous structure to behavioural function. This aim motivated even the earliest neuroscience experiments, as when Luigi Galvani reported in the late-18th century that electrically stimulating the nerves of a frog was sufficient to make its legs twitch (Galvani, 1791). In more recent years, methodological innovations have enabled fine-grained manipulation of neuronal states to an unprecedented extent. One might think these advances afford neuroscientists ever greater confidence to infer causal relationships between brain states and behaviours, yet paradoxically, as neuroscience tends towards ever-greater reductionism in its models and philosophies, behaviour itself often takes a back seat in the study of its causes.

This notion is compellingly argued by Krakauer and colleagues in their influential 2017 article, “Neuroscience needs behavior: correcting a reductionist bias”. The neural implementation of a behaviour, Krakauer et al. (2017) assert, is best probed only after the careful decomposition and analysis of the behaviour itself. Yet where behaviour was once so often at the centre of neuroscience, it has now lost its role of primacy. The de-emphasis on behaviour has contributed to a seemingly insurmountable gap between neuroethologists, who prioritise the naturalistic behaviours of the animals they study, and mainstream neurophysiologists, who tend towards reductionistic views of animal behaviour and its substrates. Yet this gap should not exist. As Jenny Read remarks with beautiful succinctness: “Evolutionarily, all that is required is useful behaviour” (Read, 2022). To understand evolution, we must understand behaviour. Furthermore, the rich world of animal behaviour is

valuable to all sorts of neurophysiologists – even those who may not consider themselves to be working on questions of evolution.

To demonstrate this, we take as an example the neuroscience of vision. Many vertebrates and invertebrates rely on visual cues to navigate and interact with their environments. Thus, the visual system presents a fantastic window into how ecological pressures have shaped different animals' behaviours and their developmental strategies. We turn our attention specifically to the *development* of the visual system, including the retina and its downstream targets in the brain, because evolution is the evolution of development (García-Moreno & Molnár, 2020; Horváth et al., 2022). Evolution must act on the developing organism, because adult animals do not transform into other adult animals. As such, to study how visual systems have evolved, we must study the development of visual systems across species.

In the field of visual development, a great deal of research has gone into the phenomenon of spontaneous retinal waves, which are bursts of action potentials that propagate across the retina early in development absent from any external sensory input. Spontaneous activity, including spontaneous retinal waves, is known to serve a variety of functions in early development, including the establishment of neuronal circuits that shall enable sensory processing later in life. In this theoretical chapter, we look particularly at retinal waves as one type of spontaneous activity in central nervous system (CNS) development known to guide the development of the visual system. Despite the importance of spontaneous retinal waves, little work has characterised inter-species differences in the presence or function of retinal waves, let alone considered how retinal waves relate to an animal's lifestyle. Implementing a neuroethological perspective, we develop a new theory of retinal waves across the

vertebrate lineage, demonstrating the value of neuroethology for understanding development and evolution.

2. Retinal waves: A neuroethological perspective

Early in development, in some species, bursts of action potentials spontaneously initiate and travel across the retina in a wave-like fashion. These spontaneous, correlated action potentials, termed “retinal waves”, are known to play an important role in several processes of mammalian visual development, such as regulating the formation of gap junctions between retinal ganglion cells (RGCs) (Arroyo et al., 2016); modulating inter-retinal coordinated activity (Failor et al., 2018); influencing the receptive fields of neurons in visual cortex, superior colliculus, and lateral geniculate nucleus (reviewed in Thompson et al., 2017); and guiding refinement of retinotopic maps (Huberman et al., 2008; Murcia-Belmonte et al., 2019). Despite their profound importance for mammalian visual development, and despite the early seminal work on spontaneous retinal activity carried out in turtles – first, with multiunit electrophysiological recordings (Sernagor & Grzywacz, 1999; Sernagor & Mehta, 2001), then with the direct observation of waves via calcium imaging (Sernagor et al., 2003) – few researchers have systematically addressed the presence and function of spontaneous retinal waves in the non-mammalian vertebrate lineage.

2.1. How widespread are retinal waves?

Since their first observation in rats, spontaneous retinal waves have been studied in the development of a variety of species, including mice, ferrets, cats, rabbits, non-human primates, chicks, turtles, and zebrafish (Figure 2.1; Table 2.1). These species comprise a moderate diversity of the vertebrate family tree, demonstrating the presence of retinal waves across myriad mammalian species as well as two species of sauropsids (the chick and the turtle), and most recently, a ray-finned fish (the zebrafish).

Notably, studies have failed to observe spontaneous retinal waves in two species: the fruit fly (*Drosophila melanogaster*) (Akin et al., 2019; Hiesinger et al., 2006) and the African clawed frog (*Xenopus laevis*) (Demas et al., 2012). First, we will consider the fruit fly. Spontaneous activity serves a role in the development of the *Drosophila* visual system (Akin et al., 2019; Choi et al., 2021), though this activity likely originates in the brain rather than the retina, as it is described even in mutants whose retinal function has been abolished (Akin et al., 2019). It seems likely, then, that retinal waves are a uniquely vertebrate phenomenon, though outstanding questions remain about the role and character of spontaneous activity in invertebrate CNS development.

Next, we will consider *Xenopus laevis*, the African clawed frog. Within the vertebrate lineage, it was theorised prior to the observation of retinal waves in zebrafish that retinal waves occur exclusively in amniotes (i.e., animals that develop with an amnion – mammals, birds, and reptiles) (Ackman & Crair, 2014; Kutsarova et al., 2017; Pratt et al., 2016). Retinal waves had been documented in a diversity of amniotic species and were believed to be absent in *Xenopus laevis* – an anamniote –

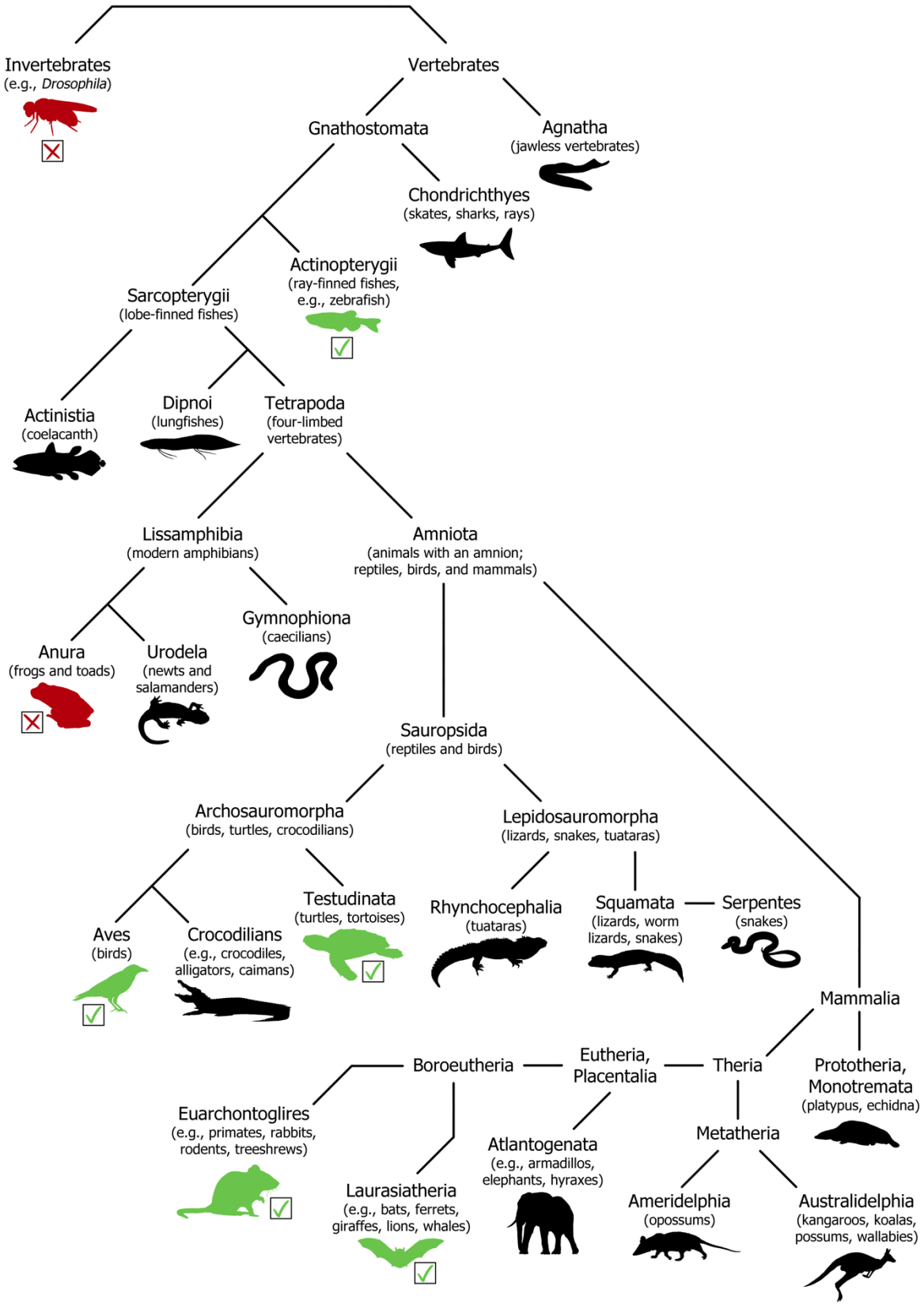


Figure 2.1. Cladogram depicting the study of spontaneous retinal waves. *A green silhouette and check mark indicate retinal waves have been observed in this phylogenetic group. A red silhouette and cross indicate that observations have failed to detect retinal waves in this group. This figure represents the current phylogenetic diversity of retinal wave research, to date.*

Species	Taxonomic group	Retinal waves?	Age at which retinal waves studied	Method	Foundational Citation(s)
Macaque (*Macaca fascicularis*)	Primates	Yes	Embryonic days 60-76	Multielectrode arrays on isolated retinae	Warland et al. (2006)
Rabbit (*Oryctolagus cuniculus*)	Lagomorpha	Yes	Postnatal days 0-6	Whole-cell patch clamp on isolated retinae	Zhou (1998)
Mouse (*Mus musculus*)	Rodentia	Yes	Postnatal days 0-4	Refers to unpublished data from isolated mice retinae	Mooney et al. (1996)
Rat (*Rattus norvegicus*)	Rodentia	Yes	Embryonic days 17-21	*In vivo* extracellular unit recordings from retinae	Galli & Maffei (1988)
Ferret (*Mustela furo*)	Carnivora	Yes	Postnatal days 5-21	Multielectrode arrays on isolated retinae	Meister et al. (1991)
Cat (*Felis catus*)	Carnivora	Yes	Embryonic day 52; postnatal day 1	Multielectrode arrays on isolated retinae	Meister et al. (1991)
Chick (*Gallus gallus*)	Galliformes	Yes	Embryonic days 6-11	Calcium imaging on isolated retinae	Catsicas et al. (1998)
Turtle (*Trachemys scripta elegans*)	Testudines	Yes	Stage 22 (approx. 3 weeks to hatching) – stage 26 (time of hatching)	*In vivo* extracellular unit recordings from retinae (1995) Calcium imaging on isolated retinae (2003)	Sernagor & Grzywacz (1995) Sernagor et al. (2003)
Frog (*Xenopus laevis*)	Anura	No	Retinal waves not found from stage 39 (approx. 2.5 days post-fertilization; dpf) to stage 60 (approx. 46 dpf)	Multielectrode arrays on isolated retinae	Demas et al. (2012)
Zebrafish (*Danio rero*)	Cypriniformes	Yes	2.5 – 3.5 days post-fertilization	*In vivo* two-photon calcium imaging; whole-cell patch clamp recording	Zhang et al. (2016)
Fruit fly (*Drosophila melanogaster*)	Diptera	No	Retinal waves not found from 40 hours after puparium formation (hAPF) – adulthood	*In vivo* two-photon calcium, voltage, and glutamate imaging	Akin et al. (2019)

Table 2.1. Summary of retinal wave studies. Species: common and binomial scientific name. Taxonomic clade: phylogenetic order of the species. Retinal waves observed*: Indication of whether retinal waves have been observed in this species.* Age at which retinal waves studied*: The developmental time points at which retinal waves were studied in the foundational studies.* Method*: The method used to study retinal waves in the foundational citation(s).* Foundational Citation*: Exemplary, seminal literature regarding the observation or failure to observe spontaneous retinal activity in this species.*

---

supporting a theory that amniotes evolved retinal waves as a strategy to achieve visual system refinement whilst relatively deprived of visual stimuli, as would be the case *in ovo* or *in utero* (Kutsarova et al., 2017; Pratt et al., 2016). However, the observation of retinal waves in zebrafish (Zhang et al., 2016, 2019) now offers compelling justification to revisit this apparent demarcation between amniotes and anamniotes. If retinal waves are present in zebrafish, why might they be absent in *Xenopus*? Furthermore, can the environment and ecological niche of the developing zebrafish shed light upon a possible divergence in retinal wave function within the vertebrate tree?

2.2. The ethological role of retinal waves

Within both mammals and zebrafish, retinal waves have a known tendency to progress temporally-to-nasally (Figure 2.2A) (Ackman et al., 2012; Elstrott & Feller, 2010; Stafford et al., 2009; Zhang et al., 2016). This temporal-to-nasal bias makes sense only in light of ethological considerations. The directionality of spontaneous retinal waves corresponds to the optic flow of sensory information across the retina as an animal moves around its environment, such as when a developing tadpole swims

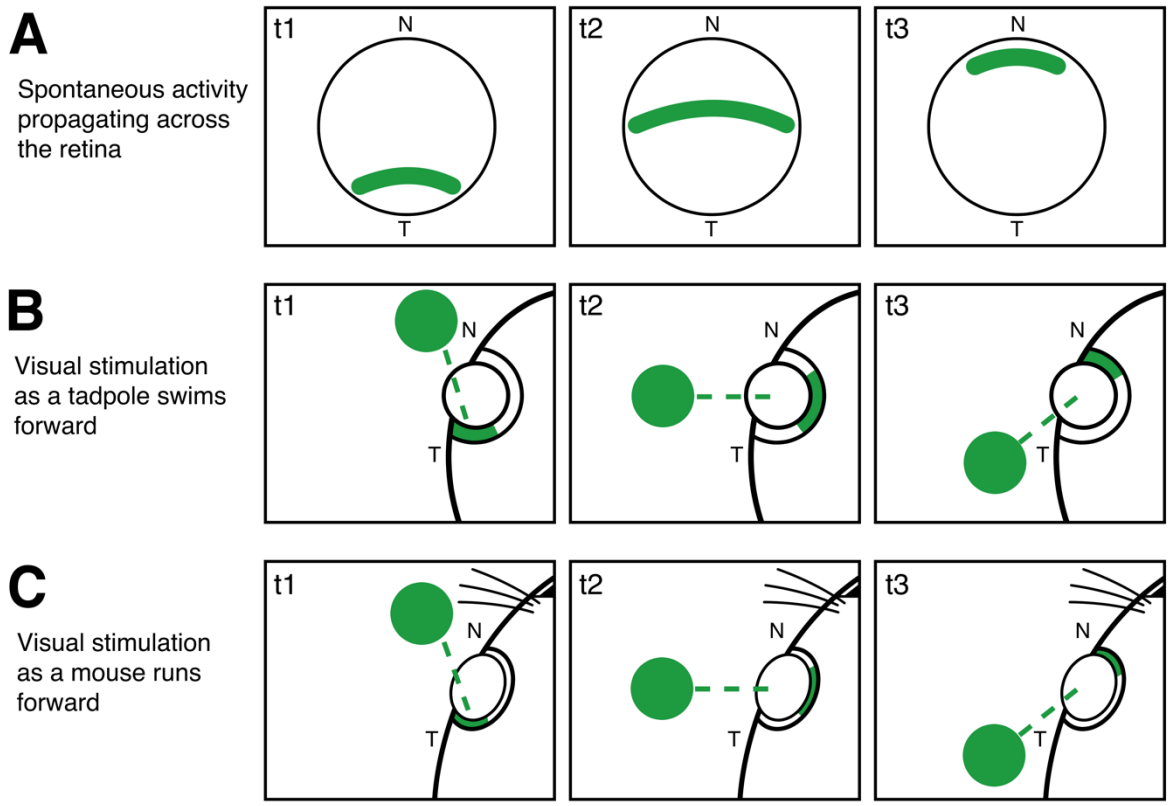


Figure 2.2. Temporal-to-nasal patterned retinal activity. *(A) Spontaneous retinal waves stereotypically propagate from the temporal side of the retina to the nasal side. (B) As a tadpole swims forward, the visual scene stimulates the retina in the same temporal-to-nasal fashion. (C) Similarly, the visual environment stimulates the mouse's retina temporally-to-nasally as the mouse runs forward.*

---

around its environment (Figure 2.2B) or an older mouse navigates on the ground (Figure 2.2C). In each case, patterned retinal activity – whether spontaneous or evoked by light – progresses from the temporal side of the retina first to the nasal side last. In other words, the directionality of spontaneous retinal waves corresponds to the directionality of visually evoked sensory information animals will receive as they navigate their environments.

This is not a coincidence. The nasal-to-temporal optic flow produced by spontaneous retinal waves (Figure 2.2A), swimming forward (Figure 2.2B), and running forward (Figure 2.2C) is important for the development of the visual system.

In a provocative series of experiments, Hiramoto and Cline (2014) find that exposing developmental stage 47 tadpoles to nasal-to-temporal visual stimuli – i.e., opposite to the naturalistic direction of optic flow – results in disrupted refinement of the retinotectal projection. Ge and colleagues (2021) report a strikingly similar phenomenon in mice: manipulating the directionality of retinal waves in newborn mice (postnatal day 8-11) impairs neuronal responses to visual motion in the superior colliculus. In whole, these experiments demonstrate a persistent pattern: the temporal-to-nasal directionality of optic flow is important, playing a key role in the development of a visual system that will meet the needs of an animal navigating its environment primarily through forward locomotion. Behaviour is the key to understanding this pattern: it is only by considering the behaviours of these animals – for instance, the tendency for mice to run forward and tadpoles and fish to swim forward – that the importance of directionality in retinal waves can be understood.

2.3. Retinal waves in the broader context of development

While it has been theorised that amniotes (i.e., mammals, birds, and reptiles) evolved spontaneous retinal waves as a strategy to achieve visual system refinement under conditions of relative visual deprivation (Kutsarova et al., 2017; Pratt et al., 2016), the observation that zebrafish experience spontaneous retinal waves (Zhang et al., 2016) casts doubt upon this theory. Fish, like frogs, are anamniotes (i.e., they do not develop in an amnion); developing in the open water, zebrafish are exposed to naturalistic visual stimuli throughout their development. However, just as the environment of the developing zebrafish differs substantially from that of amniotes, zebrafish retinal waves also seem to differ markedly from those observed in amniotes.

While mammals and reptiles experience distinct types of retinal waves at different time points, spanning weeks of protracted development (Maccione et al., 2014; Sernagor et al., 2003; Tiriac et al., 2018; see also review by Feller & Kerschensteiner, 2020), zebrafish retinal waves appear to be far more homogeneous and occur within a narrow window of 24 hours, from 2.5 – 3.5 days post-fertilisation (Zhang et al., 2016, 2019). In light of these profound differences, a natural question is whether retinal waves serve the same function between these species.

Among other functions, retinal waves in mammals simulate optic flow and guide the refinement of retinotopic maps (Ge et al., 2021; Murcia-Belmonte et al., 2019), thus enabling a high degree of plasticity in mammalian visual development. In contrast, it is possible that spontaneous retinal waves in zebrafish follow a different time course and show distinct dynamics because they do not serve the same functions in zebrafish development. To evaluate this possibility, it is important to consider the broader patterns of visual development in zebrafish and the ecological environment of the developing zebrafish.

The importance of visual experience for the development of the zebrafish visual system has been hotly contested for years (e.g., Avitan et al., 2017; Dixon et al., 2004; Gnuegge et al., 2001; Nevin et al., 2008; Niell & Smith, 2005; Saszik & Bilotta, 2001; Xie et al., 2019). Though it seems beyond debate that visual experience plays *some* role in the development of zebrafish vision, the deficits resulting from early visual deprivation are often subtle.

Of particular note, Niell and Smith (2005) report that dark rearing zebrafish until 84 hours post-fertilisation (i.e., 3.5 days post-fertilisation) produces small deficits in spatial acuity, while receptive field size, topography, and direction

selectivity are wholly spared. The timing of this manipulation corresponds to the timing of spontaneous retinal waves in zebrafish; where spontaneous retinal waves cease at 3.5 days post-fertilisation (Zhang et al., 2016), this is also the stage at which (Niell & Smith, 2005) ended their visual deprivation for zebrafish. Hence, retinal waves are occurring at a time when visual experience doesn't seem to play much of a role in zebrafish visual development. It is important to note that while dark-rearing zebrafish for short periods early in life produces only subtle deficits, longer periods of dark-rearing produce more substantial and behaviourally-relevant visual deficits. For instance, (Avitan et al., 2017) report that dark-rearing zebrafish until 6 days post-fertilisation is sufficient to produce long-lasting deficits in prey-capturing behaviours. Altogether, these experiments indicate that while visual experience plays a role in zebrafish visual development, retinal waves occur at an early time point when visual experience is less important. How does this compare with the timeline of retinal waves in amniotes, like mammals?

Zebrafish develop in open water under a constant threat of predation. Their sensory systems must develop in a rapid and stereotyped fashion, to allow for the quick deployment of sensory-driven behaviours. In contrast, amniotes develop in the relative safety of a womb or protective egg. This relative safety allows for a more protracted and experience-dependent development of sensory systems, including the visual system. Indeed, illustrating the protracted nature of amniotic sensory development, stage I retinal waves – the earliest retinal waves – initiate at around embryonic day 17 in mice, while stage III retinal waves – the final stage of retinal waves – terminate at around the time of eye opening on postnatal day 14 (Maccione et al., 2014; see also reviews by Kerschensteiner, 2016 and Feller & Kerschensteiner,

2020). In contrast, zebrafish retinal waves occur entirely within a 24-hour period from 2.5 – 3.5 days post-fertilisation (Zhang et al., 2016, 2019). The role of retinal waves in mammalian visual development is also far more dynamic and experience-dependent than what has been observed in zebrafish. As discussed in the paragraphs that follow, the characteristics of later retinal waves in mammals are influenced by both internal states (i.e., sleep and wakefulness) and the external environment (i.e., light exposure through the eyelid).

In mice, eye opening typically occurs around postnatal day 14 (Rochefort et al., 2011; Shen & Colonnese, 2016). In the days immediately before eye opening, during which Stage III retinal waves occur (Kerschensteiner, 2016), sudden changes in luminance (e.g., flashes of light) are sufficient to produce responses in visual cortical neurons (Rochefort et al., 2011). While the majority of visual cortical activity is driven by retinal waves at this age (Mukherjee et al., 2017), recent work by Tiriac et al. (2018) has demonstrated that visual stimulation through the eyelid can trigger retinal waves with indistinguishable dynamics to spontaneous retinal waves. Furthermore, retinal waves interact with sleep in the developing mouse; bouts of wakefulness from postnatal days 8-12 dramatically suppress visual cortical activity by suppressing retinal wave-driven activity (Mukherjee et al., 2017). Altogether, the most recent evidence suggests that the dynamics and effects of amniotic retinal waves are experience-dependent, modulated by both external stimuli (i.e., light) and internal states (i.e., wakefulness).

The literature paints a compelling picture: through the extended period during which retinal waves drive refinement within the mammalian visual system, there is a complex interplay between three stages of retinal waves, light exposure, and sleep

over the course of weeks. Zebrafish, in contrast, experience one type of retinal wave from 2.5 – 3.5 days post-fertilisation, at a time when sensory experience plays a lesser role in development of the visual system. Altogether, these studies suggest that very early development of the zebrafish visual system may be less dependent upon visual experience than that of mammals, at least during the developmental stages at which retinal waves are known to occur in each species.

Now, turning our attention to other anamniotic species, it is important to note that the experience-independent nature of early zebrafish visual development parallels the experience-independent development of visually-guided behaviours in the African clawed frog (*Xenopus laevis*). Just as early dark-rearing produces only subtle deficits in zebrafish visual development, in *Xenopus*, dark-rearing does not impede the development of early visually-guided, adaptive behaviours such as colour-guided phototaxis (Bruno et al., 2022; Hunt et al., 2020). Just as dark-rearing zebrafish for longer periods of time produces deficits in prey-capturing behaviours (Avitan et al., 2017), the visually-guided behaviours of older *Xenopus* tadpoles (i.e., stage 43-44 and older; approximately 3.5 – 4 days post-fertilisation) are influenced by visual experience (Bertolesi et al., 2021; Moriya et al., 1996). These similarities in early visual development might be explained, in part, by the similar ecological niches of these animals. Both larval zebrafish and *Xenopus* tadpoles, as aquatic species, develop in the danger of open water with the threat of predation. The environment necessitates a rapid development of sensory and motor systems to adequately respond to this threat. Might the similar ecological niche between zebrafish and tadpoles be reflected in the early development of their sensory systems?

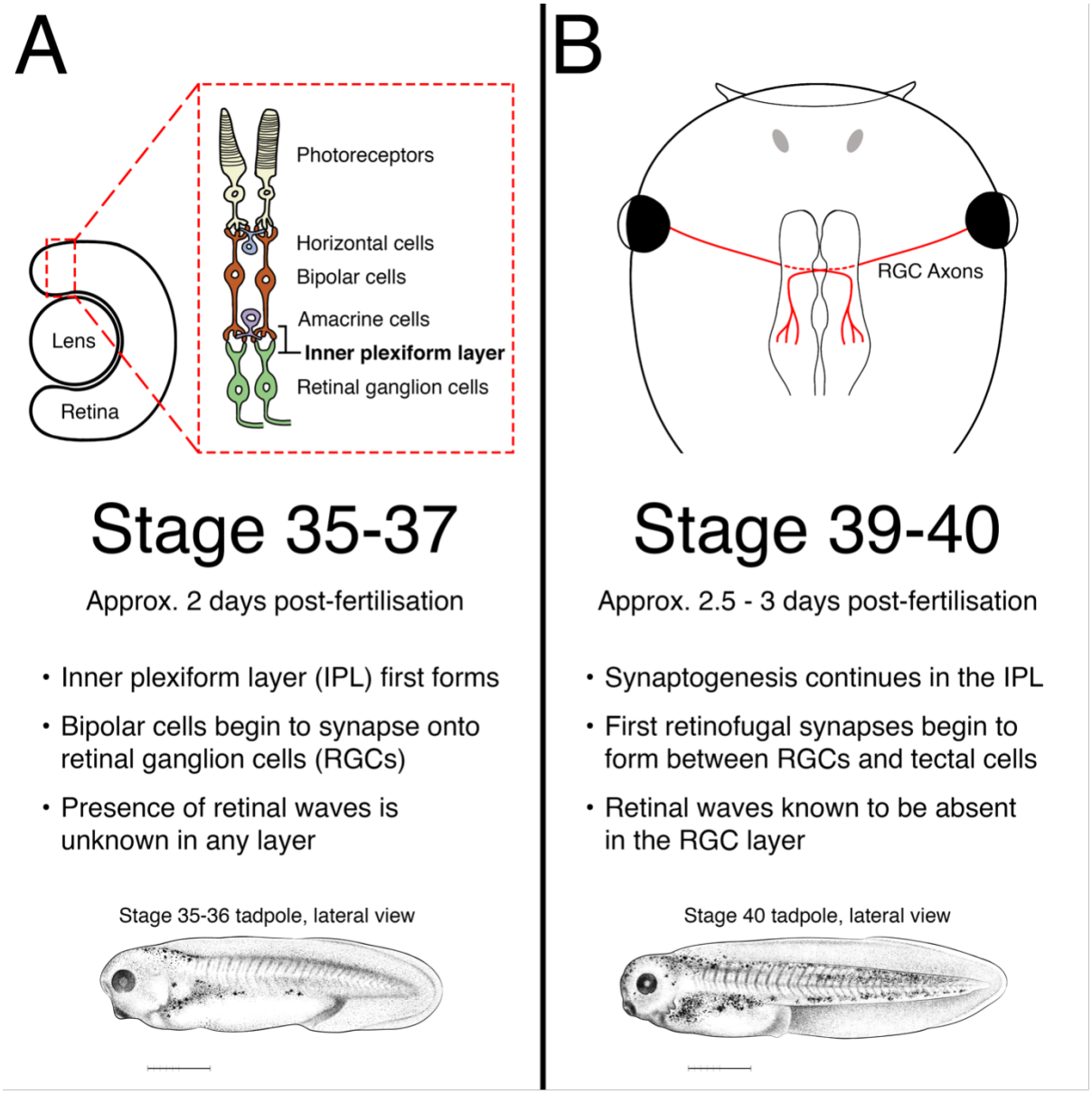


Figure 2.3. Development of the* Xenopus *visual system. *(A) At stage 35-37, approximately two days post-fertilisation, the inner plexiform layer (IPL) first forms. At this time, bipolar cells begin to synapse onto retinal ganglion cells (RGCs). It is unknown whether retinal waves occur in any layer at this stage. Schematic shows the organisation of the* Xenopus *retina, including the IPL. (B) At stage 39-40, approximately 2.5 – 3 days post-fertilisation, synaptogenesis continues in the IPL. The first retinofugal synapses begin to form between RGCs and tectal cells. Retinal waves do not occur in the RGC layer, per experiments reported by Demas et al. (2012).* Xenopus *illustrations, stage 37-38 (panel A, bottom) and 40 (panel B, bottom) © Natalya Zahn (2022), via Xenbase (www.xenbase.org RRID:SCR_003280). Scale bars: 1 mm.*

2.4. Revisiting retinal waves in frogs

While zebrafish are more distantly related to amniotes than amphibians, retinal waves have been observed in zebrafish yet are thought to be absent in amphibians (Figure 2.1). This poses an interesting problem. Were retinal waves a convergent evolution among amniotes and at least some ray-finned fishes? Did a common ancestor exhibit retinal waves, which were subsequently lost in the amphibian lineage? Or do amphibians experience retinal waves, but in a manner unlike those experienced by amniotes? To make sense of this conundrum, it is important to revisit the experiments looking for retinal waves in amphibians, bearing in mind the commonalities between zebrafish and amphibian visual development.

In the only study – to our knowledge – examining the question of retinal waves in frogs, (Demas et al., 2012) used a microelectrode array to record from the retinal ganglion cell (RGC) layer of retinae isolated from *Xenopus laevis* tadpoles staged 39-40 (approximately 2.5 days post-fertilisation) and older. Subsequent to the formation of the inner plexiform layer at stage 35-37 (Figure 2.3A), stage 39-40 is when the first RGC axons begin to innervate the optic tectum, forming the retinotectal circuit, the main retinofugal pathway in the frog (Figure 2.3B) (Holt & Harris, 1983). When Demas and colleagues (2012) recorded from stage 39-40 tadpole retinae, they could not detect any spontaneous retinal waves. The retina is still responsive – light exposure reliably evokes responses in these isolated retinae (Demas et al., 2012) – yet there is no evidence of spontaneous retinal waves or other spontaneous correlated activity. The observations reported by Demas and colleagues yield three possible interpretations: (a) *Xenopus laevis* tadpoles do not experience spontaneous retinal waves, (b) retinal waves occur in *Xenopus laevis* prior to developmental stage 39, or

(c) retinal waves cannot reliably be recorded in the RGC layer of *Xenopus laevis* retinae (e.g., perhaps they occur only within the inner plexiform layer). We note that interpretations (b) and (c) are not mutually exclusive.

The first interpretation outlined above (i.e., that *Xenopus laevis* does not experience retinal waves) has generally been preferred, supporting the theory of an amniote/anamniote division in retinal wave evolution. However, the observation of retinal waves in zebrafish offers a compelling reason to revisit this interpretation.

Intriguingly, if the second interpretation is correct (i.e., *Xenopus laevis* retinal waves occur prior to stage 39), that would mean that retinal waves occur before the retinotectal circuit forms (Holt & Harris, 1983). In other words, if *Xenopus* tadpoles experience retinal waves at all, their timing is restricted such that they cannot be involved in the refinement of the retinotectal visual circuit (Figure 2.3) – in stark contrast to the important role retinal waves play in the refinement of mammalian retinofugal pathways.

Surprising as this may be, it would not be entirely unprecedented to discover that zebrafish retinal waves are particularly important for the development of the retina, but not for retinofugal pathways. While it is reported by Zhang et al. (2016) that spontaneous retinal waves in zebrafish always originate with bipolar cell activity, in mammals, studies in both ferret (Feller et al., 1997; Wong et al., 1995) and mouse (Blankenship et al., 2009; Tian & Copenhagen, 2003) have shown that bipolar cells contribute only to the initiation of Stage III glutamatergic retinal waves. This cross-species difference in the intra-retinal dynamics of wave activity hints that retinal waves in zebrafish might play a different role with respect to the development of the retina itself. Further supporting this idea is the fact that, at postnatal day 2.5, when

zebrafish retinal waves begin, RGC axons have only reached about half of the regions of the zebrafish optic tectum which will eventually be innervated (Burrill & Easter Jr., 1994). This is consistent with the retinal waves playing a more important role for the development of the zebrafish retina itself, rather than retinofugal projections.

Conversely, mammalian retinal waves are known to play an important role in the refinement of retinofugal projections as well as intra-retinal and inter-retinal development. Mammalian retinal waves not only guide the formation of connections between the retina and the lateral geniculate nucleus (Butts et al., 2007; Lee et al., 2014), but they also regulate the formation of gap junctions between RGCs within the retina (Arroyo et al., 2016). Intriguingly, retinal waves additionally modulate inter-retinal activity in mammals, with monocular enucleation influencing the dynamics of retinal waves in the remaining eye (Failor et al., 2018). These observations could be explained, at least in part, by a transient retino-retinal projection that may serve to synchronise retinal wave activity between the two eyes (Murcia-Belmonte et al., 2019). This emphasises, once again, the complex character of retinal waves in mammalian visual development, which does not seem to be present in zebrafish. If *Xenopus laevis* retinal waves occur entirely prior to stage 39, then they likely play a role in the development of the retinae, entirely before the formation of retinofugal projections. This would be consistent with the limited time scale of retinal waves in zebrafish which experience retinal waves only at 2.5 – 3.5 days post-fertilisation.

An alternative, though not exclusive, interpretation is that retinal waves occur primarily outside of the RGC layer in the developing *Xenopus laevis* retina. Correlated activity was not found when recording from the RGC layer of isolated *Xenopus* retinae (Demas et al., 2012), but as stated earlier, retinal waves in zebrafish were found to

always originate with bipolar cell activity in the inner plexiform layer (IPL) and then propagate to the somata of only *some* RGCs (Zhang et al., 2016). The *Xenopus laevis* IPL forms at stage 35 and refines through stage 42 (Figure 2.3A) (Grant et al., 1980). If *Xenopus laevis* retinal waves similarly initiate in the IPL, they might not reliably propagate to the RGC layer, as is the case in zebrafish. This would explain why Demas and colleagues (2012) could not detect retinal waves in the RGC layer. This would once again point to a more important role for retinal waves in the formation of the retina itself; if these waves do not reliably propagate to RGC somata, they would be unlikely to play much of a role in the formation and refinement of retinofugal projections, and likely play a more important role in the formation of the retinae themselves. Thus, while previous work has demonstrated that *Xenopus laevis* retinofugal pathways are unlikely to be guided by retinal wave activity, it is highly possible that *Xenopus laevis* tadpoles experience a more limited form of retinal wave activity, like those observed in zebrafish.

2.5. The origin of retinal waves

Before their observation in zebrafish (Zhang et al., 2016), it was thought that spontaneous retinal waves were evolved by amniotes to compensate for the visual deprivation that occurs *in ovo* or *in utero*. However, it is time to revisit this theory. It seems unlikely that zebrafish would develop retinal waves where no other anamniotes have. Instead, we propose the possibility of a relatively simple ancestral retinal wave, which has been expanded upon by amniotes who leverage the relatively safe environment *in ovo* or *in utero*. Enjoying the safety of a womb or egg, amniotes

tend to undergo a more protracted development of sensorimotor systems, utilising greater experience-dependent plasticity in the early development of sensory systems.

Unlike amniotes, anamniotes – including zebrafish – develop in an external environment and frequently require a functioning visual system that develops quickly and reliably. The environment necessitates the rapid development of stereotypical, visually-guided behaviours, precluding much of the experience-dependent plasticity and protracted development seen in amniotic sensory system development.

The key to understanding the evolutionary origin of retinal waves lies in the environment. In turtles, spontaneous retinal waves play a part in the development of a functional visual system which can aid in sea-finding (i.e., the process of crawling from the egg to the water). Sea-finding is a complex, visually-guided process which relies upon multiple kinds of visual information. Turtle hatchlings are known to integrate the brightness of visual inputs from multiple angles, in order to determine the brightest direction (Salmon et al., 1992; Verheijen & Wildschut, 1973; Witherington, 1992); to prefer some spectral wavelengths over others, irrespective of light intensity (Sella et al., 2006); and to use shape/form perception to orient away from high silhouettes (Limpus & Kamrowski, 2013; Salmon et al., 1992; Tuxbury & Salmon, 2005). (The intricacies of turtle hatchling sea-finding are reviewed excellently by Lohmann et al., 1996.) It is highly possible that the spontaneous retinal waves which occur during sea turtle embryogenesis are a necessary step for the development of a retina which can make comparisons on the basis of luminance, spectral intensity, and form vision to guide hatchling turtles to the sea. In other words, the turtle's ecological niche likely demands retinal waves as a means to

form the visual system which can subserve visually-guided decisions from shortly after hatching.

With the discovery of spontaneous retinal waves in zebrafish, retinal waves are now known to exist in both amniotes and anamniotes, yet these waves seem to differ markedly between the two groups. A definitive reason behind this difference remains to be established, but the most promising explanation to date comes from considering the environment and the behaviours required of many anamniotes early in life. We propose that the protection offered by wombs and eggs has enabled amniotes to build upon the retinal waves experienced by many anamniotes. Put another way, in anamniotes, retinal waves are important for the development of the retinae, but in amniotes, retinal waves take on an additional significance for the wiring of retinofugal pathways.

3. Concluding remarks

The finding of retinal waves in zebrafish opens a new and exciting chapter in the study of how the visual system has evolved across the vertebrate lineage. Since adult animals do not transform into other adult animals, evolution is the evolution of development (García-Moreno & Molnár, 2020; Horváth et al., 2022). It is by considering the environment of a developing fish, amphibian, reptile, bird, or mammal, and the most adaptive behavioural repertoires for these respective environments, that we arrive at a novel theory of retinal wave evolution. Yet this is far from the first time that behaviour has driven advances in neurophysiology.

3.1. The roads paved by behaviour

Behaviour has long paved the roads for discoveries in neurophysiology. As one brief example of this longstanding pattern, we consider Hodgkin and Huxley's Nobel Prize-winning work on the initiation and propagation of action potentials in the squid giant axon (Hodgkin et al., 1952; Hodgkin & Huxley, 1952a, 1952b). Decades prior to the work of Hodgkin and Huxley, it was John Zachary Young (1938, 1939) who described how the squid's giant motor nerve fibres enable muscular contractions that expel powerful jets of water from the squid's body. The incredible speed of this elegant escape mechanism is enabled by the enormous size of the squid giant axon; greater axon diameter is associated with higher conduction velocity, as demonstrated early on by Hursh (1939) and others. The squid's ecological surroundings drove the evolution of a speedy escape mechanism for the squid, by selecting for those squids which could most competently escape predation. By acting on the level of behavioural fitness, evolutionary processes selected for the giant axon that subserves this unique behaviour.

The squid giant axon enabled Hodgkin and Huxley to dissect the physiological basis of the action potential in the 1950s, but this outstanding discovery was enabled only by the earlier work of others, like Young, who described the physiological basis for the squid's naturalistic behaviours. Fortuitous as it was that Young had done this work decades prior, this is a repeating pattern in the history of physiology: behavioural understanding often precedes physiological understanding.

Despite the important role that behavioural understanding plays in the discovery of physiological mechanisms, it would – in general – be impractical for a

neurophysiologist to take on the additional roles of comparative physiologist, zoologist, ecologist, and animal behaviourist. So what might be done?

3.2. The future of behaviour

To the great fortune of physiologists, plenty of experimental work and theory has been done already in the study of naturalistic animal behaviours. Much has already been described across a wide-ranging variety of species, and this work needs only to be applied by physiologists.

Indeed, in the 1920s, it was the physiologist August Krogh who joked about the animals that were seemingly created to answer specific questions in physiology, just as the squid giant axon was "created" to study the action potential in the 1950s. Krogh writes (1929):

> I have no doubt that there is quite a number of animals which are… "created" for special physiological purposes, but I am afraid that most of them are unknown to the men for whom they were "created," and we must apply to the zoölogists to find them and lay our hands on them.

Bearing in mind the century-old wisdom of Krogh, neurophysiologists should once more begin to appreciate the incredible diversity of species that inhabit this world. To this end, we have considered the influence of ecological niche on visual system development. Specifically, we examined the emergence of retinal waves within the vertebrate lineage from a behavioural point of view. Using the specialisation of animals to their environments as our guide, we have developed a novel theory of the emergence of retinal waves among vertebrates. From this theory, we predicted the presence of retinal waves across a larger swathe of the vertebrate lineage than

previously appreciated, and we made predictions regarding the function of retinal waves in the context of broader patterns of visual development.

Most immediately, future work should investigate the possibility of retinal waves prior to stage 39 and in the IPL of *Xenopus laevis*. However, this theoretical work predicts the presence of retinal waves in other anamniotes as well. By considering not only the environments of developing animals, but also the behaviours and adaptations required by these environments, neuroethological considerations have the power to bring forward new explanations and identify unappreciated patterns in neurophysiology.

References

Ackman, J. B., Burbridge, T. J., & Crair, M. C. (2012). Retinal waves coordinate patterned activity throughout the developing visual system. *Nature*, *490*(7419), 219–225. https://doi.org/10.1038/nature11529

Ackman, J. B., & Crair, M. C. (2014). Role of emergent neural activity in visual map development. *Current Opinion in Neurobiology*, *24*, 166–175. https://doi.org/10.1016/j.conb.2013.11.011

Akin, O., Bajar, B. T., Keles, M. F., Frye, M. A., & Zipursky, S. L. (2019). Cell-type-Specific Patterned Stimulus-Independent Neuronal Activity in the Drosophila Visual System during Synapse Formation. *Neuron*, *101*(5), 894-904.e5. https://doi.org/10.1016/j.neuron.2019.01.008

Arroyo, D. A., Kirkby, L. A., & Feller, M. B. (2016). Retinal Waves Modulate an Intraretinal Circuit of Intrinsically Photosensitive Retinal Ganglion Cells. *Journal of Neuroscience*, *36*(26), 6892–6905. https://doi.org/10.1523/JNEUROSCI.0572-16.2016

Avitan, L., Pujic, Z., Mölter, J., Van De Poll, M., Sun, B., Teng, H., Amor, R., Scott, E. K., & Goodhill, G. J. (2017). Spontaneous Activity in the Zebrafish Tectum Reorganizes over Development and Is Influenced by Visual Experience. *Current Biology*, *27*(16), 2407-2419.e4. https://doi.org/10.1016/j.cub.2017.06.056

Bertolesi, G. E., Debnath, N., Atkinson-Leadbeater, K., Niedzwiecka, A., & McFarlane, S. (2021). Distinct type II opsins in the eye decode light properties for background adaptation and behavioural background preference. *Molecular Ecology*, *30*(24), 6659–6676. https://doi.org/10.1111/mec.16203

Blankenship, A. G., Ford, K. J., Johnson, J., Seal, R. P., Edwards, R. H., Copenhagen, D. R., & Feller, M. B. (2009). Synaptic and Extrasynaptic Factors Governing Glutamatergic Retinal Waves. *Neuron*, *62*(2), 230–241. https://doi.org/10.1016/j.neuron.2009.03.015

Bruno, J. R., Udoh, U. G., Landen, J. G., Osborn, P. O., Asher, C. J., Hunt, J. E., & Pratt, K. G. (2022). A circadian-dependent preference for light displayed by Xenopus tadpoles is modulated by serotonin. *iScience*, *25*(11), 105375. https://doi.org/10.1016/j.isci.2022.105375

Burrill, J. D., & Easter Jr., S. S. (1994). Development of the retinofugal projections in the embryonic and larval zebrafish (Brachydanio rerio). *Journal of Comparative Neurology*, *346*(4), 583–600. https://doi.org/10.1002/cne.903460410

Butts, D. A., Kanold, P. O., & Shatz, C. J. (2007). A Burst-Based "Hebbian" Learning Rule at Retinogeniculate Synapses Links Retinal Waves to Activity-Dependent Refinement. *PLOS Biology*, *5*(3), e61. https://doi.org/10.1371/journal.pbio.0050061

Choi, B. J., Chen, Y.-C. D., & Desplan, C. (2021). Building a circuit through correlated spontaneous neuronal activity in the developing vertebrate and invertebrate visual systems. *Genes & Development*, *35*(9–10), 677–691. https://doi.org/10.1101/gad.348241.121

Demas, J. A., Payne, H., & Cline, H. T. (2012). Vision drives correlated activity without patterned spontaneous activity in developing Xenopus retina. *Developmental Neurobiology*, *72*(4), 537–546. https://doi.org/10.1002/dneu.20880

Dixon, L. J., McDowell, A. L., Houchins, J. D., & Bilotta, J. (2004). Effects of restricted spectral rearing on the development of zebrafish retinal physiology. *Documenta Ophthalmologica*, *109*(1), 17–33. https://doi.org/10.1007/s10633-004-1124-y

Elstrott, J., & Feller, M. B. (2010). Direction-Selective Ganglion Cells Show Symmetric Participation in Retinal Waves During Development. *Journal of Neuroscience*, *30*(33), 11197–11201. https://doi.org/10.1523/JNEUROSCI.2302-10.2010

Failor, S. W., Ng, A., & Cheng, H.-J. (2018). Monocular enucleation alters retinal waves in the surviving eye. *Neural Development*, *13*(1), 4. https://doi.org/10.1186/s13064-018-0101-1

Feller, M. B., Butts, D. A., Aaron, H. L., Rokhsar, D. S., & Shatz, C. J. (1997). Dynamic Processes Shape Spatiotemporal Properties of Retinal Waves. *Neuron*, *19*(2), 293–306. https://doi.org/10.1016/S0896-6273(00)80940-X

Feller, M. B., & Kerschensteiner, D. (2020). Retinal waves and their role in visual system development. In *Synapse Development and Maturation* (pp. 367–382). Elsevier. https://doi.org/10.1016/B978-0-12-823672-7.00016-8

Galvani, L. (1791). De viribus electricitatis in motu musculari. Commentarius. *De Bonoiensi Scientiarum et Artium Intituo Atque Academie Commentarii*, *7*, 363–418.

García-Moreno, F., & Molnár, Z. (2020). Chapter 25—The impact of different modes of neuronal migration on brain evolution. In J. Rubenstein, P. Rakic, B. Chen, K. Y. Kwan, A. Kolodkin, & E. Anton (Eds.), *Cellular Migration and Formation of Axons and Dendrites (Second Edition)* (pp. 555–576). Academic Press. https://doi.org/10.1016/B978-0-12-814407-7.00025-0

Ge, X., Zhang, K., Gribizis, A., Hamodi, A. S., Sabino, A. M., & Crair, M. C. (2021). Retinal waves prime visual motion detection by simulating future optic flow. *Science*, *373*(6553), eabd0830. https://doi.org/10.1126/science.abd0830

Gnuegge, L., Schmid, S., & Neuhauss, S. C. F. (2001). Analysis of the Activity-Deprived Zebrafish Mutant macho Reveals an Essential Requirement of Neuronal Activity for the Development of a Fine-Grained Visuotopic Map. *Journal of Neuroscience*, *21*(10), 3542–3548. https://doi.org/10.1523/JNEUROSCI.21-10-03542.2001

Grant, P., Rubin, E., & Cima, C. (1980). Ontogeny of the retina and optic nerve in Xenopus laevis. I. Stages in the early development of the retina. *Journal of Comparative Neurology*, *189*(4), 593–613. https://doi.org/10.1002/cne.901890403

Hiesinger, P. R., Zhai, R. G., Zhou, Y., Koh, T.-W., Mehta, S. Q., Schulze, K. L., Cao, Y., Verstreken, P., Clandinin, T. R., Fischbach, K.-F., Meinertzhagen, I. A., & Bellen, H. J. (2006). Activity-Independent Prespecification of Synaptic Partners in the Visual Map of Drosophila. *Current Biology*, *16*(18), 1835–1843. https://doi.org/10.1016/j.cub.2006.07.047

Hiramoto, M., & Cline, H. T. (2014). Optic flow instructs retinotopic map formation through a spatial to temporal to spatial transformation of visual information. *Proceedings of the National Academy of Sciences*, *111*(47), E5105–E5113. https://doi.org/10.1073/pnas.1416953111

Hodgkin, A. L., & Huxley, A. F. (1952a). Currents carried by sodium and potassium ions through the membrane of the giant axon of Loligo. *The Journal of Physiology*, *116*(4), 449–472.

Hodgkin, A. L., & Huxley, A. F. (1952b). The components of membrane conductance in the giant axon of Loligo. *The Journal of Physiology*, *116*(4), 473–496.

Hodgkin, A. L., Huxley, A. F., & Katz, B. (1952). Measurement of current-voltage relations in the membrane of the giant axon of Loligo. *The Journal of Physiology*, *116*(4), 424–448.

Holt, C. E., & Harris, W. A. (1983). Order in the initial retinotectal map in Xenopus: A new technique for labelling growing nerve fibres. *Nature*, *301*(5896), Article 5896. https://doi.org/10.1038/301150a0

Horváth, T. L., Hirsch, J., & Molnár, Z. (2022). Chapter 1 - Zoltán Molnár: The developing brain. In T. L. Horváth, J. Hirsch, & Z. Molnár (Eds.), *Body, Brain, Behavior* (pp. 1–66). Academic Press. https://doi.org/10.1016/B978-0-12-818093-8.00005-7

Huberman, A. D., Feller, M. B., & Chapman, B. (2008). Mechanisms Underlying Development of Visual Maps and Receptive Fields. *Annual Review of Neuroscience*, *31*(1), 479–509. https://doi.org/10.1146/annurev.neuro.31.060407.125533

Hunt, J. E., Bruno, J. R., & Pratt, K. G. (2020). An Innate Color Preference Displayed by Xenopus Tadpoles Is Persistent and Requires the Tegmentum. *Frontiers in Behavioral Neuroscience*, *14*. https://doi.org/10.3389/fnbeh.2020.00071

Hursh, J. B. (1939). Conduction Velocity and Diameter of Nerve Fibers. *American Journal of Physiology*, *127*(1), 131–139. https://doi.org/10.1152/ajplegacy.1939.127.1.131

Kerschensteiner, D. (2016). Glutamatergic Retinal Waves. *Frontiers in Neural Circuits*, *10*, 38. https://doi.org/10.3389/fncir.2016.00038

Krakauer, J. W., Ghazanfar, A. A., Gomez-Marin, A., MacIver, M. A., & Poeppel, D. (2017). Neuroscience Needs Behavior: Correcting a Reductionist Bias. *Neuron*, *93*(3), 480–490. https://doi.org/10.1016/j.neuron.2016.12.041

Krogh, A. (1929). The Progress of Physiology. *American Journal of Physiology*, *90*(2), 243–251. https://doi.org/10.1152/ajplegacy.1929.90.2.243

Kutsarova, E., Munz, M., & Ruthazer, E. S. (2017). Rules for Shaping Neural Connections in the Developing Brain. *Frontiers in Neural Circuits*, *10*. https://doi.org/10.3389/fncir.2016.00111

Lee, H., Brott, B. K., Kirkby, L. A., Adelson, J. D., Cheng, S., Feller, M. B., Datwani, A., & Shatz, C. J. (2014). Synapse elimination and learning rules co-regulated by MHC class I H2-Db. *Nature*, *509*(7499), Article 7499. https://doi.org/10.1038/nature13154

Limpus, C., & Kamrowski, R. L. (2013). Ocean-finding in marine turtles: The importance of low horizon elevation as an orientation cue. *Behaviour*, *150*(8), 863–893. https://doi.org/10.1163/1568539X-00003083

Lohmann, K. J., Witherington, B. E., Lohmann, C. M. F., & Salmon, M. (1996). Orientation, Navigation, and Natal Beach Homing in Sea Turtles. In *The Biology of Sea Turtles, Volume I*. CRC Press.

Maccione, A., Hennig, M. H., Gandolfo, M., Muthmann, O., van Coppenhagen, J., Eglen, S. J., Berdondini, L., & Sernagor, E. (2014). Following the ontogeny of retinal waves: Pan-retinal recordings of population dynamics in the neonatal mouse. *The Journal of Physiology*, *592*(7), 1545–1563. https://doi.org/10.1113/jphysiol.2013.262840

Moriya, T., Kito, K., Miyashita, Y., & Asami, K. (1996). Preference for background color of the Xenopus laevis tadpole. *Journal of Experimental Zoology*, *276*(5), 335–344. https://doi.org/10.1002/(SICI)1097-010X(19961201)276:5<335::AID-JEZ4>3.0.CO;2-P

Mukherjee, D., Yonk, A. J., Sokoloff, G., & Blumberg, M. S. (2017). Wakefulness suppresses retinal wave-related neural activity in visual cortex. *Journal of Neurophysiology*, *118*(2), 1190–1197. https://doi.org/10.1152/jn.00264.2017

Murcia-Belmonte, V., Coca, Y., Vegar, C., Negueruela, S., de Juan Romero, C., Valiño, A. J., Sala, S., DaSilva, R., Kania, A., Borrell, V., Martinez, L. M., Erskine, L., & Herrera, E. (2019). A Retino-retinal Projection Guided by Unc5c Emerged in Species with Retinal Waves. *Current Biology*, *29*(7), 1149-1160.e4. https://doi.org/10.1016/j.cub.2019.02.052

Nevin, L. M., Taylor, M. R., & Baier, H. (2008). Hardwiring of fine synaptic layers in the zebrafish visual pathway. *Neural Development*, *3*(1), 36. https://doi.org/10.1186/1749-8104-3-36

Niell, C. M., & Smith, S. J. (2005). Functional Imaging Reveals Rapid Development of Visual Response Properties in the Zebrafish Tectum. *Neuron*, *45*(6), 941–951. https://doi.org/10.1016/j.neuron.2005.01.047

Pratt, K. G., Hiramoto, M., & Cline, H. T. (2016). An Evolutionarily Conserved Mechanism for Activity-Dependent Visual Circuit Development. *Frontiers in Neural Circuits*, *10*. https://doi.org/10.3389/fncir.2016.00079

Read, J. C. A. (2022). Stereopsis without correspondence. *Philosophical Transactions of the Royal Society B: Biological Sciences*, *378*(1869), 20210449. https://doi.org/10.1098/rstb.2021.0449

Rochefort, N. L., Narushima, M., Grienberger, C., Marandi, N., Hill, D. N., & Konnerth, A. (2011). Development of Direction Selectivity in Mouse Cortical Neurons. *Neuron*, *71*(3), 425–432. https://doi.org/10.1016/j.neuron.2011.06.013

Salmon, M., Wyneken, J., Fritz, E., & Lucas, M. (1992). Seafinding By Hatchling Sea Turtles: Role of Brightness, Silhouette and Beach Slope as Orientation Cues. *Behaviour*, *122*(1–2), 56–77. https://doi.org/10.1163/156853992X00309

Saszik, S., & Bilotta, J. (2001). Constant dark-rearing effects on visual adaptation of the zebrafish ERG. *International Journal of Developmental Neuroscience*, *19*(7), 611–619. https://doi.org/10.1016/S0736-5748(01)00051-X

Sella, K. N., Salmon, M., & Witherington, B. E. (2006). Filtered Streetlights Attract Hatchling Marine Turtles. *Chelonian Conservation and Biology*, *5*(2), 255–261. https://doi.org/10.2744/1071-8443(2006)5[255:FSAHMT]2.0.CO;2

Sernagor, E., & Grzywacz, N. M. (1999). Spontaneous Activity in Developing Turtle Retinal Ganglion Cells: Pharmacological Studies. *Journal of Neuroscience*, *19*(10), 3874–3887. https://doi.org/10.1523/JNEUROSCI.19-10-03874.1999

Sernagor, E., & Mehta, V. (2001). The role of early neural activity in the maturation of turtle retinal function. *Journal of Anatomy*, *199*(4), 375–383. https://doi.org/10.1046/j.1469-7580.2001.19940375.x

Sernagor, E., Young, C., & Eglen, S. J. (2003). Developmental Modulation of Retinal Wave Dynamics: Shedding Light on the GABA Saga. *Journal of Neuroscience*, *23*(20), 7621–7629. https://doi.org/10.1523/JNEUROSCI.23-20-07621.2003

Shen, J., & Colonnese, M. T. (2016). Development of Activity in the Mouse Visual Cortex. *Journal of Neuroscience*, *36*(48), 12259–12275. https://doi.org/10.1523/JNEUROSCI.1903-16.2016

Stafford, B. K., Sher, A., Litke, A. M., & Feldheim, D. A. (2009). Spatial-Temporal Patterns of Retinal Waves Underlying Activity-Dependent Refinement of Retinofugal Projections. *Neuron*, *64*(2), 200–212. https://doi.org/10.1016/j.neuron.2009.09.021

Thompson, A., Gribizis, A., Chen, C., & Crair, M. C. (2017). Activity-dependent development of visual receptive fields. *Current Opinion in Neurobiology*, *42*, 136–143. https://doi.org/10.1016/j.conb.2016.12.007

Tian, N., & Copenhagen, D. R. (2003). Visual Stimulation Is Required for Refinement of ON and OFF Pathways in Postnatal Retina. *Neuron*, *39*(1), 85–96. https://doi.org/10.1016/S0896-6273(03)00389-1

Tiriac, A., Smith, B. E., & Feller, M. B. (2018). Light Prior to Eye Opening Promotes Retinal Waves and Eye-Specific Segregation. *Neuron*, *100*(5), 1059-1065.e4. https://doi.org/10.1016/j.neuron.2018.10.011

Tuxbury, S. M., & Salmon, M. (2005). Competitive interactions between artificial lighting and natural cues during seafinding by hatchling marine turtles. *Biological Conservation*, *121*(2), 311–316. https://doi.org/10.1016/j.biocon.2004.04.022

Verheijen, F. J., & Wildschut, J. T. (1973). The photic orientation of hatchling sea turtles during water finding behaviour. *Netherlands Journal of Sea Research*, *7*, 53–67. https://doi.org/10.1016/0077-7579(73)90032-X

Witherington, B. E. (1992). *Sea-finding behavior and the use of photic orientation cues by hatchling sea turtles* [Ph.D., University of Florida]. https://www.proquest.com/docview/303980507/abstract/F08706079D3746D4PQ/1

Wong, R. O. L., Chernjavsky, A., Smith, S. J., & Shatz, C. J. (1995). Early functional neural networks in the developing retina. *Nature*, *374*(6524), Article 6524. https://doi.org/10.1038/374716a0

Xie, J., Jusuf, P. R., Bui, B. V., & Goodbourn, P. T. (2019). Experience-dependent development of visual sensitivity in larval zebrafish. *Scientific Reports*, *9*(1), 18931. https://doi.org/10.1038/s41598-019-54958-6

Young, J. Z. (1938). The Functioning of the Giant Nerve Fibres of the Squid. *Journal of Experimental Biology*, *15*(2), 170–185. https://doi.org/10.1242/jeb.15.2.170

Young, J. Z. (1939). Fused neurons and synaptic contacts in the giant nerve fibres of cephalopods. *Philosophical Transactions of the Royal Society of London. Series B, Biological Sciences*, *229*(564), 465–503. https://doi.org/10.1098/rstb.1939.0003

Zahn, N., James-Zorn, C., Ponferrada, V. G., Adams, D. S., Grzymkowski, J., Buchholz, D. R., Nascone-Yoder, N. M., Horb, M., Moody, S. A., Vize, P. D., & Zorn, A. M. (2022). Normal Table of Xenopus development: A new graphical resource. *Development*, *149*(14), dev200356. https://doi.org/10.1242/dev.200356

Zhang, R., Du, W., Prober, D. A., & Du, J. (2019). Müller Glial Cells Participate in Retinal Waves via Glutamate Transporters and AMPA Receptors. *Cell Reports*, *27*(10), 2871-2880.e2. https://doi.org/10.1016/j.celrep.2019.05.011

Zhang, R., Li, X., Kawakami, K., & Du, J. (2016). Stereotyped initiation of retinal waves by bipolar cells via presynaptic NMDA autoreceptors. *Nature Communications*, *7*(1), 12650. https://doi.org/10.1038/ncomms12650

Chapter 3

Development of a data-driven approach to investigate white matter connectivity in lesser-studied brains.

Declarations

Publication history

Parts of this chapter have previously been published in the following preprint, distributed under the terms of the Creative Commons Attribution-NonCommercial 4.0 International (CC BY-NC 4.0) license.

Hunt, J. E., Warrington., S., Roumazeilles, L., Jbabdi, S., Molnár, Z., Sotiropoulous, S. N., & Mars, R. B. (2025). An anthropoid/strepsirrhine divergence in ventral visual stream connectivity. *bioRxiv*. doi:10.1101/2025.05.19.653861

Contribution statement

JEH designed and carried out experiments, contributed to the NFacT toolbox, analysed data, interpreted results, drafted the manuscript, and produced all figures which appear in this chapter. SW and SNS created the NFacT toolbox and assisted with its implementation. LR preprocessed the macaque data. SJ assisted with analysis code for data preprocessing. ZM assisted in editing the manuscript and designing figures. RBM designed experiments, assisted with data analysis and interpretation, assisted in editing the manuscript and designing figures, and supervised the project.

Acknowledgements

JEH is funded by a Wellcome Trust Doctoral Studentship in Neuroscience (222368/Z/21/Z). Data were provided in part by the Human Connectome Project, MGH-USC Consortium (Principal Investigators: Bruce R. Rosen, Arthur W. Toga and Van Wedeen; U01MH093765) funded by the NIH Blueprint Initiative for Neuroscience Research grant; the National Institutes of Health grant P41EB015896; and the Instrumentation Grants S10RR023043, 1S10RR023401, 1S10RR019307. The Oxford Centre for Integrative Neuroimaging was supported by core funding from the Wellcome Trust (203139/Z/16/Z). SW and SNS acknowledge funding from the European Research Council (ERC Consolidator 101000969 to SNS). RBM is supported by the Biotechnology and Biological Sciences Research Council UK (BB/N019814/1). The funders had no role in the design or writing of this report, nor in the collection, analysis, and interpretation of data.

Abstract

Comparative anatomical studies of white matter organisation hold great potential to improve our understanding of basic human brain organisation, assist in the translation of preclinical studies of neuropsychiatric disorders, and inform wildlife conservation and management efforts. Yet most of our knowledge of brain anatomy exists in a few model organisms. Why is this?

This dearth of information is due in large part to technical challenges in data collection and analysis. While neuroimaging now allows for the relatively cheap acquisition of high-quality, whole-brain data from animals that are not sacrificed specifically for scientific research, the challenge of comparative neuroimaging studies is that the brains under investigation are often little-studied and have few ready-made processing tools available. Atlas-based tractography can be used to extract specific pathways, but only if researchers already know a connection's origin, course, and termination. Such knowledge is by-and-large absent for many primate species.

To overcome these challenges, we develop the use of an unsupervised machine learning algorithm, non-negative matrix factorisation (NMF), to extract white matter connections across species. Based on probabilistic inference of white matter trajectories and cortical endpoints, NMF can be used to separate white matter into likely white matter tracts, even in brains for which white matter atlases are not available. This chapter presents a series of experiments which establish the suitability of NMF-based techniques for the reconstruction of white matter tracts at low sample sizes and in non-human brains.

1. Introduction: How do we compare unusual brains?

The first chapter of this thesis introduced some of the benefits of comparative neuroanatomy. To briefly summarise a few of the most compelling benefits:

i) Most preclinical studies for neuropsychiatric disorders are carried out in non-human animals. Comparative neuroanatomy is key to accurately predicting whether and how experimental treatments may translate to humans.

ii) Comparative work is key to understanding evolution.

iii) Comparing nervous systems is key to certain branches of philosophical enquiry.

iv) Understanding how animals transduce and process sensory information is key to designing and implementing effective wildlife conservation and management efforts.

It is clear that comparative neuroanatomy serves a combination of practical and theoretical scientific goals. Yet despite the numerous benefits to comparative studies, neuroscience continues to rely on a small number of model organisms. Why is this?

Over 100 years of scientific literature have yielded a deep understanding of a few model organisms, including rich information about each species' development, behaviour, and life course. Among the more practicable information in this deep corpus of literature is genetic profiling (Aitman et al., 2011), molecular descriptions of developmental processes (Anderson & Ingham, 2003), cortical grey matter maps (Rosa & Tweedale, 2005), and more recently, tractographic atlases (Assimopoulos et al., 2024). The pioneering work of early investigators, and those who have stood on their shoulders, has yielded what Rosa and Tweedale (2005) call the "solid

foundation of knowledge" upon which further studies can be more easily completed. In the primate lineage, this solid foundation has been built for the macaque, yet the foundation is less sturdy for other species. This chapter thus seeks to establish a toolset for the characterisation of white matter connectivity in lesser-studied brains.

In the human, macaque, and chimpanzee, atlas-based tractography protocols can extract specific white matter pathways (Assimopoulos et al., 2024; Bryant et al., 2020, 2025; Warrington et al., 2020). Such protocols require foreknowledge of a connection's origin, course, and termination, information which is largely absent in other species. While white matter atlases are being developed for additional primate species with varying degrees of formalisation (Bryant et al., 2020, 2021, 2024; Liu et al., 2020), these atlases have not yet been incorporated into tractography protocols and their implementation remains labour-intensive. As such, a discovery approach is needed. There are well-established exploratory methods for analysing MRI data in the human brain (O'Muircheartaigh & Jbabdi, 2018; Singh & Wong, 2010), though their use in comparative studies is still relatively rare (Mars et al., 2019).

An intriguing possibility comes with the increasing accessibility of data-driven approaches based on machine learning algorithms. Non-negative matrix factorisation (NMF; Lee & Seung, 1999, 2000) and related algorithms (Yang & Oja, 2010) show great promise for the analysis of neuroimaging data, having recently found purchase in the analysis of white matter in the developing human brain (Thompson et al., 2020) and the grey matter of the adult human and chimpanzee brains (Varikuti et al., 2018; Vickery et al., 2024).

NMF is an unsupervised dimensionality reduction algorithm with an inherent clustering property, similar to independent component analysis. Briefly, NMF

factorises a matrix into the linear product of two other matrices (the factor matrices), wherein all three matrices contain only positive values. By specifying a lower dimensionality for the factor matrices, NMF generates factors with fewer dimensions than the original matrix, and thereby clusters data. The non-negative nature of NMF makes it well-suited for phenomena which are inherently non-negative (e.g., the firing rates of neurons or the intensity of white matter). If NMF can be used to identify white matter bundles that correspond to known tracts, then it could be used to interrogate data in lesser-studied species without losing sight of anatomical rigour.

Here, we assess the suitability of NMF for reconstructing white matter tracts, in particular its ability to find clusters that resemble known white matter connectivity. We used the Python-based NFacT pipeline (Thompson et al., 2020; https://github.com/SPMIC-UoN/NFacT), which is a tractography-focused wrapper for Scikit-learn's NMF algorithm (Pedregosa et al., 2011). In order to assess the suitability of this data-driven approach for reconstructing white matter and better understand the properties of this approach, we performed NMF decomposition in the human and macaque, the two species for which the best-established atlas-based tractography protocols exist. We adjusted the parameters of the NMF decomposition, and compared the outcome of each decomposition against atlas-based tractography.

2. Methods

2.1. Data sources

Because comparative studies often have limited sample sizes, we sought to assess the performance of non-negative matrix factorisation (NMF)-based analysis

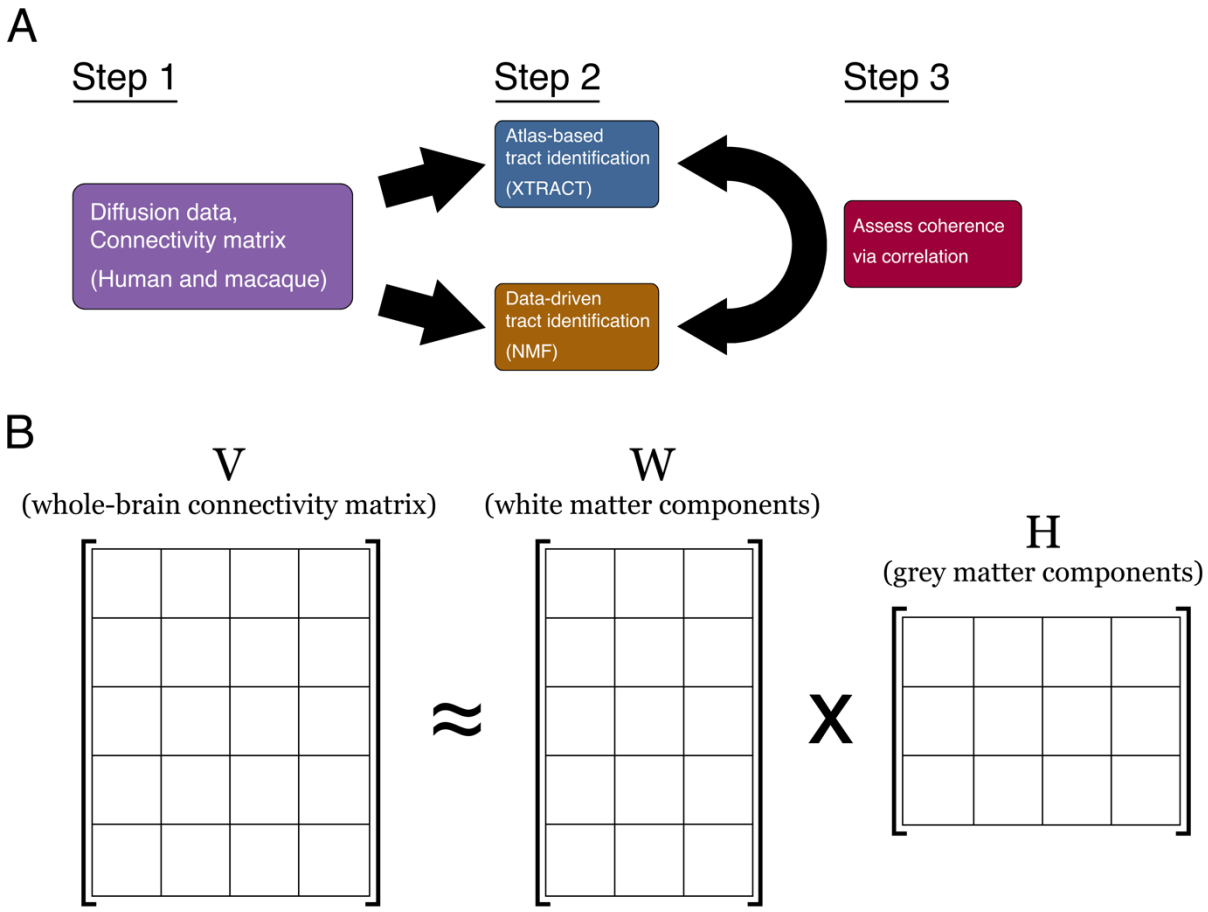


Figure 3.1. NMF validation procedure and methods overview. (A) *Study overview. Connectivity matrices were produced for one human and one macaque, based on diffusion MRI scans in each species. Tracts were then identified using traditional, atlas-based and data-driven, NMF-based approaches. Data-driven tractography output was then assessed for coherence with atlas-based tractography output by computing a matrix of correlation values.* ***(B)*** *Summary of the NMF algorithm. A whole-brain connectivity matrix (*V*) is decomposed into two smaller matrices (*W *and* H*), which approximate* V *when multiplied together. Because* W *and* H *are lower in dimensionality than* V*, white matter voxels and grey matter vertices with similar properties cluster together. These clustered voxels and vertices comprise putative tracts and their associated connectivity profiles.*

---

with small sample sizes. We thus compared the results of NMF-based analysis against atlas-based tractography (Figure 3.1A), using diffusion MRI data from one randomly-selected adult human participant in the Human Connectome Project's "40 unrelated subjects" dataset (Van Essen et al., 2013), and diffusion MRI data from one

postmortem adult macaque brain, the acquisition and early processing of which has been previously described by Roumazeilles et al. (2022). Briefly, the macaque brain was extracted and fixed in formalin after the animal was euthanised for reasons unrelated to this study. No evidence of neuropathology was found, and the brain was stored in a 10% neutral buffered formalin solution with azide.

2.2. Data acquisition and preprocessing

Human data were collected and preprocessed as described by the Human Connectome Project (see Setsompop et al., 2013; Van Essen et al., 2013 and https://www.humanconnectome.org/). The macaque brain was rehydrated in a phosphate buffer for one week prior to scanning, and scanned in a fluorocarbon-based fluid to displace air inclusions at the tissue surface. The 7T preclinical scanner used for data acquisition (Varian, Oxford UK) has a birdcage transmit/receive coil with an inner diameter of 72 mm (Rapid Biomedical GmbH, Rimpar Germany). To minimise image distortions, 2-D diffusion-weighted images were collected using a spin-echo multi-slice (DW-SEMS) protocol with single line readout. Data are of high spatial resolution, at 0.6 mm isotropic resolution with a single-shell protocol. The acquisition parameters are as follows: TE/TR = 26 ms/10 s; matrix size = 128x128 (variable number of slices); b = 0 s/mm^2 (non-diffusion-weighted; 16 volumes), 4000 s/mm^2 (diffusion-weighted, 128 volumes). Data quality characteristics including computed signal-to-noise ratio, mean fractional anisotropy, and mean diffusivity are computed and reported by Roumazeilles et al. (2022).

Diffusion MRI data were preprocessed using the *phoenix* module of the in-house MR Comparative Anatomy Toolbox (Mr Cat; www.neuroecologylab.org), which

relies on FSL (Jenkinson et al., 2012; http://www.fmrib.ox.ac.uk/fsl). A three-fibre ball and stick model was then fitted to the data using FSL's *BedpostX* (Behrens et al., 2007). *BedpostX* models crossing fibres in diffusion MRI data by building a distribution of diffusion parameters at each voxel using a Markov Chain Monte Carlo sampling technique (Behrens et al., 2007), addressing the shortcomings of early tractography techniques at modelling crossing fibres (e.g., Lin et al., 2003). Species-specific brain templates were then created using multimodal iterative registration using the MMORF pipeline (Lange et al., 2020). A cortical surface representation of each template was created using the *precon_all* (Benn et al., 2025; https://github.com/neurabenn/precon_all) adaptation of Freesurfer's *recon-all* pipeline (Fischl, 2012) and downsampled to 10,000 vertices per hemisphere. These steps produced a dataset which was then used as input for tractography.

2.3. Data-driven tractography

Probabilistic tractography was run from the cortical surface towards the white matter via *Probtrackx2* (Behrens et al., 2007) to create a connectivity matrix, wherein each row corresponds to a surface-based (vertex) seed and each column to a volume-based (voxel) target. By tracking from the grey matter surface, this approach avoids the difficulties with fanning fibres that frequently affect tractographic inference (see discussions by Jeurissen et al., 2019 and Savadjiev et al., 2008), as fibres are expected to merge rather than fan out in this direction (Warrington et al., 2020). Individual subject matrices were produced with 10,000 seed points, 1,000 samples per seed, and a step length of 0.2 with distance correction applied. Among other

reasons, a step length of 0.2 was used to reduce the likelihood of tractography streamlines underrepresenting tight curves among genuine white matter tracts.

The resultant connectivity matrix, wherein rows correspond to grey matter and columns correspond to white matter, was then decomposed via NMF into two matrices: one comprising white matter by components, and one comprising components by grey matter (Figure 3.1B). In other words, for each component, there is a corresponding volumetric representation of that component's white matter voxels and a grey matter surface array of vertices representing the innervation pattern of that component. NMF decomposition was used to decompose the results of probabilistic tractography in a single human brain and a single macaque brain.

NMF requires the user to specify the number of components (K) to be used in decomposition, similar to the specification of a k value in k-means clustering. Previous work in humans has shown that NMF is able to reconstruct known white matter bundles reliably when applied to data from hundreds of subjects (Thompson et al., 2020), but changing the number of components produced substantial changes to connectivity results. Therefore, to assess the properties of NMF when applied to single subjects, we performed NMF decomposition with $K = 10$, 50, 60, 100, and 200 components for the individuals of both species in our study. Other NMF hyperparameters were selected according to the default parameters in the Scikit-learn Python package, version 1.7, with the exception of the following. NMF was initialised using the "non-negative double singular value decomposition" (NNDSVD) method (Boutsidis & Gallopoulos, 2008), which is particularly well-suited to NMF with sparse factors, such as the tracts we wish to derive from probabilistic tractography data in the present study. As Boutsidis and Gallopoulos report (2008), for NMF with sparse

factors, the NNDSVD initialisation method leads to a faster error reduction and convergence during the matrix factorisation, as well as a reduction in final approximation error. Additionally, to increase the sparsity and interpretability of the NMF output, the regularisation terms “alpha_W” and “alpha_H” were both increased from the default of 0.0 to 0.1. Increasing the regularisation of the NMF algorithm results in sparser, more interpretable outputs, with greater independence between components (Hoyer, 2004; Thompson et al., 2020).

2.4 Atlas-based tractography and statistical comparison

To produce the atlas-based tractography against which NMF performance was compared, we ran probabilistic tractography on a set of 42 combinations of seed, waypoint, and exclusion masks designed to reliably identify the major white matter bundles in the human and macaque brain, as implemented in the FSL tool *XTRACT* (Warrington et al., 2020). We then ran *XTRACT Blueprint* (Mars et al., 2018; Warrington et al., 2020) to generate surface-space connectivity blueprints. A surface-space connectivity blueprint is a representation of the grey matter cortical surface that is innervated by a given white matter fibre bundle, so this analysis produced a set of 42 innervation patterns, corresponding to the 42 known major white matter bundles in human and macaque.

The NMF and XTRACT results were then compared to assess similarity of innervation patterns, using a Pearson’s correlation applied to vectorised data, implemented via Python’s *numpy* library. This approach is well-suited for characterising standardised covariance between two sets of values (Rodgers & Nicewander, 1988), and has been used previously to assess the performance of data-

driven tractography in human brains (Thompson et al., 2020). Furthermore, Pearson's correlation was deemed appropriate here due to the identical structure between the two matrices being compared. The ordering of data points comprising a given NMF-derived component or XTRACT-derived tract within a brain is identical between both sets of decompositions, such that a given cell corresponds to the same grey matter region across both matrices. Given the univariate nature of each matrix in our datasets, multivariate matrix correlation measures such as the RV-coefficient (Kherif et al., 2003; Robert & Escoufier, 1976) would have been inappropriate. After the calculation of a correlation between each NMF-derived component and each XTRACT-derived tract, maximal correlations were identified for each XTRACT-derived tract and plotted using custom Python and R scripts.

3. Results

Non-negative matrix factorisation (NMF) can be used to perform data-driven tractography and at large participant numbers, the output closely resembles known white matter tracts in human brains (Thompson et al., 2020). Here, we extend this finding in two ways. First, we demonstrate that even within a single subject, NMF can reproduce known white matter tracts. Second, we demonstrate that NMF is capable of reproducing known white matter tracts in the macaque brain, also at a sample size of $n = 1$.

3.1. NMF output recapitulates known white matter tracts in human and macaque, at small sample sizes

NMF and related algorithms require users to specify a number of components for parcellation. To assess the effect of component number on the coherence between NMF output and atlas-based tractography, we decomposed connectivity matrices via NMF while specifying component values of $K = 10$, 50, 60, 100, and 200. Each NMF component corresponds to a white matter volumetric map and a grey matter surface endpoint map, representing the grey matter regions innervated by the fibre bundles comprising the white matter map. We used a Pearson's correlation to compare grey matter surface endpoint maps for all NMF components with connectivity maps for known white matter tracts, identified using the XTRACT and XTRACT Blueprint atlas-based tractography protocols for human and macaque (Mars et al., 2018; Warrington et al., 2020).

For each white matter tract, we identified the single best-correlated NMF component at each component number, ranging from $K = 10$ through $K = 200$. These maximal correlations are presented for both species in Figure 3.2 and examples are presented in Figure 3.3. Tables 3.1 and 3.2 present the maximal correlational data on a per-tract basis. The minimum, median, and maximum of the maximal correlational values for each number of components are as follows (data visualised in Figure 3.2B). Human: $K = 10$: 0.04, 0.30, 0.77; $K = 50$: 0.17, 0.54, 0.76; $K = 60$: 0.17, 0.54, 0.76; $K = 100$: 0.26, 0.58, 0.81; $K = 200$: 0.18, 0.56, 0.85. Macaque: $K = 10$: 0.02, 0.14, 0.40; $K = 50$: 0.13, 0.38, 0.65; $K = 60$: 0.13, 0.40, 0.65; $K = 100$: 0.14, 0.42, 0.69; $K = 200$: 0.15, 0.42, 0.65. Overall, correlations were higher in the human brain than in

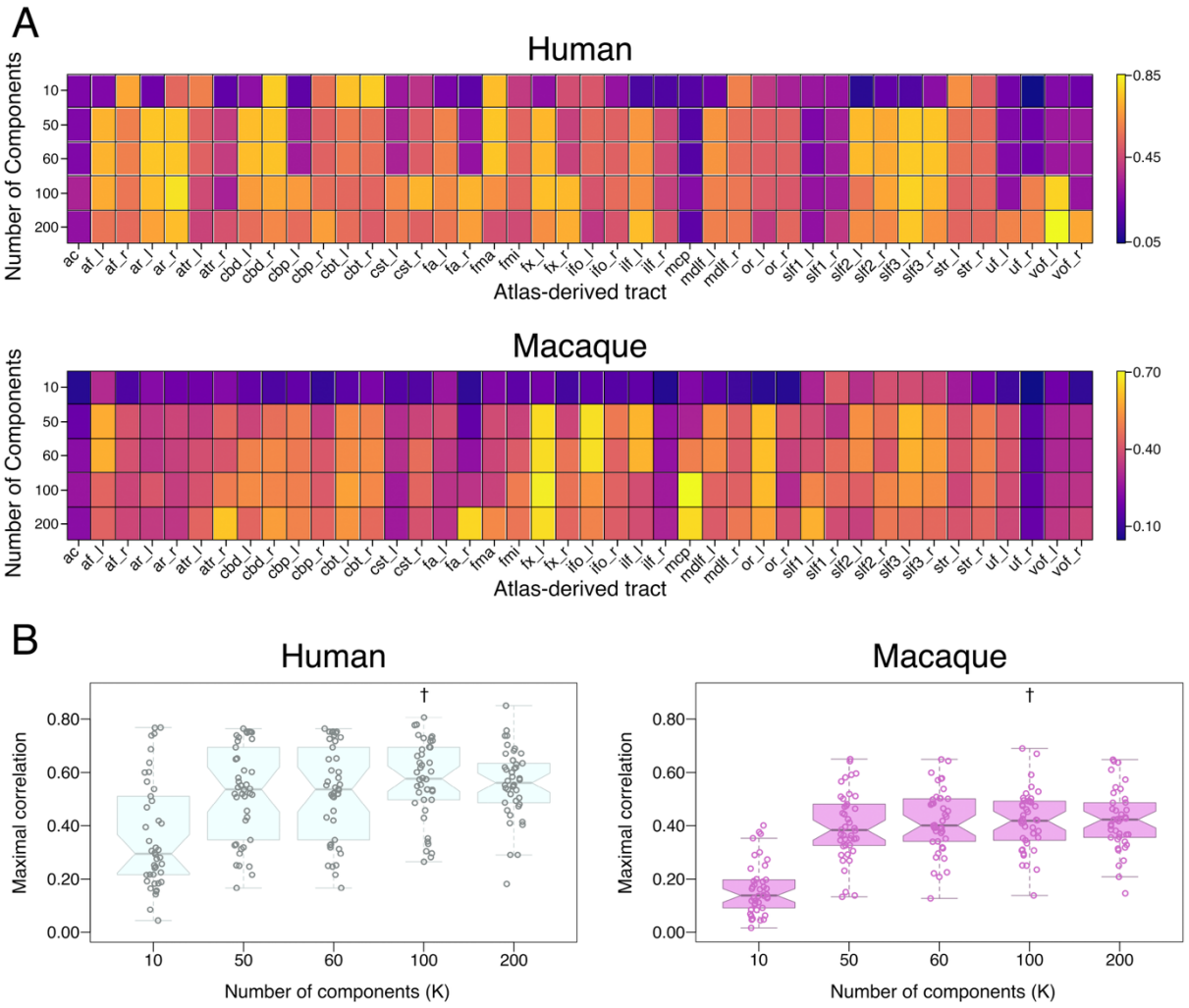


Figure 3.2. Quantitative comparison between NMF outputs and atlas-derived tracts. (A) *Correlation matrices between NMF components and atlas-derived tracks in human and macaque. Each column corresponds to a white matter tract identified via XTRACT protocols. Each cell represents the correlation between that tract's grey matter connectivity map and the best-matching NMF component. NMF was used to decompose each brain's connectivity matrix at* K *= 10, 50, 60, 100, and 200 components. Abbreviations are per Table 3.1.* ***(B)*** *Distributions of maximal correlations for different component numbers. Box-and-whisker plots show the distributions of maximal correlations for different numbers of components. Each marker represents one XTRACT-derived tract's correlation with its best-matching NMF component. Notches indicate the 95% confidence interval of the median (median ± 1.57 × IQR/$n^{0.5}$). † indicates the model order with the highest median among maximal correlations in each species.*

---

the macaque brain. For both species, the highest median among maximal correlations was at $K = 100$. Interestingly, the results at $K = 50$ and $K = 60$ were identical in

human, but not in macaque. This suggests that small changes to NMF hyperparameters may be affect decomposition in one brain, whilst remaining inconsequential in another. We note that the distributions of maximal correlations change as a function of component number similarly, across both human and macaque. In both species, $K = 10$ yielded the lowest maximal correlations between NMF-based components and XTRACT-derived tracts. Maximal correlations increased with higher model orders in both species, before peaking at $K = 100$ and plateauing

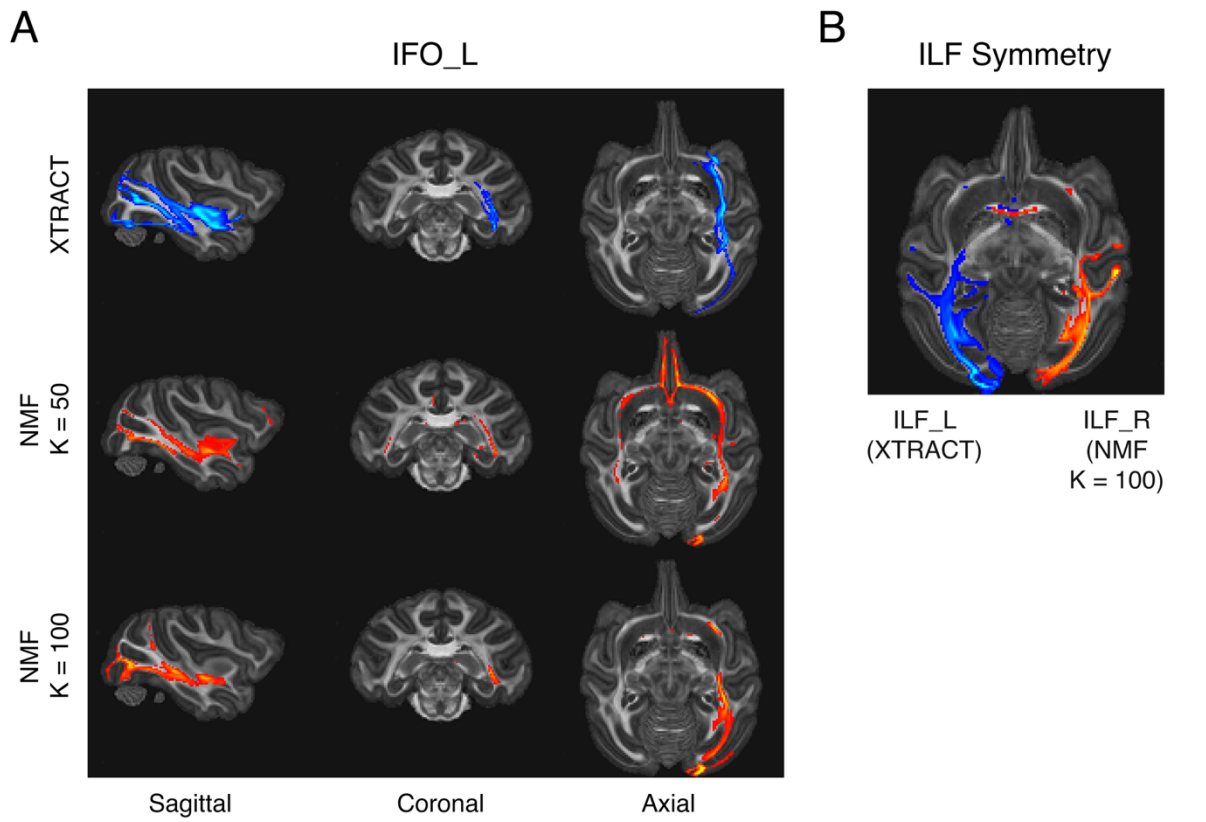


Figure 3.3. Visual anatomical characteristics of NMF-derived tracts in macaque. (A) *Comparison between XTRACT-derived left inferior fronto-occipital fasciculus (IFO_L) and NMF-derived IFO_L, at low and high component numbers. At* K *= 50, the NMF component which best corresponds to the IFO_L includes nonspecific white matter in the contralateral hemisphere and dorsal prefrontal cortex. At* K *= 100, the best-corresponding component comprises a posterior subsection of the IFO_L.* ***(B)*** *Visual symmetry between XTRACT-derived and NMF-derived inferior longitudinal fasciculi (ILFs), axial view. The shape and morphology of the NMF-derived ILF (right) closely mirrors that of the XTRACT-derived ILF (left), despite a modest correlation of* r *= 0.25 between the XTRACT- and NMF-derived right ILF.*

or slightly decreasing at $K = 200$. These results suggest that NMF-based, data-driven tractography has similar properties across both species.

Visualising the data, we observed that at low component numbers (i.e., $K = 50$ and 60), components tend to include white matter that is nonspecific to the tracts of interest and at high component numbers (i.e., $K = 100$ and 200), components are more likely to correspond to subdivisions of tracts, consistent with previous findings (Figure 3.3A; Thompson et al., 2020; see further discussion in Chapter 4). Despite the lower correlations reported for some XTRACT-derived tracts, visual inspection reveals generally good coherence between NMF-derived tracts and their XTRACT-derived counterparts. This is visualised in Figure 3.3B, using the example of the inferior longitudinal fasciculi (ILFs) in macaque. Despite a lower-than-average correlation of $r = 0.25$ with the XTRACT-derived right ILF, the best-matching NMF component at $K = 100$ shows good spatial and morphological symmetry with the left ILF that was identified via XTRACT. In other words, while the quantitative comparison suggests that the NMF-derived right ILF coheres worse than usual with the XTRACT-derived right ILF, anatomical examination reveals that the NMF-derived right ILF has the morphology one would expect.

To reconcile this apparent contradiction, it is helpful to note the lateral temporal projection of the NMF-derived ILF which shows much higher signal intensity than the corresponding projection reconstructed via XTRACT (Figure 3.3B). This difference in signal intensity pattern results in a deceptively modest correlation despite high visual morphological coherence between the two methods' outputs, emphasising the need to incorporate data visualisation into NMF-based analyses.

Tract name	Abbrev-iation	10 comp.	50 comp.	60 comp.	100 comp.	200 comp.
Anterior commissure	ac	0.25	0.25	0.25	0.35	0.29
Arcuate fasciculus (left)	af_l	0.25	0.72	0.72	0.70	0.57
Arcuate fasciculus (right)	af_r	0.69	0.60	0.60	0.58	0.55
Acoustic radiation (left)	ar_l	0.22	0.75	0.75	0.74	0.68
Acoustic radiation (right)	ar_r	0.54	0.75	0.75	0.81	0.74
Anterior thalamic radiation (left)	atr_l	0.60	0.52	0.52	0.46	0.44
Anterior thalamic radiation (right)	atr_r	0.19	0.42	0.42	0.34	0.48
Cingulum subsection: dorsal (left)	cbd_l	0.28	0.74	0.74	0.67	0.55
Cingulum subsection: dorsal (right)	cbd_r	0.77	0.75	0.75	0.70	0.62
Cingulum subsection: perigenual (left)	cbp_l	0.18	0.33	0.33	0.66	0.55
Cingulum subsection: perigenual (right)	cbp_r	0.57	0.52	0.52	0.55	0.67
Cingulum subsection: temporal (left)	cbt_l	0.75	0.58	0.58	0.54	0.55
Cingulum subsection: temporal (right)	cbt_r	0.77	0.56	0.56	0.53	0.51
Corticospinal tract (left)	cst_l	0.32	0.35	0.35	0.62	0.57
Corticospinal tract (right)	cst_r	0.40	0.51	0.51	0.72	0.52
Frontal aslant (left)	fa_l	0.24	0.61	0.61	0.63	0.58
Frontal aslant (right)	fa_r	0.18	0.30	0.30	0.72	0.67
Forceps major	fma	0.74	0.75	0.75	0.64	0.47
Forceps minor	fmi	0.42	0.53	0.53	0.54	0.46
Fornix (left)	fx_l	0.29	0.73	0.73	0.74	0.64
Fornix (right)	fx_r	0.47	0.43	0.43	0.73	0.70
Inferior fronto-occipital fasciculus (left)	ifo_l	0.49	0.54	0.54	0.49	0.40
Inferior fronto-occipital fasciculus (right)	ifo_r	0.30	0.52	0.52	0.55	0.49
Inferior longitudinal fasciculus (left)	ilf_l	0.14	0.65	0.65	0.64	0.74
Inferior longitudinal fasciculus (right)	ilf_r	0.15	0.46	0.46	0.43	0.49
Middle cerebellar peduncle	mcp	0.17	0.17	0.17	0.27	0.18
Middle longitudinal fasciculus (left)	mdlf_l	0.22	0.65	0.65	0.60	0.60

Middle longitudinal fasciculus (right)	mdlf_r	0.60	0.55	0.55	0.58	0.58
Optic radiation (left)	or_l	0.41	0.51	0.51	0.50	0.42
Optic radiation (right)	or_r	0.34	0.52	0.52	0.50	0.54
Superior longitudinal fasciculus 1 (left)	slf1_l	0.31	0.25	0.25	0.30	0.29
Superior longitudinal fasciculus 1 (right)	slf1_r	0.31	0.33	0.33	0.33	0.41
Superior longitudinal fasciculus 2 (left)	slf2_l	0.09	0.73	0.73	0.57	0.63
Superior longitudinal fasciculus 2 (right)	slf2_r	0.19	0.70	0.70	0.69	0.62
Superior longitudinal fasciculus 3 (left)	slf3_l	0.16	0.77	0.77	0.78	0.76
Superior longitudinal fasciculus 3 (right)	slf3_r	0.28	0.75	0.75	0.73	0.65
Superior thalamic radiation (left)	str_l	0.64	0.57	0.57	0.53	0.53
Superior thalamic radiation (right)	str_r	0.51	0.54	0.54	0.54	0.54
Uncinate fasciculus (left)	uf_l	0.23	0.25	0.25	0.28	0.61
Uncinate fasciculus (right)	uf_r	0.04	0.22	0.22	0.60	0.62
Vertical occipital fasciculus (left)	vof_l	0.26	0.31	0.31	0.78	0.85
Vertical occipital fasciculus (right)	vof_r	0.22	0.32	0.32	0.31	0.69

Table 3.1. Best-matching NMF components per tract, human. *Table of Pearson correlation coefficient values for the best-matching NMF components, for each atlas-identified white matter tract. These data are visualised in Figure 3.2.*

3.2. NMF output effectively reconstructs different tracts at different component numbers

In both the human and macaque brain, the median correlation between tracts and their best-matching components increased slightly above $K = 60$, suggesting that decomposition should be run with higher component numbers in large primate brains, like the ones analysed here. However, it is important to note that the component number which produced the best-matching component varied on a per-

tract basis. For example, in the human brain, the best-matching component for the left superior thalamic radiation (str_l) was found at $K = 10$ components ($r = 0.64$) while the best-matching components for the left and right optic radiation (or_l, or_r) were found at 50/60 components ($r = 0.51$) and 200 components ($r = 0.54$), respectively. In macaque, the left inferior fronto-occopital fasciculus (ifo_l) was best reconstructed at $K = 50/60$ ($r = 0.65$), while the right frontal aslant (fa_r) found a much higher correlation at $K = 200$ ($r = 0.64$) than at any other component number ($r \leq 0.31$).

In sum, these results indicate that there is no global optimal parameter set for NMF-based tractography. The best configuration with which to reconstruct a particular tract in a given brain must be experimentally validated and cannot necessarily be predicted based on other tract reconstructions in the same brain.

4. Discussion

This chapter has used a data-driven approach to reconstruct known white matter tracts in human and macaque. Extending previous work, we show for the first time that non-negative matrix factorisation (NMF) can be used to perform data-driven tractography in human and non-human brains, even at a sample size of $n = 1$. In the absence of anatomical priors sufficient to specify exclusion masks and other

Tract name	Abbrev-iation	10 comp.	50 comp.	60 comp.	100 comp.	200 comp.
Anterior commissure	ac	0.05	0.15	0.21	0.24	0.21
Arcuate fasciculus (left)	af_l	0.29	0.57	0.57	0.42	0.42
Arcuate fasciculus (right)	af_r	0.11	0.39	0.38	0.35	0.36
Acoustic radiation (left)	ar_l	0.20	0.32	0.31	0.39	0.33

Acoustic radiation (right)	ar_r	0.16	0.35	0.34	0.33	0.32
Anterior thalamic radiation (left)	atr_l	0.16	0.33	0.37	0.38	0.42
Anterior thalamic radiation (right)	atr_r	0.20	0.42	0.39	0.47	0.61
Cingulum subsection: dorsal (left)	cbd_l	0.14	0.35	0.48	0.50	0.43
Cingulum subsection: dorsal (right)	cbd_r	0.10	0.44	0.50	0.49	0.54
Cingulum subsection: perigenual (left)	cbp_l	0.14	0.47	0.46	0.48	0.49
Cingulum subsection: perigenual (right)	cbp_r	0.07	0.33	0.39	0.40	0.42
Cingulum subsection: temporal (left)	cbt_l	0.13	0.50	0.50	0.55	0.52
Cingulum subsection: temporal (right)	cbt_r	0.18	0.48	0.50	0.50	0.43
Corticospinal tract (left)	cst_l	0.12	0.29	0.30	0.25	0.25
Corticospinal tract (right)	cst_r	0.11	0.35	0.44	0.43	0.38
Frontal aslant (left)	fa_l	0.24	0.37	0.32	0.31	0.31
Frontal aslant (right)	fa_r	0.06	0.14	0.22	0.31	0.64
Forceps major	fma	0.19	0.36	0.35	0.35	0.50
Forceps minor	fmi	0.13	0.34	0.40	0.47	0.46
Fornix (left)	fx_l	0.17	0.64	0.64	0.67	0.65
Fornix (right)	fx_r	0.09	0.35	0.45	0.45	0.43
Inferior fronto-occipital fasciculus (left)	ifo_l	0.14	0.65	0.65	0.52	0.49
Inferior fronto-occipital fasciculus (right)	ifo_r	0.12	0.46	0.42	0.42	0.40
Inferior longitudinal fasciculus (left)	ilf_l	0.14	0.58	0.58	0.37	0.37
Inferior longitudinal fasciculus (right)	ilf_r	0.04	0.23	0.23	0.25	0.27
Middle cerebellar peduncle	mcp	0.19	0.27	0.48	0.69	0.64
Middle longitudinal fasciculus (left)	mdlf_l	0.13	0.51	0.51	0.42	0.40
Middle longitudinal fasciculus (right)	mdlf_r	0.08	0.41	0.40	0.41	0.46
Optic radiation (left)	or_l	0.05	0.60	0.60	0.59	0.54
Optic radiation (right)	or_r	0.05	0.40	0.34	0.29	0.37
Superior longitudinal fasciculus 1 (left)	slf1_l	0.27	0.36	0.38	0.49	0.57

Superior longitudinal fasciculus 1 (right)	slf1_r	0.40	0.31	0.43	0.44	0.37
Superior longitudinal fasciculus 2 (left)	slf2_l	0.30	0.51	0.50	0.41	0.34
Superior longitudinal fasciculus 2 (right)	slf2_r	0.38	0.45	0.39	0.49	0.46
Superior longitudinal fasciculus 3 (left)	slf3_l	0.37	0.59	0.58	0.53	0.44
Superior longitudinal fasciculus 3 (right)	slf3_r	0.35	0.52	0.54	0.50	0.43
Superior thalamic radiation (left)	str_l	0.25	0.38	0.39	0.36	0.39
Superior thalamic radiation (right)	str_r	0.17	0.47	0.48	0.46	0.43
Uncinate fasciculus (left)	uf_l	0.08	0.39	0.39	0.37	0.36
Uncinate fasciculus (right)	uf_r	0.02	0.13	0.13	0.14	0.15
Vertical occipital fasciculus (left)	vof_l	0.16	0.27	0.28	0.30	0.31
Vertical occipital fasciculus (right)	vof_r	0.06	0.29	0.28	0.31	0.35

Table 3.2. Best-matching NMF components per tract, macaque. *Table of Pearson correlation coefficient values for the best-matching NMF components, for each atlas-identified white matter tract. These data are visualised in Figure 3.2.*

criteria for atlas-based tractography, this technique will enable researchers to compare white matter organisation across species.

By performing atlas-based tractography and data-driven tractography in the same brains, we were able to benchmark the performance of our NMF-based pipeline against the current "gold standard" methodology for the reconstruction of white matter tracts from neuroimaging data. NMF decomposition was generally able to faithfully reproduce white matter tracts identified via atlas-based methods in both the human and the macaque. However, it is worth noting that both approaches are subject to the concerns inherent to the usage of tractography to infer white matter connectivity. Although correlations between NMF-derived components and atlas-

derived tracts in the human brain are similar in magnitude to what has been reported previously (Thompson et al., 2020), correlation values in the macaque were lower, which may reflect different aspects of the data sources, acquisition, and processing. First, the macaque brain is smaller than the human brain; this difference in brain sizes necessitates the usage of different tractographic parameters, including streamline step size. Second, while the resolution of scans was comparable between brains, the spatial resolution, angular resolution, and number of shells of each scan did indeed differ between species. Third, the macaque brain, unlike the human brain, was scanned *ex vivo* following fixation in formalin. Formalin fixation is known to cause a reduction in overall diffusivity, though this reduction appears to be uniform across the brain, thus leaving anisotropy values unchanged (Sun et al., 2005). Formalin fixation of the brain is thus unlikely to have unduly affected tractography, but the possibility should be considered nonetheless. Finally, only five NMF decomposition component numbers were tested due to computational constraints, with K values ranging from 10 to 200. It is possible that the macaque brain would have benefited from a decomposition with a different number of components from those tested here.

Nonetheless, even when NMF decomposition yielded components with lower correlation values with a given tract, visual inspection revealed that the anatomical features of the best-matching NMF component cohere reasonably with the known tract, emphasising the need for visual inspection of NMF output in any analysis workflows. Visual inspection additionally confirmed the prior finding (Thompson et al., 2020) that lower component numbers tended to produce components which included white matter that is nonspecific to tracts of interest, and higher component

numbers tended to produce components corresponding to subdivisions of tracts. However, it is important to note that within a single brain, tracts differed in which component number yielded the best reconstruction, suggesting there is no universal optimum number of components for NMF decomposition in a given brain.

By performing tractography on a single brain, these results represent a "worst-case" scenario. With sample sizes far greater than those presented here, Thompson and colleagues (2020) are able to present much higher correlations between NMF-derived connections and atlas-derived tracts in the human brain. In light of the reasonable correlation we find between NMF decomposition and atlas-based tractography with a sample size of one brain per species, our results paint an optimistic picture for the future of data-driven tractography, both in humans and in non-human species.

More generally, our results demonstrate how data-driven methods for analysing complex neuroimaging data can be used to test hypotheses in comparative neuroscience. Large-scale comparative anatomy is now possible through the increasing availability of high-quality, whole-brain imaging data from a range of species, including many primates (Assaf et al., 2020; Tendler et al., 2022). The availability of these data presents both opportunities and challenges, as many of the species from which data are now available have been studied only sparsely. The use of a data-driven approach such as NMF opens the possibility of interrogating these data without losing sight of anatomical rigour. Indeed, Chapters 4 and 5 of this thesis apply the NMF-based analysis pipeline developed here to four non-human primate brains, to test hypotheses about the evolution of white matter across the primate lineage.

References

Aitman, T. J., Boone, C., Churchill, G. A., Hengartner, M. O., Mackay, T. F. C., & Stemple, D. L. (2011). The future of model organisms in human disease research. *Nature Reviews Genetics*, *12*(8), 575–582. https://doi.org/10.1038/nrg3047

Anderson, K. V., & Ingham, P. W. (2003). The transformation of the model organism: A decade of developmental genetics. *Nature Genetics*, *33*(3), 285–293. https://doi.org/10.1038/ng1105

Assaf, Y., Bouznach, A., Zomet, O., Marom, A., & Yovel, Y. (2020). Conservation of brain connectivity and wiring across the mammalian class. *Nature Neuroscience*, *23*(7), 805–808. https://doi.org/10.1038/s41593-020-0641-7

Assimopoulos, S., Warrington, S., Bryant, K. L., Pszczolkowski, S., Jbabdi, S., Mars, R. B., & Sotiropoulos, S. N. (2024). Generalising XTRACT tractography protocols across common macaque brain templates. *Brain Structure and Function*. https://doi.org/10.1007/s00429-024-02760-0

Behrens, T. E. J., Berg, H. J., Jbabdi, S., Rushworth, M. F. S., & Woolrich, M. W. (2007). Probabilistic diffusion tractography with multiple fibre orientations: What can we gain? *NeuroImage*, *34*(1), 144–155. https://doi.org/10.1016/j.neuroimage.2006.09.018

Benn, R. A., Xu, T., Mars, R. B., Boch, M., Roumazeilles, L., Heuer, K., Toro, R., Margulies, D. S., Manzano-Patron, J. P., Montesinos, P., Galan-Arriola, C., Lopez-Martin, G., Sanchez-Gonzalez, J., Duff, E. P., & Ibañez, B. (2025). *Precon_all: A species-agnostic automated pipeline for non-human cortical surface*

reconstruction (p. 2025.04.16.649072). bioRxiv. https://doi.org/10.1101/2025.04.16.649072

Boutsidis, C., & Gallopoulos, E. (2008). SVD based initialization: A head start for nonnegative matrix factorization. *Pattern Recognition*, *41*(4), 1350–1362. https://doi.org/10.1016/j.patcog.2007.09.010

Bryant, K. L., Ardesch, D. J., Roumazeilles, L., Scholtens, L. H., Khrapitchev, A. A., Tendler, B. C., Wu, W., Miller, K. L., Sallet, J., van den Heuvel, M. P., & Mars, R. B. (2021). Diffusion MRI data, sulcal anatomy, and tractography for eight species from the Primate Brain Bank. *Brain Structure and Function*, *226*(8), 2497–2509. https://doi.org/10.1007/s00429-021-02268-x

Bryant, K. L., Camilleri, J., Warrington, S., Freches, G. B., Sotiropoulos, S. N., Jbabdi, S., Eickhoff, S., & Mars, R. B. (2025). Connectivity Profile and Function of Uniquely Human Cortical Areas. *Journal of Neuroscience*, *45*(15). https://doi.org/10.1523/JNEUROSCI.2017-24.2025

Bryant, K. L., Li, L., Eichert, N., & Mars, R. B. (2020). A comprehensive atlas of white matter tracts in the chimpanzee. *PLOS Biology*, *18*(12), e3000971. https://doi.org/10.1371/journal.pbio.3000971

Bryant, K. L., Manger, P. R., Bertelsen, M. F., Khrapitchev, A. A., Sallet, J., Benn, R. A., & Mars, R. B. (2024). A map of white matter tracts in a lesser ape, the lar gibbon. *Brain Structure and Function*, *229*(8), 1839–1854. https://doi.org/10.1007/s00429-023-02709-9

Fischl, B. (2012). FreeSurfer. *NeuroImage*, *62*(2), 774–781. https://doi.org/10.1016/j.neuroimage.2012.01.021

Hoyer, P. O. (2004). Non-negative Matrix Factorization with Sparseness Constraints. *Journal of Machine Learning Research*, *5*(Nov), 1457–1469.

Jenkinson, M., Beckmann, C. F., Behrens, T. E. J., Woolrich, M. W., & Smith, S. M. (2012). FSL. *NeuroImage*, *62*(2), 782–790. https://doi.org/10.1016/j.neuroimage.2011.09.015

Jeurissen, B., Descoteaux, M., Mori, S., & Leemans, A. (2019). Diffusion MRI fiber tractography of the brain. *NMR in Biomedicine*, *32*(4), e3785. https://doi.org/10.1002/nbm.3785

Kherif, F., Poline, J.-B., Mériaux, S., Benali, H., Flandin, G., & Brett, M. (2003). Group analysis in functional neuroimaging: Selecting subjects using similarity measures. *NeuroImage*, *20*(4), 2197–2208. https://doi.org/10.1016/j.neuroimage.2003.08.018

Lange, F. J., Ashburner, J., Smith, S. M., & Andersson, J. L. R. (2020). A Symmetric Prior for the Regularisation of Elastic Deformations: Improved anatomical plausibility in nonlinear image registration. *NeuroImage*, *219*, 116962. https://doi.org/10.1016/j.neuroimage.2020.116962

Lee, D. D., & Seung, H. S. (1999). Learning the parts of objects by non-negative matrix factorization. *Nature*, *401*(6755), Article 6755. https://doi.org/10.1038/44565

Lee, D. D., & Seung, H. S. (2000). Algorithms for Non-negative Matrix Factorization. *Advances in Neural Information Processing Systems*, *13*. https://proceedings.neurips.cc/paper_files/paper/2000/hash/f9d1152547c0bde01830b7e8bd60024c-Abstract.html

Lin, C.-P., Wedeen, V. J., Chen, J.-H., Yao, C., & Tseng, W.-Y. I. (2003). Validation of diffusion spectrum magnetic resonance imaging with manganese-enhanced rat optic tracts and ex vivo phantoms. *NeuroImage*, *19*(3), 482–495. https://doi.org/10.1016/S1053-8119(03)00154-X

Liu, C., Ye, F. Q., Newman, J. D., Szczupak, D., Tian, X., Yen, C. C.-C., Majka, P., Glen, D., Rosa, M. G. P., Leopold, D. A., & Silva, A. C. (2020). A resource for the detailed 3D mapping of white matter pathways in the marmoset brain. *Nature Neuroscience*, *23*(2), 271–280. https://doi.org/10.1038/s41593-019-0575-0

Mars, R. B., O'Muircheartaigh, J., Folloni, D., Li, L., Glasser, M. F., Jbabdi, S., & Bryant, K. L. (2019). Concurrent analysis of white matter bundles and grey matter networks in the chimpanzee. *Brain Structure and Function*, *224*(3), 1021–1033. https://doi.org/10.1007/s00429-018-1817-8

Mars, R. B., Sotiropoulos, S. N., Passingham, R. E., Sallet, J., Verhagen, L., Khrapitchev, A. A., Sibson, N., & Jbabdi, S. (2018). Whole brain comparative anatomy using connectivity blueprints. *eLife*, *7*, e35237. https://doi.org/10.7554/eLife.35237

O'Muircheartaigh, J., & Jbabdi, S. (2018). Concurrent white matter bundles and grey matter networks using independent component analysis. *NeuroImage*, *170*, 296–306. https://doi.org/10.1016/j.neuroimage.2017.05.012

Pedregosa, F., Varoquaux, G., Gramfort, A., Michel, V., Thirion, B., Grisel, O., Blondel, M., Prettenhofer, P., Weiss, R., Dubourg, V., Vanderplas, J., Passos, A., Cournapeau, D., Brucher, M., Perrot, M., & Duchesnay, É. (2011). Scikit-learn:

Machine Learning in Python. *Journal of Machine Learning Research*, *12*(85), 2825–2830.

Robert, P., & Escoufier, Y. (1976). A Unifying Tool for Linear Multivariate Statistical Methods: The RV-Coefficient. *Journal of the Royal Statistical Society. Series C (Applied Statistics)*, *25*(3), 257–265. https://doi.org/10.2307/2347233

Rodgers, J. L., & Nicewander, W. A. (1988). Thirteen Ways to Look at the Correlation Coefficient. *The American Statistician*, *42*(1), 59–66. https://doi.org/10.2307/2685263

Rosa, M. G. P., & Tweedale, R. (2005). Brain maps, great and small: Lessons from comparative studies of primate visual cortical organization. *Philosophical Transactions of the Royal Society B: Biological Sciences*, *360*(1456), 665–691. https://doi.org/10.1098/rstb.2005.1626

Roumazeilles, L., Lange, F. J., Benn, R. A., Andersson, J. L. R., Bertelsen, M. F., Manger, P. R., Flach, E., Khrapitchev, A. A., Bryant, K. L., Sallet, J., & Mars, R. B. (2022). Cortical Morphology and White Matter Tractography of Three Phylogenetically Distant Primates: Evidence for a Simian Elaboration. *Cerebral Cortex*, *32*(8), 1608–1624. https://doi.org/10.1093/cercor/bhab285

Savadjiev, P., Campbell, J. S. W., Descoteaux, M., Deriche, R., Pike, G. B., & Siddiqi, K. (2008). Labeling of ambiguous subvoxel fibre bundle configurations in high angular resolution diffusion MRI. *NeuroImage*, *41*(1), 58–68. https://doi.org/10.1016/j.neuroimage.2008.01.028

Setsompop, K., Kimmlingen, R., Eberlein, E., Witzel, T., Cohen-Adad, J., McNab, J. A., Keil, B., Tisdall, M. D., Hoecht, P., Dietz, P., Cauley, S. F., Tountcheva, V., Matschl, V., Lenz, V. H., Heberlein, K., Potthast, A., Thein, H., Van Horn, J.,

Toga, A., … Wald, L. L. (2013). Pushing the limits of *in vivo* diffusion MRI for the Human Connectome Project. *NeuroImage*, *80*, 220–233. https://doi.org/10.1016/j.neuroimage.2013.05.078

Singh, M., & Wong, C.-W. (2010). Independent component analysis-based multifiber streamline tractography of the human brain. *Magnetic Resonance in Medicine*, *64*(6), 1676–1684. https://doi.org/10.1002/mrm.22509

Sun, S.-W., Neil, J. J., Liang, H.-F., He, Y. Y., Schmidt, R. E., Hsu, C. Y., & Song, S.-K. (2005). Formalin fixation alters water diffusion coefficient magnitude but not anisotropy in infarcted brain. *Magnetic Resonance in Medicine*, *53*(6), 1447–1451. https://doi.org/10.1002/mrm.20488

Tendler, B. C., Hanayik, T., Ansorge, O., Bangerter-Christensen, S., Berns, G. S., Bertelsen, M. F., Bryant, K. L., Foxley, S., van den Heuvel, M. P., Howard, A. F., Huszar, I. N., Khrapitchev, A. A., Leonte, A., Manger, P. R., Menke, R. A., Mollink, J., Mortimer, D., Pallebage-Gamarallage, M., Roumazeilles, L., … Miller, K. L. (2022). The Digital Brain Bank, an open access platform for post-mortem imaging datasets. *eLife*, *11*, e73153. https://doi.org/10.7554/eLife.73153

Thompson, E., Mohammadi-Nejad, A. R., Robinson, E. C., Andersson, J. L. R., Jbabdi, S., Glasser, M. F., Bastiani, M., & Sotiropoulos, S. N. (2020). Non-negative data-driven mapping of structural connections with application to the neonatal brain. *NeuroImage*, *222*, 117273. https://doi.org/10.1016/j.neuroimage.2020.117273

Van Essen, D. C., Smith, S. M., Barch, D. M., Behrens, T. E. J., Yacoub, E., & Ugurbil, K. (2013). The WU-Minn Human Connectome Project: An overview. *NeuroImage*, *80*, 62–79. https://doi.org/10.1016/j.neuroimage.2013.05.041

Varikuti, D. P., Genon, S., Sotiras, A., Schwender, H., Hoffstaedter, F., Patil, K. R., Jockwitz, C., Caspers, S., Moebus, S., Amunts, K., Davatzikos, C., & Eickhoff, S. B. (2018). Evaluation of non-negative matrix factorization of grey matter in age prediction. *NeuroImage*, *173*, 394–410. https://doi.org/10.1016/j.neuroimage.2018.03.007

Vickery, S., Patil, K. R., Dahnke, R., Hopkins, W. D., Sherwood, C. C., Caspers, S., Eickhoff, S. B., & Hoffstaedter, F. (2024). The uniqueness of human vulnerability to brain aging in great ape evolution. *Science Advances*, *10*(35), eado2733. https://doi.org/10.1126/sciadv.ado2733

Warrington, S., Bryant, K. L., Khrapitchev, A. A., Sallet, J., Charquero-Ballester, M., Douaud, G., Jbabdi, S., Mars, R. B., & Sotiropoulos, S. N. (2020). XTRACT - Standardised protocols for automated tractography in the human and macaque brain. *NeuroImage*, *217*, 116923. https://doi.org/10.1016/j.neuroimage.2020.116923

Yang, Z., & Oja, E. (2010). Linear and Nonlinear Projective Nonnegative Matrix Factorization. *IEEE Transactions on Neural Networks*, *21*(5), 734–749. https://doi.org/10.1109/TNN.2010.2041361

Chapter 4

An anthropoid/strepsirrhine divergence in ventral visual stream connectivity.

Declarations

Publication history

Parts of this chapter have previously been published in the following preprint, distributed under the terms of the Creative Commons Attribution-NonCommercial 4.0 International (CC BY-NC 4.0) license.

Hunt, J. E., Warrington., S., Roumazeilles, L., Jbabdi, S., Molnár, Z., Sotiropoulous, S. N., & Mars, R. B. (2025). An anthropoid/strepsirrhine divergence in ventral visual stream connectivity. *bioRxiv*. doi:10.1101/2025.05.19.653861

Contribution statement

JEH designed and carried out experiments, contributed to the NFacT toolbox, analysed data, interpreted results, drafted the manuscript, and produced all figures which appear in this chapter. SW and SNS created the NFacT toolbox and assisted with its implementation. LR preprocessed data. SJ assisted with analysis code for data preprocessing. ZM assisted in editing of the manuscript and designing figures. RBM designed experiments, assisted with data analysis and interpretation, assisted in editing the manuscript and designing figures, and supervised the project.

Acknowledgements

JEH is funded by a Wellcome Trust Doctoral Studentship in Neuroscience (222368/Z/21/Z). The Wellcome Centre for Integrative Neuroimaging is supported by core funding from the Wellcome Trust (203139/Z/16/Z). SW and SNS acknowledge funding from the European Research Council (ERC Consolidator 101000969 to SNS). RBM is supported by the Biotechnology and Biological Sciences Research Council UK (BB/N019814/1). The funders had no role in the design or writing of this report, nor in the collection, analysis, and interpretation of data.

Abstract

The ventral visual stream has undergone extensive reorganisation within the primate lineage. While some work has examined restructuring of the ventral prefrontal cortical grey matter across primates, comparative studies of white matter connectivity are lacking primarily due to difficulties in data acquisition and processing. Here, we apply the data-driven approach developed in the previous chapter to study white matter connectivity across three primate species, using post-mortem diffusion MRI data.

Using this technique, we reconstruct anterior temporal-frontal and occipitotemporal-frontal connections across two anthropoids and one strepsirrhine: the rhesus macaque, the black-capped squirrel monkey, and the ring-tailed lemur. We find that the anthropoids exhibit a broader range of prefrontal innervation from these ventral visual connections. This study supports the hypothesis that anthropoid primates underwent extensive reorganisation of both grey and white matter during their emergence as visual foragers in a complex ecological niche.

Furthermore, we quantify the extent of between-species variance compared with other sources of variance in this dataset, showing that the variation between species far outweighs that arising from individual differences or analysis parameterization. This result provides an important validation of earlier studies on between-species differences in connectivity.

1. Introduction: The visual primate brain

Primates are thought to have descended from a common ancestor adapted for life in the fine branches of trees, who developed a leaping-grasping form of locomotion and used frontally directed eyes to guide visual foraging (Cartmill, 1992; Fleagle, 2013; Kaas et al., 2021). This visuomotor history is reflected in the anatomical organisation of the primate brain. Variations in the size of the brain and of aspects of the visual system across the primate order are correlated with the visual specialisations of the different lineages (Barton, 1998). Anthropoid primates in particular moved into the daylight foraging niche, developed a fovea for highly detailed vision, and, in some lineages, trichromatic vision (Williams et al., 2010). As the organisation of an organism's visual system reflects its ecological niche (Hunt et al., 2024), these anthropoid visual specialisations would be expected to be reflected in the organisation of the cortical visual pathways in anthropoids. One particularly prominent aspect of the primate visual system is the existence of two cortical pathways in the neocortex. Starting in the striate visual cortex, two visual pathways process different aspects of visual information (Baizer et al., 1991; Goodale & Milner, 1992). The dorsal pathway processes visual information for visually guided actions (Rizzolatti & Matelli, 2003), and is believed to have evolved in primates to incorporate primary visual cortical inputs to the posterior parietal cortex via the middle temporal visual area (Kaas & Baldwin, 2020). The ventral pathway to inferior temporal cortex was traditionally seen as important in object recognition or more generally the processing of object representations (Kravitz et al., 2013). However, while the dorsal stream is relatively well studied and its role in the visuomotor niche of primates is well understood, the variation and role of the ventral stream are less

often interpreted within such an ecological framework. Recently, however, Murray and colleagues proposed that the role of the ventral stream can be understood in this context as providing the visual context (Murray et al., 2017). They proposed that the inferior temporal cortex provides this information to ventral parts of the prefrontal cortex to guide decision making during foraging and that the ventral stream connections are particularly elaborated upon in anthropoids (Eldridge et al., 2021). We undertake a study to provide a first test of this hypothesis.

In primates, the orbitofrontal cortex and the ventrolateral prefrontal cortex receive the bulk of the prefrontal inputs from the ventral visual stream. The ventrolateral prefrontal cortex is argued to have emerged in the anthropoid lineage (Eldridge et al., 2021), though it is also possible that it existed prior to anthropoids and has simply expanded dramatically in anthropoids. In either case, whether the ventrolateral prefrontal cortex is reduced or absent in the strepsirrhines, this model of ventral stream evolution yields a prediction that the orbitofrontal cortex receives a relatively larger share of ventral stream inputs in strepsirrhines, and a relatively smaller share of such inputs in anthropoids. The present chapter seeks to test these predictions.

Understanding the anthropoid elaborations of the general primate neural infrastructure for visuomotor processing requires methods that can study these pathways in a range of species, relatively fast, and at reasonable costs. Detailed tracer studies, although commonly hailed as the gold standard, still face substantial challenges: they require sacrifice of numerous animals per species, are expensive, and are time- and labour-intensive (Nectow & Nestler, 2020). In contrast, recent advances in neuroimaging allow high quality, whole brain data to be collected relatively

cheaply either in vivo or from post-mortem brains that are not sacrificed specifically for scientific research (Prescott & Poirier, 2021; Thiebaut de Schotten et al., 2019). Diffusion MRI and related tractography methods in particular have proven successful for comparing brain organisation across species (Hecht et al., 2013; Mars et al., 2018). However, the challenge of such studies is that the brains under investigation are often little studied and have fewer ready-made processing tools available. Standard atlas-based tractography protocols can be used to extract specific pathways, but only if researchers already know a connection's origin, course, and termination. Such knowledge is increasingly available in human and macaque (Assimopoulos et al., 2024; Warrington et al., 2020), but by and large absent in other species. As such, without the substantial foreknowledge required for *a priori* specification of masks and logical operations, a discovery approach is needed to compare brain organisation across species. Exploratory methods for analysing MRI data are well-established (O'Muircheartaigh & Jbabdi, 2018; Singh & Wong, 2010), though their use in comparative studies is still relatively rare (Mars et al., 2019). Data-driven approaches, such as the non-negative matrix factorisation (NMF; Lee & Seung, 1999, 2000)-based approach investigated in the previous chapter, open the unique possibility of interrogating data in lesser-studied species without losing sight of anatomical rigour.

Here, we reconstruct ventral visual stream connections in the brains of three primate species: the anthropoid Old World macaque monkey, the anthropoid New World squirrel monkey, and the strepsirrhine ring-tailed lemur. We use an unsupervised decomposition algorithm based on NMF to extract connectivity components based on the tractographic inference of white matter trajectories and cortical endpoints (Thompson et al., 2020). We then identify components comprising

connections between the temporal and prefrontal cortices and connections between the visual and prefrontal cortices in each species. We predict that among these connections, prefrontal innervation is mostly confined to the orbitofrontal cortex in the lemur, but extends more dorsally in the anthropoid primates.

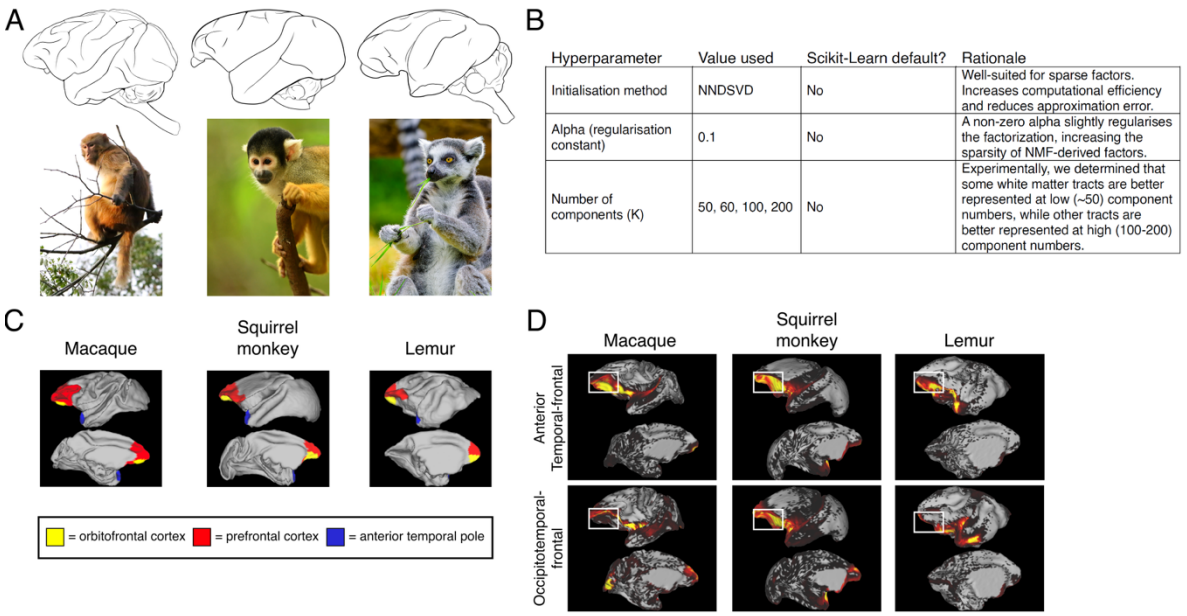


Figure 4.1. Study overview. (A) *Diffusion MRI data were collected in three species (left-to-right): the rhesus macaque, the black-capped squirrel monkey, and the ring-tailed lemur. Above: drawing of each brain's left hemisphere, lateral aspect. Below: photographic illustration of each species.* ***(B)*** *The following NMF hyperparameters were modified from default values: initialisation method, regularisation constant (i.e., alpha), and number of components (*K*).* ***(C)*** *Binary masks were drawn on each cortical surface to specify regions of interest. Note that the prefrontal cortical mask includes all of the orbitofrontal cortical mask, as well as additional regions as indicated by colour.* ***(D)*** *Depth of prefrontal innervation was visualised and quantitatively compared across species. Each image shows a left-hemisphere brain surface with an example NMF grey matter map overlaid. White boxes illustrate qualitatively that ventral visual stream connections in lemur innervate less dorsal prefrontal cortex than in macaque and squirrel monkey. A quantitative comparison of prefrontal innervation patterns is presented in Results and Figure 4.4.*

2. Methods

2.1. Data sources

This study used an existing postmortem primate dataset, whose acquisition and early processing has been previously described by Roumazeilles et al. (2022). We used nine post-mortem brains obtained from Copenhagen Zoo, the Zoological Society of London, and the primate research facility at the University of Oxford. These brains (Figure 4.1A) comprise three rhesus macaques (*M. mulatta*; 1 female, 2 males; aged 11-15 years), the first of which was analysed in the previous chapter; three black-capped squirrel monkeys (*S. boliviensis*; 1 female, 2 males; aged 2-9 years); and three ring-tailed lemurs (*L. catta*, 3 males; aged 3-11 years).

Brains were extracted and formalin fixed. No evidence of neuropathology was found in any of the brains studied. Brains were stored in formalin or a phosphate-buffer saline (PBS) solution. Further details of the brain extraction and storage protocols are reported in Roumazeilles et al. (2022).

2.2. Data acquisition and preprocessing

Imaging data were collected for all brains using a 7-tesla preclinical MRI scanner (Varian, Oxford UK). All brains were rehydrated in a phosphate buffer for one week prior to scanning, and scanned in Fomblin or Fluorinert. The 7T preclinical scanner used for data acquisition (Varian, Oxford UK) has a birdcage transmit/receive coil with an inner diameter of 72 mm (Rapid Biomedical GmbH, Rimpar Germany).

To minimise image distortions, all 2-D diffusion-weighted images were collected using a spin-echo multi-slice (DW-SEMS) protocol with single line readout.

Data are high spatial resolution, at 0.5 mm isotropic resolution for lemurs and squirrel monkeys and 0.6 mm isotropic resolution for macaques, with a single-shell protocol. The acquisition parameters are as follows: TE/TR = 26 ms/10 s; matrix size = 128x128 (variable number of slices); b = 0 s/mm^2 (non-diffusion-weighted; 16 volumes), 4000 s/mm^2 (diffusion-weighted, 128 volumes). Data quality characteristics including computed signal-to-noise ratio, mean fractional anisotropy, and mean diffusivity are computed and reported for each individual by Roumazeilles et al. (2022).

All data were preprocessed as described by Roumazeilles et al. (2022). Diffusion MRI data were preprocessed using the phoenix module of the in-house MR Comparative Anatomy Toolbox (Mr Cat; www.neuroecologylab.org), which relies on FSL (Jenkinson et al., 2012; www.fmrib.ox.ac.uk/fsl). A three-fibre ball and stick model was then fitted to the data using FSL's BedpostX (Behrens et al., 2007). Species-specific brain templates were then created using multimodal iterative registration using the MMORF pipeline (Lange et al., 2020). A cortical surface representation of each template was created using the precon_all (Benn et al., 2025; github.com/neurabenn/precon_all) adaptation of Freesurfer's recon-all pipeline (Fischl, 2012) and downsampled to 10,000 vertices per hemisphere.

2.3. Data-driven tractography

We performed data-driven connection mapping using non-negative matrix factorisation (NMF; Lee & Seung, 1999, 2000), the properties of which are discussed in more detail in the previous chapter. As before, NMF was run via the NFacT toolbox in Python (Thompson et al., 2020; github.com/SPMIC-UoN/NFacT), which is a

tractography-focused wrapper for Scikit-learn's (Pedregosa et al., 2011) NMF algorithm. NMF was run on a group average of the three brains from each species, and results were then regressed back to individual brains.

As in the previous chapter, NMF hyperparameters were selected according to the default parameters in the Scikit-learn Python package, version 1.7, with the exception of hyperparameters controlling initialisation, regularisation, and component number (Figure 4.1B). NMF was initialised using the "non-negative double singular value decomposition" (NNDSVD) method (Boutsidis & Gallopoulos, 2008) and the regularization terms "alpha_W" and "alpha_H" were changed from the default of 0.0 to 0.1, as before. Finally, we specified the number of components (K) to be used in decomposition. In the previous chapter, we reported that there is no universally optimal number of components to reconstruct white matter tracts in a given brain. As such, we once again performed NMF decomposition with several component numbers: $K = 50$, 60, 100, and 200 components.

To generate the input data for NMF, probabilistic tractography (Behrens et al., 2007) was run from the cortical surface towards the white matter to create a connectivity matrix, wherein each row corresponds to a surface-based (vertex) seed and each column to a volume-based (voxel) target. Individual subject matrices were produced with 10,000 seed points, 1,000 samples per seed, and a step length of 0.2 mm with distance correction applied, then averaged across individuals of each species. The average connectivity matrix was then decomposed via NMF into two matrices: one comprising white matter by components and one comprising components by grey matter. Thus, for each resultant component, both a grey matter surface array of vertices and a volumetric representation of the component's white

matter voxels were produced. These matrices were then regressed from the group decomposition to subject-level decomposition to achieve the individual decomposition data used in subsequent analysis.

2.4. Tractography comparison

To identify whether NMF-based, data-driven tractography shows better performance in the macaque with a sample size of three brains, we also performed atlas-based tractography using the macaque brains and performed a similar comparison to that reported in the previous chapter, using the dataset of three macaque brains. We ran probabilistic tractography on a set of 42 combinations of seed, waypoint, and exclusion masks designed to reliably identify the major white matter bundles in the macaque brain, as implemented in the FSL tool XTRACT (Warrington et al., 2020). We then ran XTRACT Blueprint (Mars et al., 2018; Warrington et al., 2020) to generate surface-space connectivity blueprints. The NMF and XTRACT results were then compared as before, using a Pearson's correlation implemented in Python's *numpy* library (Harris et al., 2020), to generate a correlation matrix and identify maximal correlations for each tract. In addition to the decomposition at $K = 50$, 60, 100, and 200 reported throughout the rest of this chapter, we additionally performed NMF decomposition at $K = 10$ for the XTRACT comparison, to maintain parity with the analysis described in the previous chapter. NMF performance was visualised and described using R (R Core Team, 2025).

Finally, we directly compared the performance of NMF decomposition at reconstructing each tract with an n of one brain compared to an n of three brains, using the single-macaque decomposition data reported in the previous chapter as well

as the group average of the three macaque brains analysed here. We identified the single-highest correlated component for each tract from all NMF decomposition values, and calculated a Pearson's correlation between the results with $n = 1$ and $n = 3$ brains. To test for equivalence of mean maximal correlations at $n = 1$ and $n = 3$, a Student's *t*-test was run in R using the default "t.test" function. Finally, to answer the distinct yet related question of whether there was consistency in which tracts are well-represented in the output of NMF decomposition with different numbers of brains, we ranked the performance of NMF for each brain based on Pearson's correlation values with XTRACT results, with 1 being the tract with the single-highest correlated NMF component and 42 being the tract with the lowest correspondence among all NMF components. We compared these ranks at $n = 1$ brain and $n = 3$ brains by computing a Kendall's correlation (Kendall, 1938) between these ranked lists, using R's default "cor.test()" function, which implements Kendall's correlation in the manner described by Hollander and Wolfe (1973).

2.5. Component selection

To reconstruct connections of interest from NMF output, we developed a processing pipeline, described in the paragraphs which follow, utilising FSL (Jenkinson et al., 2012), Connectome Workbench (Marcus et al., 2011), and custom tools written in MATLAB (MathWorks, Natick, MA, USA), including the MR Comparative Analysis Toolbox (Mr Cat; Mars et al., 2016; www.neuroecologylab.org).

NMF outputs were analysed to identify and characterise the anterior temporal-frontal and occipitotemporal-frontal connections, in each species. To do so, regions of

interest were drawn on the grey matter surface (Figure 4.1C) using Connectome Workbench (Marcus et al., 2011). These regions of interest were specified based on reports in prior literature. In macaque, the orbitofrontal cortex was specified anterior to the infraprincipal dimple in the manner reported by (Saleem et al., 2014), who identified the orbitofrontal cortex based on cytoarchitectonic and tracer data in macaques. In squirrel monkey, the orbitofrontal cortex was specified according to Deshpande & Kohut's (2023) regions of interest, which are based on Yuan and colleagues' (2021) functional parcellation of the squirrel monkey prefrontal cortex, derived from fMRI data. The squirrel monkey orbitofrontal cortical region of interest was cross-validated against the cytoarchitectonic mapping in the common squirrel monkey by Rosabal (1967). In lemur, the orbitofrontal cortex was specified as the ventral part of the prefrontal cortex, comprising the grey matter regions ventral to the principal sulcus as specified by Roumazeilles et al. (2022), and bounded posteriorly by the edge of prefrontal cortex that was identified cytoarchitectonically by Mott and Kelley (1908). The lemur orbitofrontal cortical mask was cross-validated against the cytoarchitectonic mapping by Brodmann (1909).

Temporal regions of interest were drawn to include either the anterior temporal pole or a larger swathe of the temporal lobe. Occipital regions of interest used either the primary visual cortical regions of interest reported by Roumazeilles et al. (2022) or larger regions of interest comprising most of the occipital lobe. It was found that the specification of temporal and occipital regions of interest did not affect the selection of components comprising the anterior temporal-frontal or occipitotemporal-frontal. Furthermore, the temporal and occipital regions of interest

were not used in the calculation of prefrontal innervation metrics or the statistical analysis of cross-species differences.

Using the regions of interest described above, we identified components comprising anterior temporal-frontal and occipitotemporal-frontal connections based on the signal intensity in temporal and prefrontal or occipital and prefrontal surface regions. To identify which components had high signal intensity in both regions of interest, the mean signal intensity in each region was computed for each component using custom MATLAB code, and these averages were multiplied to produce plots showing which NMF components have high signal intensity in both regions of interest. Those components which had high signal intensity in both regions were then visualised in both surface and volume space, to identify anterior temporal-frontal and occipitotemporal-frontal connections. Because the connections we studied are all ipsilateral, contra-hemispheric values were zeroed to aid in visualisation.

Identification of connections took place on the basis of the following criteria. Anterior temporal-frontal connections were identified based on termination sites in the anterior temporal pole and prefrontal cortex, a hook-shaped morphology around the lateral sulcus, minimal parietal involvement, and minimal occipital involvement. Occipitotemporal-frontal connections were identified based on termination sites in the ventral occipital cortex and prefrontal cortex, a morphology running principally along the anterior-posterior axis, minimal parietal involvement, and a ventral position in volume space. It has been previously reported that particularly at higher NMF component numbers, fibre bundles may be divided into multiple sub-components which together comprise a single projection of interest (Thompson et al., 2020), and we have identified this pattern in our own work as well (see previous chapter). To

counteract this issue, whenever multiple components matched the anatomical criteria outlined above at higher NMF model orders, these components were summed to produce a single connection.

2.6. Statistical analysis of innervation patterns

After identifying anterior temporal-frontal and occipitotemporal-frontal connections for each species and at each number of components, we visualised and quantified the distribution of termination sites in the prefrontal cortex (Figure 4.1D), enabling comparison of the depth of prefrontal innervation across species. For each connection, a value called the Non-Orbitofrontal Innervation Bias (NOIB) index was computed. This index is defined by calculating the density of innervation in both the orbitofrontal cortex and the remainder of the prefrontal cortex. The density of prefrontal cortical innervation is then divided by the density of orbitofrontal innervation, as follows:

$$NOIB = \frac{Density\ of\ innervation\ in\ PFC\ (less\ OFC)}{Density\ of\ innervation\ in\ OFC}$$

("PFC" stands for "prefrontal cortex" and OFC stands for "orbitofrontal cortex".)

NOIB therefore describes the relationship between a connection's orbitofrontal cortical innervation and its innervation of the rest of the prefrontal cortex. A high NOIB value means more of the connection terminates outside of the orbitofrontal cortex, while a low NOIB value means more of the connection terminates within the orbitofrontal cortex.

To compare NOIB values, a nested ANOVA was implemented using the spreadsheet provided by the *Handbook of Biological Statistics* (3rd ed.; McDonald John H., 2014). This approach allows for statistical comparison of the contribution to variance by cross-species differences (macaque, squirrel monkey, or lemur); within-species differences; and number of components. This comparison yields a percentage of variance explained by each hierarchical variable in the nested ANOVA. In other words, nested ANOVA allows us to identify what percentage of variation in our dataset comes from cross-species differences, what percentage originates from differences between brain hemispheres, and what percentage originates from adjusting NMF component numbers. For cross-species comparisons, data on the lowest level of the nested ANOVA are averaged together, making the comparison statistically equivalent to a one-way ANOVA. To assess differences between groups, post-hoc analyses were completed by *t*-test with a Bonferroni correction for multiple comparisons.

3. Results

In this study, we identify and characterise differences in the prefrontal innervation of anterior temporal-frontal and occipitotemporal-frontal connections between two anthropoid species and one strepsirrhine species: the rhesus macaque, the black-capped squirrel monkey, and the ring-tailed lemur (Figure 4.1A). These connections are reconstructed using a data-driven method based on non-negative matrix factorisation (NMF; hyperparameters summarised in Figure 4.1B).

First, we assessed the performance of NMF decomposition using an average of three macaque brains. We compared these group-average NMF decomposition results

against atlas-based tractography and the output of NMF decomposition using a single macaque brain. Having benchmarked NMF's performance, we then identified anterior temporal-frontal and occipitotemporal-frontal connections in each species, based on regions of interest on the cortical surface (Figure 4.1C). Next, we quantified and compared the prefrontal innervation of both connections in each species (Figure 4.1D). Finally, we assessed the contributions to overall variance in the data from cross-species differences, within-species differences, and algorithmic parameterisation, to conclude that the cross-species differences reported here are far greater than individual (within-species) differences or differences in the parameterisation of the NMF algorithm.

3.1. NMF performs similarly with one brain and three brains

Having previously assessed the performance of NMF decomposition with a single macaque brain against XTRACT-based tractography, we adopted the same analytical approach here to enable a direct comparison of results. Briefly, we used a Pearson's correlation to compare each NMF component's grey matter map against each known tract's connectivity map, as identified using XTRACT and XTRACT Blueprint (Mars et al., 2018; Warrington et al., 2020). We then assessed the group-average results against those achieved using a single macaque brain.

The correlations between XTRACT-derived tracts and their best-matching components, using the group average of $n = 3$ macaque brains, are summarised in Figure 4.2A-B. The minimum, median, and maximum values for each component number are as follows. $K = 10$: 0.04, 0.30, 0.48; $K = 50$: 0.14, 0.41, 0.64; $K = 60$: 0.14, 0.42, 0.70; $K = 100$: 0.15, 0.43, 0.66; $K = 200$: 0.23, 0.41, 0.65. As Figure 4.2B

visualises, maximal correlations vary as a function of K value such that the median maximal correlation is lowest at $K = 10$ and highest at $K = 100$. This is a similar pattern to that observed with $n = 1$ brain (see previous chapter, Figure 3.2B).

Next, we directly compared the performance of NMF decomposition with a group average of $n = 3$ brains against the results for a single macaque brain ($n = 1$; data reported in previous chapter). For each sample size, $n = 1$ and $n = 3$, we identified the single optimal reconstruction for each tract (i.e., the single-highest correlated NMF component from all NMF decompositions). Optimal reconstructions are well-correlated between the two datasets (Pearson's $r = 0.66$, 40 *d.f.*; visually presented in Figure 4.2C). A Student's *t*-test suggests equivalence of means between both sets of optimal reconstructions (one-brain mean: 0.47, three-brain mean: 0.48; $t = 0.64803$, 82 *d.f.*, $p = 0.52$; 95% CI for difference between means: -0.03 – 0.06). We therefore conclude that increasing the sample size from $n = 1$ to $n = 3$ brains does not improve tract reconstruction.

Having established via Pearson's correlation that optimal tract reconstructions are similar at $n = 1$ and $n = 3$ brains, we additionally assessed the two datasets for equivalence in rank-order of tract reconstructions. Based on the optimal reconstructions presented in Figure 4.3C, tracts were ranked from one to 42, with one being the tract with the highest-correlated NMF component from among all decompositions at a given sample size, and 42 being the tract with the lowest-correlated best-match among NMF components. These rank orders are compared for $n = 1$ and $n = 3$ in Figure 4.3D. The five tracts with the best reconstructions at $n = 1$

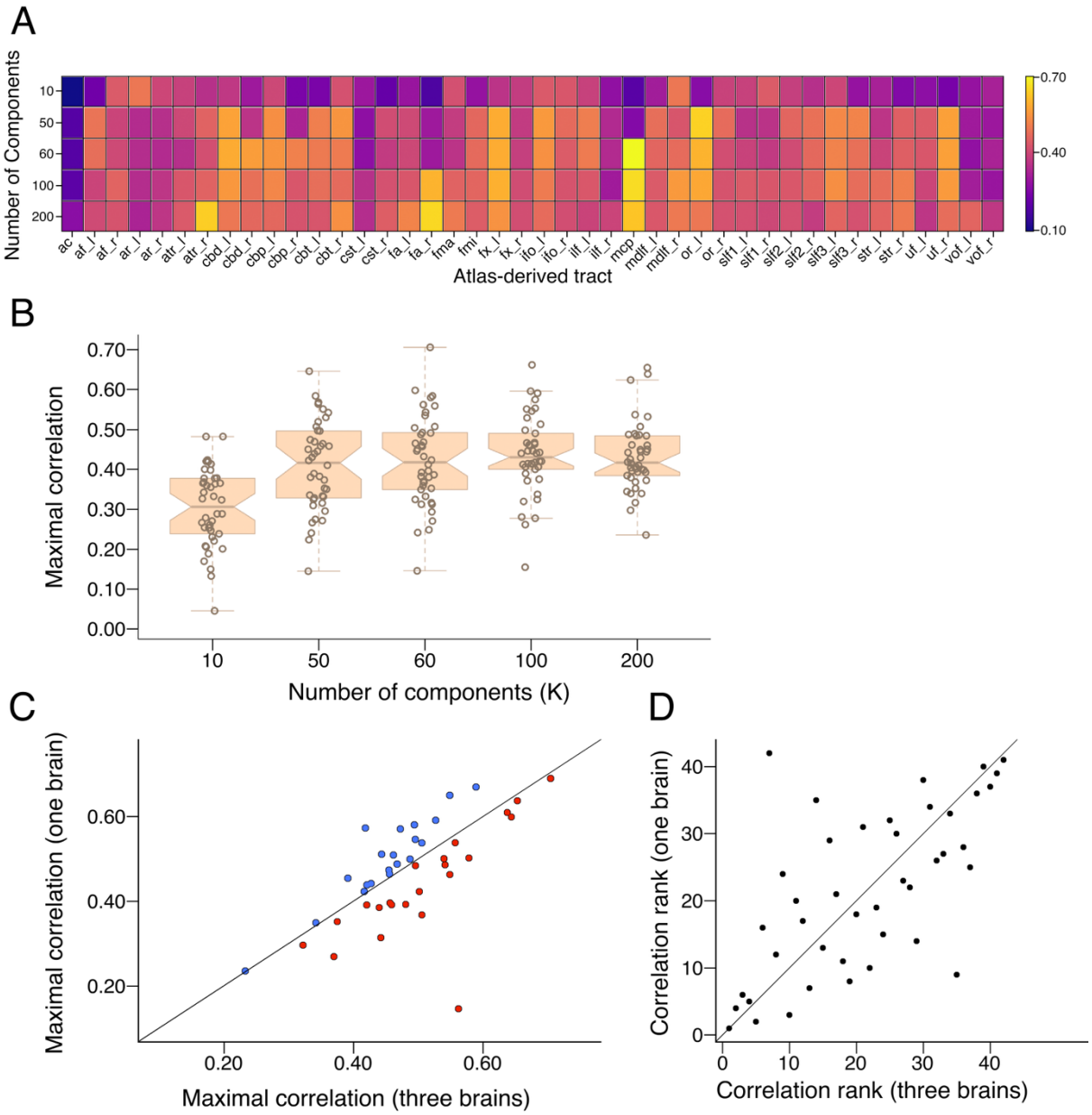


Figure 4.2. Performance of NMF decomposition in macaque with three brains. ***(A)*** *Correlation matrix between NMF components and atlas-derived tracks in macaque. As in Figure 3.2, each column corresponds to a white matter tract identified via XTRACT protocols. Each cell represents the correlation between that tract's grey matter connectivity map and the best-matching NMF component. NMF was used to decompose each brain's connectivity matrix at* K *= 10, 50, 60, 100, and 200 components. Abbreviations are per Table 3.1.* ***(B)*** *Distributions of maximal correlations for different component numbers. Box-and-whisker plots show the distributions of maximal correlations for different numbers of components. Notches indicate the 95% confidence interval of the median (median ± 1.57 × IQR/$n^{0.5}$).* ***(C)*** *NMF performance at different sample sizes, per tract. Single-highest correlations among all NMF component numbers, using one brain or three brains. Each marker represents a single white matter tract. Blue markers indicate better performance with one brain (20 of 42 tracts), while red markers indicate better performance with three brains (22 of 42 tracts). NMF performance was strongly-correlated between the two*

datasets (Pearson's r = 0.66, 40 d.f.). The diagonal line represents theoretical equivalence between n = 1 and n = 3. ***(D)*** *Rank-ordering of tracts by best-matching component, using one brain or three brains. Each marker represents one tract. The diagonal line represents if all tracts ranked the same between the two datasets (i.e., equal value on both axes). There is a moderate correlation between tracts' rank-orders between the two datasets (Kendall's τ = 0.50).*

---

are also the best-reconstructed tracts at $n = 3$ (Figure 4.3D, lower-left corner). The two sets of rank-orders are moderately correlated (Kendall's $\tau = 0.50$), reflecting our finding that for many tracts, NMF performance at $n = 1$ is comparable to NMF performance at $n = 3$. In sum, each of these analyses (Pearson's correlation, *t*-test, and Kendall's correlation of rank orders) indicates that NMF performs similarly well at reconstructing tracts at $n = 1$ and $n = 3$.

3.2. Anterior temporal-frontal and occipitotemporal-frontal connections can be reliably reconstructed across primate species

To reconstruct ventral visual stream connections from NMF output, we developed the following processing pipeline. First, NMF output was sorted to find components comprising the connections of interest. A custom MATLAB script was developed to identify which NMF components have grey matter maps with high signal intensity in specific regions of interest (Figure 4.3A-B). These regions of interest were identified based on anatomical landmarks and previous literature (see *Methods*). Specifically, anterior temporal-frontal connections were screened based on high signal intensity in the anterior temporal pole and the prefrontal cortex, while occipitotemporal-frontal connections were screened based on high signal intensity in the visual cortex and prefrontal cortex. It should be noted that an additional

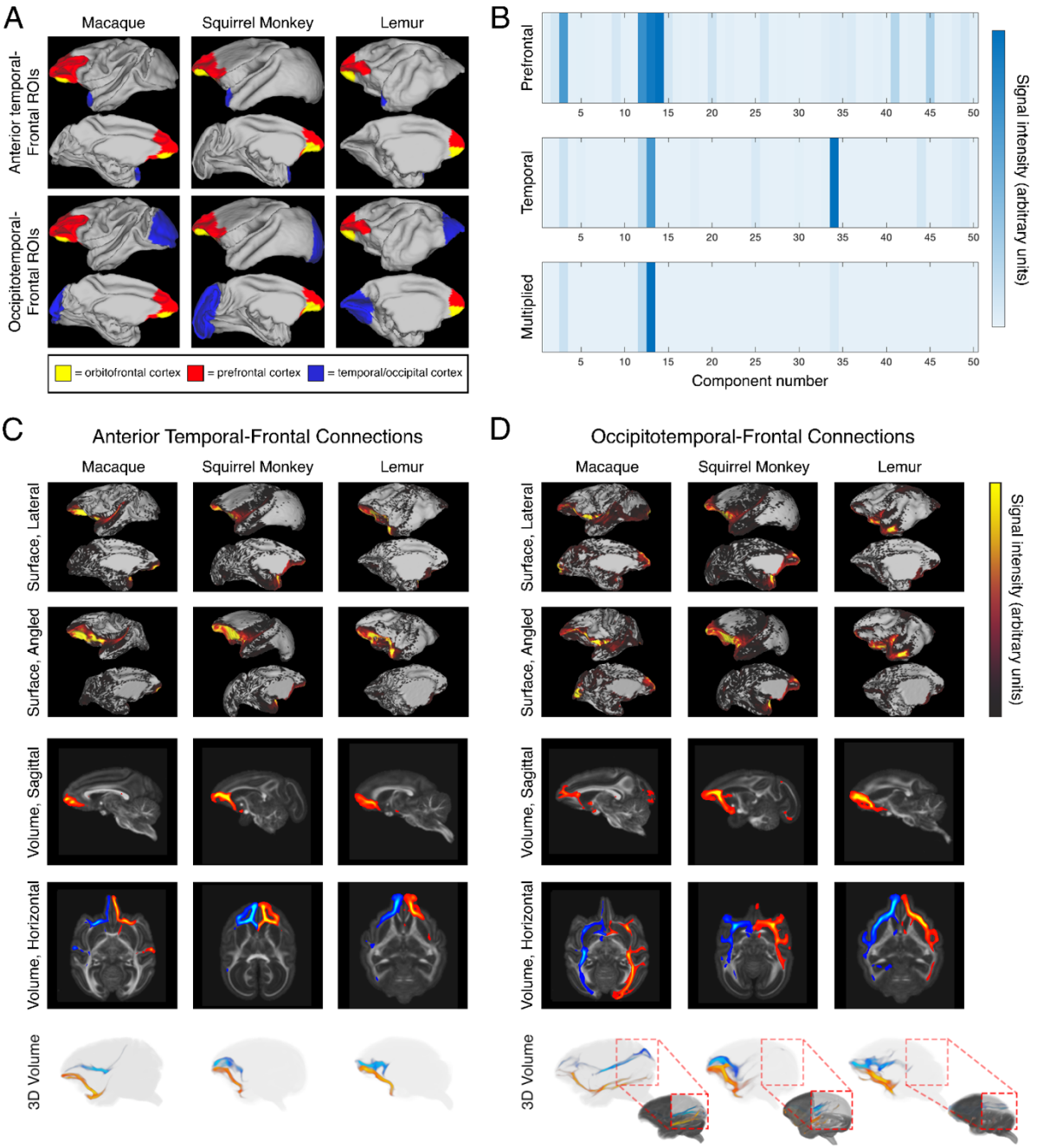


Figure 4.3. Reconstruction of anterior temporal-frontal and occipitotemporal-frontal connections. (A) *Surface projections showing regions of interest used to screen NMF components. Yellow: orbitofrontal cortex; red: prefrontal cortex; blue: anterior temporal pole (top row), visual cortex (bottom row). Note: the orbitofrontal cortex is a subregion of the prefrontal cortex; as such, the prefrontal cortical region of interest additionally includes all area within the yellow region.* ***(B)*** *Sample output of surface intensity screening. Top: each component's intensity in the prefrontal region. Middle: each component's intensity in the temporal region. Bottom: intensity values from each region multiplied. Components with moderate-to-high intensity values in both regions were selected for visualisation to identify putative connections.* ***(C)*** *Example anterior temporal-frontal connections in each species. Top two rows: surface intensity projections showing putative innervation of reconstructed*

connections. Both rows present the lateral surface (above) and medial wall (below) of the left hemisphere. The first row is a sagittal view. The second row is the same surface, with the orientation slightly tilted to show more of the prefrontal surface. Bottom three rows: volumetric reconstructions of anterior temporal-frontal connections in a left hemispheric sagittal plane (row three); horizontal plane in radiological orientation (row four); and 3D space (row five). The 3D volumetric reconstruction has been slightly angled from the sagittal plane, to better visualise the bilateral morphology of reconstructed connections. For bilateral reconstructions in rows four and five, blue indicates a right hemispheric connection while orange indicates a left hemispheric connection. ***(D)*** *Example occipitotemporal-frontal connections in each species. Rows are as described in panel C. Row five includes an additional threshold-adjusted inset volume, to visualise the posterior part of each connection where signal intensity is lower.*

---

analysis in which these regions of interest were expanded to include more visual and temporal cortex did not yield any additional components comprising the connections of interest. The visual and temporal cortical regions of interest did not contribute to the analysis of prefrontal innervation or the statistical analysis of cross-species differences.

Following sorting, components with high signal intensities in the relevant grey matter cortical regions were visually inspected in both surface and volume space to identify those that comprise anterior temporal-frontal and occipitotemporal-frontal connections. Anterior temporal-frontal connections were identified based on the following anatomical criteria: minimal parietal involvement, minimal occipital involvement, termination sites in the anterior temporal pole and prefrontal cortex, and a hook-shaped morphology around the lateral sulcus. Occipitotemporal-frontal connections were identified based on the following criteria: minimal parietal involvement, termination sites in the ventral occipital cortex and prefrontal cortex, and a morphology running principally along the anterior-posterior axis. Where connections had been split into multiple components – primarily at high NMF

component numbers – these components were then merged to form the complete connection. In each species, the reconstructed anterior temporal-frontal connections bore a strong resemblance to a known tract in the uncinate fasciculus (Figure 4.3C). Occipitotemporal-frontal connections resembled the inferior fronto-occipital fasciculus, but showed more considerable variation in constitution and may have involved other occipitotemporal-frontal connections (Figure 4.3D).

3.3. Prefrontal innervation of the anterior temporal-frontal connections is more restricted to the orbitofrontal cortex in the lemur

We quantified the depth of prefrontal innervation for each species' anterior temporal-frontal connections using a novel measure called the Non-Orbitofrontal Innervation Bias (NOIB) index. This index measures the degree to which a connection terminates outside of the orbitofrontal cortex within the prefrontal cortex. A high NOIB value indicates a high degree of innervation outside of the orbitofrontal cortex, while a low NOIB value indicates that the connection's prefrontal innervation is more restricted to the orbitofrontal cortex. NOIB is calculated as follows:

$$NOIB = \frac{Density\ of\ innervation\ in\ PFC\ (less\ OFC)}{Density\ of\ innervation\ in\ OFC}$$

("PFC" stands for "prefrontal cortex" and OFC stands for "orbitofrontal cortex".)

NOIB values were calculated for each reconstructed anterior temporal-frontal connection. These data were arranged in a hierarchical fashion, with top-level groups comprising different species and sub-groups comprising individual brain hemispheres (Figure 4.4A). Because NMF decomposition was run on each brain a total of four

A

Anterior Temporal-Frontal Connections

Macaque						Squirrel Monkey						Lemur						
Hemi 1	Hemi 2	Hemi 3	Hemi 4	Hemi 5	Hemi 6	Hemi 1	Hemi 2	Hemi 3	Hemi 4	Hemi 5	Hemi 6	Hemi 1	Hemi 2	Hemi 3	Hemi 4	Hemi 5	Hemi 6	
0.16	0.35	0.22	0.20	0.17	0.27	0.39	0.34	0.35	0.29	0.44	0.28	0.05	0.14	0.01	0.12	0.14	0.38	$K = 50$
0.15	0.34	0.22	0.28	0.18	0.21	0.46	0.45	0.39	0.40	0.45	0.30	0.07	0.15	0.05	0.11	0.15	0.29	$K = 60$
0.16	0.18	0.24	0.13	0.16	0.13	0.54	0.46	0.40	0.39	0.47	0.31	0.01	0.03	0.00	0.04	0.04	0.07	$K = 100$
0.17	0.16	0.24	0.16	0.18	0.14	0.49	0.39	0.38	0.34	0.46	0.26	0.09	0.11	0.08	0.04	0.11	0.24	$K = 200$

Species

Brain hemisphere

Different K values

Occipitotemporal-Frontal Connections

Macaque						Squirrel Monkey						Lemur						
Hemi 1	Hemi 2	Hemi 3	Hemi 4	Hemi 5	Hemi 6	Hemi 1	Hemi 2	Hemi 3	Hemi 4	Hemi 5	Hemi 6	Hemi 1	Hemi 2	Hemi 3	Hemi 4	Hemi 5	Hemi 6	
0.60	1.27	0.52	1.80	0.78	2.26	0.62	0.63	0.72	0.57	0.60	0.40	0.05	0.14	0.01	0.12	0.14	0.38	$K = 50$
0.39	0.34	0.33	0.36	0.53	0.48	0.69	0.96	0.75	1.00	0.63	0.70	0.06	0.15	0.02	0.11	0.23	0.29	$K = 60$
0.51	1.22	0.39	7.04	0.42	4.95	0.55	0.67	0.44	0.69	0.48	0.52	0.29	0.87	0.14	0.58	0.66	1.29	$K = 100$
0.46	2.33	0.59	0.45	0.93	0.26	0.77	1.42	0.76	2.05	0.73	1.56	0.05	0.09	0.04	0.07	0.12	0.26	$K = 200$

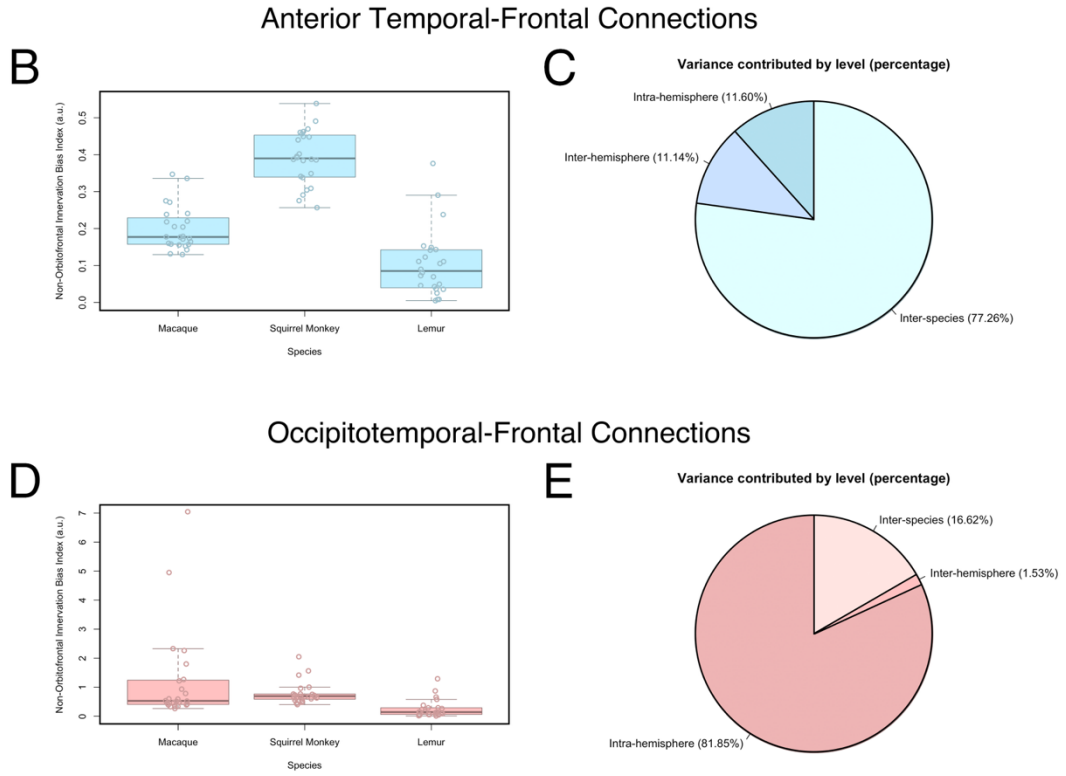


Figure 4.4. **Lemur shows the lowest non-orbitofrontal innervation bias in both sets of connections. (A)** Nested ANOVA data tables. The top level comprises different species: macaque, squirrel monkey, and lemur. The middle level comprises groupings by individual brain hemisphere. The lowest level comprises individual data points derived from running NMF with different numbers of components. Odd-numbered hemispheres are left hemispheres; even-numbered hemispheres are right hemispheres. **(B)** Box-and-whisker plots of anterior temporal-frontal non-orbitofrontal innervation bias (NOIB) index values. Whiskers extend to 1.5 × IQR. **(C)** Different contributions to variance among anterior temporal-frontal NOIB index values. **(D)** Box-and-whisker plots of occipitotemporal-frontal NOIB index values. Whiskers extend to 1.5 × IQR. Extreme macaque values are out of frame, for visualisation reasons; raw data presented in Panel A. **(E)** Different contributions to variance among occipitotemporal-frontal NOIB index values.

times at different component numbers, this hierarchical ordering of data points was chosen to respect the assumption of statistical independence among data points during inferential statistical tests. During comparisons between brain hemispheres or between species, the individual data points that arise from repeated sampling are averaged together. (See *Methods* for further detail.)

NOIB values for the anterior temporal-frontal connections in macaque, squirrel monkey, and lemur were as follows. Mean ± standard deviation: 0.20 ± 0.06 for macaque; 0.39 ± 0.07 for squirrel monkey; 0.10 ± 0.09 for lemur ($n = 24$ observations from 6 brain hemispheres per species; raw data presented in Figure 4.4A and distributions presented in Figure 4.4B). Using a nested ANOVA for inferential statistics, we observed a significant difference between species on anterior temporal-frontal OBI values (F: 34.02, $d.f. = 2$, $p = 2.67 \times 10^{-6}$). Post-hoc t-tests with a Bonferroni correction showed differences between all species (macaque v. squirrel monkey: $p = 1.23 \times 10^{-12}$; macaque v. lemur: $p = 2.92 \times 10^{-4}$; squirrel monkey v. lemur: 2.45×10^{-15}). The lemur had the smallest NOIB of the three species, indicating that the anterior temporal-frontal connections' innervation patterns are more restricted to the orbitofrontal cortex in the lemur than in the other two species.

3.4. Cross-species differences explain more variance in anterior temporal-frontal connectivity than within-species differences or algorithmic parameters

Using a nested ANOVA design, we quantified how different factors contribute to overall variance within our dataset. Because of the hierarchical organisation of a

nested ANOVA, it is possible to make statistical comparisons of the contribution to variance by each level in the hierarchy. By organising our nested ANOVA first by species (macaque, squirrel monkey, or ring-tailed lemur), then different brain hemispheres, then NMF component number, our analysis yields a percentage of variance explained by each hierarchical level in the nested ANOVA. In other words, the nested ANOVA describes what percentage of variation in our dataset comes from cross-species differences, what percentage originates from differences between brain hemispheres of the same species (e.g., due to age, sex, or hemispheric asymmetries), and what percentage originates from adjusting NMF component numbers.

Differences between species accounted for 77.26% of the variance in the dataset, whereas within-species differences accounted for only 11.14% of the variance. Running NMF with different numbers of components contributed the remaining 11.6% of the variance (Figure 4.4C). By running NMF with different numbers of components and assessing the contribution of different algorithmic parameters to overall variance in the dataset, we can conclude that the cross-species differences observed here are several times larger than inter-individual differences, inter-hemispheric differences, and variability in the identification of connections arising from the use of different NMF parameters.

3.5. The lemur's occipitotemporal-frontal connections' prefrontal innervation is more restricted to orbitofrontal cortex

Our anterior temporal-frontal results are consistent with previous work suggesting that anthropoid primates evolved to rely more on ventrolateral prefrontal

areas for visual processing in the ventral visual stream. However, it is uncertain whether other ventral visual processing tracts follow the same pattern. To address this question, we quantified the prefrontal innervation of occipitotemporal-frontal connections in the same way as we did anterior temporal-frontal connections.

We generated NOIB values for each species' reconstructed occipitotemporal-frontal connections following the same procedure as we did for anterior temporal-frontal connections. In every species, NOIB values were higher for the occipitotemporal-frontal connections than they were for anterior temporal-frontal connections. Again, connections in the macaque and squirrel monkey showed higher NOIB values than in the lemur (mean ± standard deviation: 1.22 ± 1.61 for macaque; 0.79 ± 0.38 for squirrel monkey; 0.26 ± 0.31 for lemur; $n = 24$ observations from 6 brain hemispheres per species; distributions presented graphically in Figure 4.4D). A significant difference was found between species via nested ANOVA, albeit with a lower F-statistic than for anterior temporal-frontal analysis (F: 5.54, $d.f. = 2$, $p = 0.02$), meaning that between-species differences explain less of the overall variance in the dataset. Post-hoc t-tests with a Bonferroni correction showed that differences between lemur and the two anthropoid species were the principal driver of the ANOVA's overall effect, with no statistically significant difference between the macaque and squirrel monkey (macaque v. squirrel monkey: $p = 0.64$; macaque v. lemur: $p = 0.02$; squirrel monkey v. lemur: $p = 9.36 \times 10^{-6}$).

In the macaque, four of the occipitotemporal-frontal connection reconstructions had NOIB values greater than 2 (Figure 4.4A,D). All such reconstructions occurred in right hemispheres of all three individuals, at $K = 50$, 60, and 200, resulting in a high degree of intra-hemispheric variance among

reconstructions. Indeed, differences between reconstructions within a hemisphere contributed 81.85% of the variance in this dataset (Figure 4.4E), primarily due to variance in macaque right hemispheric values (note the greater inter-quartile range for macaque in Figure 4.4D). Between-species differences contributed 16.62% of the variance and between-hemisphere differences contributed 1.53% of the variance (Figure 4.4E).

In sum, these results reflect that the lemur occipitotemporal-frontal connections are more biased towards termination in the orbitofrontal cortex, though the magnitude of this effect is more difficult to discern, owing to variability in reconstructions of the occipitotemporal-frontal connections particularly in the right hemisphere of the macaque group.

4. Discussion

This work has used a data-driven analysis of tractography data in three primates to investigate the frontal projections of the anterior temporal-frontal and visual-frontal connections of the ventral visual pathway. In the absence of anatomical priors sufficient to specify exclusion masks and other criteria for atlas-based tractography in each of our three species, this technique has enabled us to compare the ventral visual pathway across species. We have shown that the frontal connections are more widespread in the two anthropoids studied – the macaque and the squirrel monkey – than in the strepsirrhine primate – the lemur. Using the orbitofrontal cortex as a frontal reference region, we showed that prefrontal cortical innervation is more restricted to the orbitofrontal cortex in the strepsirrhine. These between-species

effects were found both for anterior temporal-frontal and ventral occipitotemporal-frontal connections.

The primate temporal lobe has been argued to be a unique specialisation to that order (Bryant & Preuss, 2018). A large part of this cortical territory is devoted to the ventral visual stream, originating in the extrastriate cortex and extending anteriorly towards the temporal pole. In recent years, it has been increasingly appreciated that the ventral stream consists of a series of reciprocally connected regions, linked to other cortical and subcortical regions, acting as a recurrent network involved in the processing of object information (Kravitz et al., 2013). Complementing this understanding, the overall model of striate and extrastriate cortex representing visual features, and increasingly anterior temporal regions representing conjunctions of visual features and ultimately whole objects and even abstract representations, has proven robust (Braunsdorf et al., 2021; Murray et al., 2017).

Recent work has interpreted the ventral visual stream in terms of its role in visually based foraging in primates. The visual representations of the temporal cortex provide a sensory context that can be used to guide foraging decisions. It has been argued that the foraging niche of anthropoid primates is more complex than that of non-anthropoid primates, with anthropoids relying on more volatile sources of food and operating in a more complex landscape (Passingham & Wise, 2012). Indeed, anthropoid primates seem to have far more complex knowledge of their environment (Janmaat et al., 2006). Consistent with this, fossil evidence suggests that early anthropoids had smaller brains than modern anthropoids, yet still possessed the sharp visual acuity that underpins the complex foraging niche of modern anthropoids (Bush

et al., 2004). This body of work is consistent with electrophysiological and anatomical studies. Eldridge and colleagues (2021) argue that many experimental results of neuronal activity in anthropoid temporal cortex, such as generalisation of items based on visual similarity and assessment of object properties based on visual information, are consistent with successful foraging behaviour in such an environment. Furthermore, Eldridge and colleagues (2021) note that the ventrolateral prefrontal cortex, as the other principal target of temporal visual cortical projections to the prefrontal cortex, is an anthropoid innovation absent in closely-related relatives, including strepsirrhines. Our results, showing that the anthropoid ventral visual stream involves relatively fewer projections to the orbitofrontal cortex than other prefrontal cortical regions, further develop the hypothesis that the ventral visual stream evolved in anthropoids to support sensory-driven foraging in complex environments.

More generally, our results demonstrate how data-driven methods for analysing complex neuroimaging data can be used successfully to test hypotheses in comparative neuroscience. Large-scale comparative anatomy is now possible through the increasing availability of high quality whole-brain imaging data from a range of species, including many primates (Assaf et al., 2020; Tendler et al., 2022). The availability of these data presents both opportunities and challenges, as many of the species from which data are now available have been studied only sparsely. The use of a data-driven approach, such as NMF, opens the possibility of interrogating these data without losing sight of anatomical rigour. Indeed, the inclusion of species that have been studied well, such as the macaque monkey, allows for a benchmarking or validation of methods. A similar approach has been taken before by Folloni and

colleagues, showing how careful tractography data is able to reconstruct tracts previously identified using tracers in the macaque (Folloni et al., 2019), before expanding the approach to other species (Folloni et al., 2024).

The availability of multiple individuals per species also allowed us to assess the performance of NMF in greater detail. Comparing our prior reconstruction of white matter tracts via NMF in a single macaque brain to NMF-based reconstruction of white matter tracts in three brains allowed us to determine that NMF can exhibit satisfactory performance for most tracts, even with a single brain. Furthermore, by reconstructing the same tracts across multiple species, we were able to determine the relative extent of within- and between-species variation in connectivity. Although the number of individuals per species in the current study is still quite low, this nevertheless allows a first quantification of the various contributions of variance in the data. To our knowledge, this has not been assessed in this manner before. We show that the between-species variance far outweighs that of individuals and of analysis parameterization. This result provides an important validation of earlier studies showing between-species differences in connectivity.

In sum, this work provides evidence of white matter reorganisation in the ventral visual stream in the anthropoid lineage. As the anthropoid primates evolved to occupy a niche as foragers capable of leveraging complex visual information, their ventral prefrontal cortex underwent extensive reorganisation. Our work confirmed that the ventral visual stream supporting this processing pathway also underwent changes in the anthropoid lineage. Furthermore, the data-driven techniques we have developed here hold the potential to address questions of white matter connectivity in additional, previously understudied species.

References

Assaf, Y., Bouznach, A., Zomet, O., Marom, A., & Yovel, Y. (2020). Conservation of brain connectivity and wiring across the mammalian class. *Nature Neuroscience*, *23*(7), 805–808. https://doi.org/10.1038/s41593-020-0641-7

Assimopoulos, S., Warrington, S., Bryant, K. L., Pszczolkowski, S., Jbabdi, S., Mars, R. B., & Sotiropoulos, S. N. (2024). Generalising XTRACT tractography protocols across common macaque brain templates. *Brain Structure and Function*. https://doi.org/10.1007/s00429-024-02760-0

Baizer, J. S., Ungerleider, L. G., & Desimone, R. (1991). Organization of visual inputs to the inferior temporal and posterior parietal cortex in macaques. *Journal of Neuroscience*, *11*(1), 168–190. https://doi.org/10.1523/JNEUROSCI.11-01-00168.1991

Barton, R. A. (1998). Visual specialization and brain evolution in primates. *Proceedings of the Royal Society of London. Series B: Biological Sciences*, *265*(1409), 1933–1937. https://doi.org/10.1098/rspb.1998.0523

Behrens, T. E. J., Berg, H. J., Jbabdi, S., Rushworth, M. F. S., & Woolrich, M. W. (2007). Probabilistic diffusion tractography with multiple fibre orientations: What can we gain? *NeuroImage*, *34*(1), 144–155. https://doi.org/10.1016/j.neuroimage.2006.09.018

Benn, R. A., Xu, T., Mars, R. B., Boch, M., Roumazeilles, L., Heuer, K., Toro, R., Margulies, D. S., Manzano-Patron, J. P., Montesinos, P., Galan-Arriola, C., Lopez-Martin, G., Sanchez-Gonzalez, J., Duff, E. P., & Ibañez, B. (2025). *Precon_all: A species-agnostic automated pipeline for non-human cortical surface*

reconstruction (p. 2025.04.16.649072). bioRxiv. https://doi.org/10.1101/2025.04.16.649072

Boutsidis, C., & Gallopoulos, E. (2008). SVD based initialization: A head start for nonnegative matrix factorization. *Pattern Recognition*, *41*(4), 1350–1362. https://doi.org/10.1016/j.patcog.2007.09.010

Braunsdorf, M., Blazquez Freches, G., Roumazeilles, L., Eichert, N., Schurz, M., Uithol, S., Bryant, K. L., & Mars, R. B. (2021). Does the temporal cortex make us human? A review of structural and functional diversity of the primate temporal lobe. *Neuroscience & Biobehavioral Reviews*, *131*, 400–410. https://doi.org/10.1016/j.neubiorev.2021.08.032

Brodmann, K. (1909). *Vergleichende Lokalisationslehre der Grosshirnrinde in ihren Prinzipien dargestellt auf Grund des Zellenbaues* (2nd unveränderte Aufl.). Barth.

Bryant, K. L., & Preuss, T. M. (2018). A Comparative Perspective on the Human Temporal Lobe. In E. Bruner, N. Ogihara, & H. C. Tanabe (Eds), *Digital Endocasts: From Skulls to Brains* (pp. 239–258). Springer Japan. https://doi.org/10.1007/978-4-431-56582-6_16

Bush, E. C., Simons, E. L., Dubowitz, D. J., & Allman, J. M. (2004). Endocranial Volume and Optic Foramen Size in Parapithecus grangeri. In C. F. Ross & R. F. Kay (Eds), *Anthropoid Origins: New Visions* (pp. 603–614). Springer US. https://doi.org/10.1007/978-1-4419-8873-7_21

Cartmill, M. (1992). New views on primate origins. *Evolutionary Anthropology: Issues, News, and Reviews*, *1*(3), 105–111. https://doi.org/10.1002/evan.1360010308

Deshpande, H. U., & Kohut, S. J. (2023). *Age-related development in prefrontal-subcortical resting-state functional connectivity in nonhuman primates* [Preprint]. Neuroscience. https://doi.org/10.1101/2023.07.19.549741

Eldridge, M. A., Hines, B. E., & Murray, E. A. (2021). The visual prefrontal cortex of anthropoids: Interaction with temporal cortex in decision making and its role in the making of 'visual animals'. *Current Opinion in Behavioral Sciences*, *41*, 22–29. https://doi.org/10.1016/j.cobeha.2021.02.012

Fischl, B. (2012). FreeSurfer. *NeuroImage*, *62*(2), 774–781. https://doi.org/10.1016/j.neuroimage.2012.01.021

Fleagle, J. G. (2013). *Primate Adaptation and Evolution*. Academic Press.

Folloni, D., Roumazeilles, L., Bryant, K. L., Manger, P. R., Bertelsen, M. F., Khrapitchev, A. A., Rudebeck, P. H., & Mars, R. B. (2024). *Comparing the limbic-frontal connectome across the primate order: Conservation of connections and implications for translational neuroscience* (p. 2024.03.06.583735). bioRxiv. https://doi.org/10.1101/2024.03.06.583735

Folloni, D., Sallet, J., Khrapitchev, A. A., Sibson, N., Verhagen, L., & Mars, R. B. (2019). Dichotomous organization of amygdala/temporal-prefrontal bundles in both humans and monkeys. *eLife*, *8*, e47175. https://doi.org/10.7554/eLife.47175

Goodale, M. A., & Milner, A. D. (1992). Separate visual pathways for perception and action. *Trends in Neurosciences*, *15*(1), 20–25. https://doi.org/10.1016/0166-2236(92)90344-8

Harris, C. R., Millman, K. J., van der Walt, S. J., Gommers, R., Virtanen, P., Cournapeau, D., Wieser, E., Taylor, J., Berg, S., Smith, N. J., Kern, R., Picus,

M., Hoyer, S., van Kerkwijk, M. H., Brett, M., Haldane, A., del Río, J. F., Wiebe, M., Peterson, P., … Oliphant, T. E. (2020). Array programming with NumPy. *Nature*, *585*(7825), 357–362. https://doi.org/10.1038/s41586-020-2649-2

Hecht, E. E., Gutman, D. A., Preuss, T. M., Sanchez, M. M., Parr, L. A., & Rilling, J. K. (2013). Process Versus Product in Social Learning: Comparative Diffusion Tensor Imaging of Neural Systems for Action Execution–Observation Matching in Macaques, Chimpanzees, and Humans. *Cerebral Cortex*, *23*(5), 1014–1024. https://doi.org/10.1093/cercor/bhs097

Hunt, J. E., Pratt, K. G., & Molnár, Z. (2024). Ocular Necessities: A Neuroethological Perspective on Vertebrate Visual Development. *Brain, Behavior and Evolution*, 1–13. https://doi.org/10.1159/000536035

Janmaat, K. R. L., Byrne, R. W., & Zuberbühler, K. (2006). Evidence for a spatial memory of fruiting states of rainforest trees in wild mangabeys. *Animal Behaviour*, *72*(4), 797–807. https://doi.org/10.1016/j.anbehav.2005.12.009

Jenkinson, M., Beckmann, C. F., Behrens, T. E. J., Woolrich, M. W., & Smith, S. M. (2012). FSL. *NeuroImage*, *62*(2), 782–790. https://doi.org/10.1016/j.neuroimage.2011.09.015

Kaas, J. H., & Baldwin, M. K. L. (2020). The Evolution of the Pulvinar Complex in Primates and Its Role in the Dorsal and Ventral Streams of Cortical Processing. *Vision*, *4*(1), 3. https://doi.org/10.3390/vision4010003

Kaas, J. H., Qi, H.-X., & Stepniewska, I. (2021). Escaping the nocturnal bottleneck, and the evolution of the dorsal and ventral streams of visual processing in

primates. *Philosophical Transactions of the Royal Society B: Biological Sciences*, *377*(1844), 20210293. https://doi.org/10.1098/rstb.2021.0293

Kendall, M. G. (1938). A New Measure of Rank Correlation. *Biometrika*, *30*(1–2), 81–93. https://doi.org/10.1093/biomet/30.1-2.81

Kravitz, D. J., Saleem, K. S., Baker, C. I., Ungerleider, L. G., & Mishkin, M. (2013). The ventral visual pathway: An expanded neural framework for the processing of object quality. *Trends in Cognitive Sciences*, *17*(1), 26–49. https://doi.org/10.1016/j.tics.2012.10.011

Lange, F. J., Ashburner, J., Smith, S. M., & Andersson, J. L. R. (2020). A Symmetric Prior for the Regularisation of Elastic Deformations: Improved anatomical plausibility in nonlinear image registration. *NeuroImage*, *219*, 116962. https://doi.org/10.1016/j.neuroimage.2020.116962

Lee, D. D., & Seung, H. S. (1999). Learning the parts of objects by non-negative matrix factorization. *Nature*, *401*(6755), Article 6755. https://doi.org/10.1038/44565

Lee, D. D., & Seung, H. S. (2000). Algorithms for Non-negative Matrix Factorization. *Advances in Neural Information Processing Systems*, *13*. https://proceedings.neurips.cc/paper_files/paper/2000/hash/f9d1152547c0bde01830b7e8bd60024c-Abstract.html

Marcus, D., Harwell, J., Olsen, T., Hodge, M., Glasser, M., Prior, F., Jenkinson, M., Laumann, T., Curtiss, S., & Van Essen, D. (2011). Informatics and Data Mining Tools and Strategies for the Human Connectome Project. *Frontiers in Neuroinformatics*, *5*. https://doi.org/10.3389/fninf.2011.00004

Mars, R. B., O'Muircheartaigh, J., Folloni, D., Li, L., Glasser, M. F., Jbabdi, S., & Bryant, K. L. (2019). Concurrent analysis of white matter bundles and grey matter networks in the chimpanzee. *Brain Structure and Function*, *224*(3), 1021–1033. https://doi.org/10.1007/s00429-018-1817-8

Mars, R. B., Sotiropoulos, S. N., Passingham, R. E., Sallet, J., Verhagen, L., Khrapitchev, A. A., Sibson, N., & Jbabdi, S. (2018). Whole brain comparative anatomy using connectivity blueprints. *eLife*, *7*, e35237. https://doi.org/10.7554/eLife.35237

Mars, R. B., Verhagen, L., Gladwin, T. E., Neubert, F.-X., Sallet, J., & Rushworth, M. F. S. (2016). Comparing brains by matching connectivity profiles. *Neuroscience & Biobehavioral Reviews*, *60*, 90–97. https://doi.org/10.1016/j.neubiorev.2015.10.008

McDonald John H. (2014). *Handbook of Biological Statistics*. Sparky House Publishing.

Mott, F. W., & Kelley, A. M. (1908). Complete survey of the cell lamination of the cerebral cortex of the lemur. *Proceedings of the Royal Society of London. Series B, Containing Papers of a Biological Character*, *80*(543), 488–506. https://doi.org/10.1098/rspb.1908.0044

Murray, E. A., Wise, S. P., & Graham, K. S. (2017). *The Evolution of Memory Systems: Ancestors, Anatomy, and Adaptations*. Oxford University Press.

Myles Hollander & Douglas A. Wolfe. (1973). *Nonparametric Statistical Methods* (1st edn). John Wiley & Sons.

Nectow, A. R., & Nestler, E. J. (2020). Viral tools for neuroscience. *Nature Reviews Neuroscience*, *21*(12), 669–681. https://doi.org/10.1038/s41583-020-00382-z

O'Muircheartaigh, J., & Jbabdi, S. (2018). Concurrent white matter bundles and grey matter networks using independent component analysis. *NeuroImage*, *170*, 296–306. https://doi.org/10.1016/j.neuroimage.2017.05.012

Passingham, R. E., & Wise, S. P. (2012). *The Neurobiology of the Prefrontal Cortex: Anatomy, Evolution, and the Origin of Insight*. OUP Oxford.

Pedregosa, F., Varoquaux, G., Gramfort, A., Michel, V., Thirion, B., Grisel, O., Blondel, M., Prettenhofer, P., Weiss, R., Dubourg, V., Vanderplas, J., Passos, A., Cournapeau, D., Brucher, M., Perrot, M., & Duchesnay, É. (2011). Scikit-learn: Machine Learning in Python. *Journal of Machine Learning Research*, *12*(85), 2825–2830.

Prescott, M. J., & Poirier, C. (2021). The role of MRI in applying the 3Rs to non-human primate neuroscience. *NeuroImage*, *225*, 117521. https://doi.org/10.1016/j.neuroimage.2020.117521

R Core Team. (2025). *R: A Language and Environment for Statistical Computing* [Computer software]. R Foundation for Statistical Computing. https://www.R-project.org/

Rizzolatti, G., & Matelli, M. (2003). Two different streams form the dorsal visual system: Anatomy and functions. *Experimental Brain Research*, *153*(2), 146–157. https://doi.org/10.1007/s00221-003-1588-0

Rosabal, F. (1967). Cytoarchitecture of the frontal lobe of the squirrel monkey. *Journal of Comparative Neurology*, *130*(2), 87–108. https://doi.org/10.1002/cne.901300202

Roumazeilles, L., Lange, F. J., Benn, R. A., Andersson, J. L. R., Bertelsen, M. F., Manger, P. R., Flach, E., Khrapitchev, A. A., Bryant, K. L., Sallet, J., & Mars, R.

B. (2022). Cortical Morphology and White Matter Tractography of Three Phylogenetically Distant Primates: Evidence for a Simian Elaboration. *Cerebral Cortex*, *32*(8), 1608–1624. https://doi.org/10.1093/cercor/bhab285

Saleem, K. S., Miller, B., & Price, J. L. (2014). Subdivisions and connectional networks of the lateral prefrontal cortex in the macaque monkey. *Journal of Comparative Neurology*, *522*(7), 1641–1690. https://doi.org/10.1002/cne.23498

Singh, M., & Wong, C.-W. (2010). Independent component analysis-based multifiber streamline tractography of the human brain. *Magnetic Resonance in Medicine*, *64*(6), 1676–1684. https://doi.org/10.1002/mrm.22509

Tendler, B. C., Hanayik, T., Ansorge, O., Bangerter-Christensen, S., Berns, G. S., Bertelsen, M. F., Bryant, K. L., Foxley, S., van den Heuvel, M. P., Howard, A. F., Huszar, I. N., Khrapitchev, A. A., Leonte, A., Manger, P. R., Menke, R. A., Mollink, J., Mortimer, D., Pallebage-Gamarallage, M., Roumazeilles, L., … Miller, K. L. (2022). The Digital Brain Bank, an open access platform for post-mortem imaging datasets. *eLife*, *11*, e73153. https://doi.org/10.7554/eLife.73153

Thiebaut de Schotten, M., Croxson, P. L., & Mars, R. B. (2019). Large-scale comparative neuroimaging: Where are we and what do we need? *Cortex*, *118*, 188–202. https://doi.org/10.1016/j.cortex.2018.11.028

Thompson, E., Mohammadi-Nejad, A. R., Robinson, E. C., Andersson, J. L. R., Jbabdi, S., Glasser, M. F., Bastiani, M., & Sotiropoulos, S. N. (2020). Non-negative data-driven mapping of structural connections with application to the neonatal

brain. *NeuroImage*, *222*, 117273. https://doi.org/10.1016/j.neuroimage.2020.117273

Warrington, S., Bryant, K. L., Khrapitchev, A. A., Sallet, J., Charquero-Ballester, M., Douaud, G., Jbabdi, S., Mars, R. B., & Sotiropoulos, S. N. (2020). XTRACT - Standardised protocols for automated tractography in the human and macaque brain. *NeuroImage*, *217*, 116923. https://doi.org/10.1016/j.neuroimage.2020.116923

Williams, B. A., Kay, R. F., & Kirk, E. C. (2010). New perspectives on anthropoid origins. *Proceedings of the National Academy of Sciences*, *107*(11), 4797–4804. https://doi.org/10.1073/pnas.0908320107

Yuan, R., Nechvatal, J. M., Buckmaster, C. L., Ayash, S., Parker, K. J., Schatzberg, A. F., Lyons, D. M., & Menon, V. (2021). Long-term effects of intermittent early life stress on primate prefrontal–subcortical functional connectivity. *Neuropsychopharmacology*, *46*(7), 1348–1356. https://doi.org/10.1038/s41386-021-00956-0

Chapter 5

Data-driven analysis of prefrontal-innervating ventral stream connections in *Galago senegalensis*.

Declarations

Contribution statement

JEH designed and carried out experiments, analysed data, interpreted results, drafted the manuscript, and produced all figures which appear in this chapter. RAB created the galago cortical surface. MB assisted with surface creation. ZM assisted in editing the manuscript and designing figures. RBM designed experiments, assisted with data analysis and interpretation, assisted in editing the manuscript and designing figures, and supervised the project.

Acknowledgements

JEH is funded by a Wellcome Trust Doctoral Studentship in Neuroscience (222368/Z/21/Z). SW and SNS acknowledge funding from the European Research Council (ERC Consolidator 101000969 to SNS). RBM is supported by the Biotechnology and Biological Sciences Research Council UK (BB/N019814/1) and the Medical Research Council UK (MR/Y010698/1). The Wellcome Centre for Integrative Neuroimaging is supported by core funding from the Wellcome Trust (203139/Z/16/Z). The funders had no role in the design or writing of this report, nor in the collection, analysis, and interpretation of data.

Abstract

Within the primate order, the ventral stream has undergone extensive reorganisation of both grey matter and white matter. Our previous work has described a divergence between two anthropoids and one strepsirrhine species – the rhesus macaque, the black-capped squirrel monkey, and the ring-tailed lemur – in the prefrontal cortical terminations of the ventral stream. Here, we extend our analysis to describe the white matter connectivity in another strepsirrhine species, the Senegal bushbaby (*Galago senegalensis*).

We use a data-driven methodology to reconstruct anterior temporal-frontal and occipitotemporal-frontal connections in the Senegal bushbaby. We find that the Senegal bushbaby exhibits a similar pattern of ventral prefrontal innervation to the lemur, with a higher density of termination sites in the orbitofrontal cortex compared to the rest of the prefrontal cortex. This study extends our previous results to the other extant branch of the strepsirrhine lineage, supporting the hypothesis that an anthropoid elaboration of the ventral stream occurred after their divergence from strepsirrhines.

1. Introduction: The strepsirrhine lineage

Extant primates are divided into two suborders: the haplorhines, consisting of the anthropoids and tarsiers, and the strepsirrhines, consisting of the lemurs and lorises. Primates are an incredibly diverse order with over 500 recognised extant species, and the strepsirrhines are no exception; a recent census identified 113 species of lemurs and 67 species of lorisoids (Fleagle & Seiffert, 2020).

The behaviours of strepsirrhines are as diverse as this suborder's phylogeny. This is well exemplified in the diets of various strepsirrhine species. During the dry season, the mongoose lemur has been observed to spend upward of 80% of its feeding time on nectar (Hilary Simons Morland, 1991; Richard & Dewar, 1991). In contrast, the nine species and subspecies of the genus *Hapalemur* (Fleagle & Seiffert, 2020) feed nearly exclusively on bamboo. Among the galagos – a branch of the lorisoids – some individuals feed primarily on fruits, others on insects, and still others primarily (Scheun et al., 2014) or entirely (Bearder & Martin, 1980) on tree gum.

As well as diet, there is considerable variation among strepsirrhines in diel activity pattern, i.e., the time of day during which an animal is active. Some lemur species are believed to be almost completely diurnal (Bearder et al., 2006), others are cathemeral (Cox & Gaston, 2024; Donati et al., 2013; LaFleur et al., 2014; Parga, 2011), and the lorisoids which are understood to be strictly nocturnal (Nekaris & Bearder, 2011; Svensson et al., 2018). Intriguingly, this diversity in strepsirrhines' diel activity patterns corresponds to cross-species differences in sensory biology.

It is thought that strepsirrhines rely more on olfactory sensation than haplorhines, overall. Yet the primates, including strepsirrhines, are an incredibly visually-oriented order among mammals. Even among nocturnal strepsirrhines, vision

guides complex decision-making tasks (Bearder et al., 2006). However, nocturnality is associated with some marked differences in visual anatomy – for instance, nocturnal strepsirrhines have a larger corneal diameter than diurnal or cathemeral strepsirrhines (Kirk, 2006). What is unknown is whether differences in diel activity pattern among strepsirrhines might be related to large-scale differences in the neuroanatomical substrates which support visual processing.

Our previous work (Chapter 4; Hunt et al., 2025) has shown that the ventral visual stream of the ring-tailed lemur does not innervate as extensive an area of the prefrontal cortex as is the case in anthropoids. Using a construct called the Non-Orbitofrontal Innervation Bias (NOIB) index, which is a measurement of a tract's prefrontal terminations in the orbitofrontal cortex compared to the terminations in the entirety of the prefrontal cortex, we identified that the lemur's ventral stream termination sites are restricted primarily to the orbitofrontal cortex, particularly in comparison to anthropoid species. This finding coheres with our theoretical framework, which asserts that the ventrolateral prefrontal cortex and the ventral stream expanded concomitantly in anthropoids. However, given the diversity of lifestyle adaptations within the strepsirrhines, a more rigorous test of our framework would benefit from examining a lorisoid species with a nocturnal lifestyle. Here, we undertake such a test by reconstructing ventral stream connections within the Senegal bushbaby, *Galago senegalensis*.

The NMF-based, data-driven approach we have described previously (Chapters 3-4; Hunt et al., 2025) is well-suited for this task, because there is no white matter atlas in the galago brain by which to perform atlas-based tractography. However, given the small size and smoothness of the galago brain, an additional goal of this

study is more broadly to assess the suitability of NMF-based approaches for reconstructing connections within smaller brains, such as the galago's.

2. Methods

2.1. Data sources

This study used an existing postmortem neuroimaging data set obtained from the Digital Brain Zoo (Tendler et al., 2022; open.win.ox.ac.uk/DigitalBrainBank), whose acquisition and early processing has previously been described by Bryant et al. (2021). The brain is that of a male Senegal bushbaby, aged 20.9 years at time of death, acquired on loan from the Netherlands Institute of Neuroscience Primate Brain Bank for scanning. Although the brain's frontal regions are slightly asymmetrical (see Figure 5.1A, below), this was identified and accommodated for in the specification of regions of interest. No evidence of neuropathology or surgical damage from brain extraction was observed.

2.2. Data acquisition and preprocessing

Imaging data were collected using a similar protocol to that reported in the previous chapter. The brain was rehydrated in a phosphate buffer solution prior to scanning, and scanned in Fluorinert. A 7-tesla preclinical MRI scanner (Varian, Oxford UK) with a birdcage transmit/receive coil with an inner diameter of 72 mm (Rapid Biomedical GmbH, Rimpar Germany) was used to collect diffusion-weighted images via a spin-echo multi-slice (DW-SEMS) protocol with single line readout. Data are at 0.3 mm isotropic resolution, with a single-shell protocol. The acquisition

parameters are as follows: TE/TR = 25 ms/10 s; matrix size = 128x128x128; b = 4000 s/mm^2 (diffusion-weighted, 128 volumes).

Diffusion MRI data were preprocessed using the Phoenix module of the in-house MR Comparative Anatomy Toolbox (Mr Cat; Mars et al., 2016; www.neuroecologylab.org), which relies on FSL (Jenkinson et al., 2012; www.fmrib.ox.ac.uk/fsl). A three-fibre ball and stick model was then fitted to the data using FSL's BedpostX (Behrens et al., 2007). A cortical surface representation of each template was created using the precon_all (Benn et al., 2025; github.com/neurabenn/precon_all) adaptation of Freesurfer's recon-all pipeline (Fischl, 2012).

2.3. Data-driven tractography

We performed data-driven connection mapping using non-negative matrix factorisation (NMF; Lee & Seung, 1999, 2000). In this study, NMF was run via the NFacT toolbox in Python (Thompson et al., 2020; github.com/SPMIC-UoN/NFacT), which is a tractography-focused wrapper for Scikit-learn's (Pedregosa et al., 2011) NMF algorithm.

As in previous chapters, NMF hyperparameters were selected according to the default parameters in the Scikit-learn Python package, version 1.7, with the exception of hyperparameters controlling initialisation, regularisation, and component number. NMF was initialised using the "non-negative double singular value decomposition" (NNDSVD) method (Boutsidis & Gallopoulos, 2008). Additionally, we changed the regularization terms "alpha_W" and "alpha_H" from the default of 0.0 to 0.1, in order to increase the sparsity and interpretability of the NMF output. Finally, we specified

the number of components (K) to be used in decomposition. As we reported previously (Chapter 3; Hunt et al., 2025), there is no universally optimal number of components to reconstruct white matter tracts in a given brain. Consistent with this, we found that in the galago brain, NMF output did not decompose anterior temporal-frontal and occipitotemporal-frontal connections into separate components at $K = 50$ or $K = 60$ components. As such, we performed NMF decomposition at $K = 50$, 60, 100, 200, 300, and 400 components for this study. Prefrontal innervation was quantified for all values except $K = 50$ and $K = 60$.

To generate the input data for NMF, probabilistic tractography (Behrens et al., 2007) was run from the cortical surface towards the white matter to create a connectivity matrix, wherein each row corresponds to a surface-based (vertex) seed and each column to a volume-based (voxel) target. A matrix was produced with 10,000 seed points, 1,000 samples per seed, and a step length of 0.2 mm with distance correction applied. This connectivity matrix was then decomposed via NMF into two matrices: one comprising white matter by components and one comprising components by grey matter. Thus, for each resultant component, both a grey matter surface array of vertices and a volumetric representation of the component's white matter voxels were produced. Each component was then screened to identify the components comprising ventral stream connections with prefrontal terminations.

2.4. Component selection

To reconstruct connections of interest in the galago brain, we utilised the processing pipeline we previously developed (Chapter 4; Hunt et al., 2025), allowing us to make direct comparisons between the galago brain and the brains of the three

species previously studied. This processing pipeline utilises FSL (Jenkinson et al., 2012), Connectome Workbench (Marcus et al., 2011), and custom tools written in MATLAB (MathWorks, Natick, MA, USA), including the MR Comparative Analysis Toolbox (Mr Cat; Mars et al., 2016; www.neuroecologylab.org).

NMF outputs were analysed to identify and characterise the anterior temporal-frontal and occipitotemporal-frontal connections in both hemispheres. To do so, regions of interest were drawn on the grey matter surface (visualised in the Results section, Figure 5.1A) using Connectome Workbench (Marcus et al., 2011). These regions of interest were specified based on cytoarchitecture reported in prior literature. Due to a lack of cytoarchitectonic data in *Galago senegalensis*, prefrontal and orbitofrontal cortical regions of interest were specified based on the cytoarchitecture reported for the brown greater galago, *Otolemur crassicaudatus*, by Preuss and Goldman-Rakic (1991). The temporal region of interest was drawn to include the anterior temporal pole, while the visual cortical region of interest was based on the parcellation in the northern greater galago, *Otolemur garnettii*, reported by Kaas et al. (2011). As in Chapter 4 and Hunt et al. (2025), the temporal and occipital regions of interest were not used in the calculation of prefrontal innervation metrics or the statistical analysis of cross-species differences.

Using the regions of interest described above, we identified components comprising anterior temporal-frontal and occipitotemporal-frontal connections based on the signal intensity in temporal and prefrontal or occipital and prefrontal surface regions. To identify which components had high signal intensity in both regions of interest, the mean signal intensity in each region was computed for each component using custom MATLAB code, and these averages were multiplied to produce plots

showing which NMF components have high signal intensity in both regions of interest. Those components which had high signal intensity in both regions were then visualised in both surface and volume space, to identify anterior temporal-frontal and occipitotemporal-frontal connections. Identification of connections took place on the basis of the following criteria. Anterior temporal-frontal connections were identified based on termination sites in the anterior temporal pole and prefrontal cortex, a hook-shaped morphology around the lateral sulcus, minimal parietal involvement, and minimal occipital involvement. Occipitotemporal-frontal connections were identified based on termination sites in the ventral occipital cortex and the prefrontal cortex, a morphology running principally along the anterior-posterior axis, minimal parietal involvement, and a ventral position in volume space. At higher NMF component numbers, whenever a connection was split between multiple components as identified using the anatomical criteria outlined above, these components were then summed to produce a single connection.

2.5. Statistical analysis of orbitofrontal innervation

To describe the distribution of prefrontal terminations in the galago brain's ventral visual stream, we calculated Non-Orbitofrontal Innervation Bias (NOIB) index values, using the same formula described previously (Chapter 4):

$$NOIB = \frac{Density\ of\ innervation\ in\ PFC\ (less\ OFC)}{Density\ of\ innervation\ in\ OFC}$$

("PFC" stands for "prefrontal cortex" and OFC stands for "orbitofrontal cortex".)

Then, to compare the distribution of prefrontal terminations in the galago brain to that in the three species studied previously, a many-to-one comparison was carried out for each set of connections using the parametric bootstrap methodology described by Alver and Zhang (2024). The parametric bootstrap is analogous to Dunnett's test (Dunnett, 1955), which is a many-to-one comparison with similarities with Tukey's range test. Dunnett's test performs well on homoscedastic data (i.e., equal variance between groups) and balanced designs. However, because our data show substantial heteroscedasticity between groups and we have an unbalanced design with fewer data points for the galago, Dunnett's test would be inappropriate here. The parametric bootstrap method we employed is more robust under these conditions, and has been established to control the type I error rate (i.e., the false positive rate) more effectively than Dunnett's test when applied to unequal, heteroscedastic data such as ours (Alver & Zhang, 2024). To compare NOIB values between species, we therefore conducted the parametric bootstrap test with the *pbANOVA* package (Alver & Zhang, 2022) in R, using 10,000 simulated values to generate the distributions.

3. Results

In this study, we have identified and characterised ventral stream prefrontal connections in the Senegal bushbaby, *Galago senegalensis*. These connections are reconstructed using a data-driven method based on non-negative matrix factorisation (NMF). Using the cortical innervation patterns and volumetric white matter paths of NMF components, we identified the components which comprise each connection in both hemispheres of the galago brain. We then quantified the extent of prefrontal

innervation of each set of connections, and compared these results to data we previously generated for the macaque, squirrel monkey, and lemur.

3.1. NMF identifies occipitotemporal-frontal connections in the galago, but does not distinguish between ventral stream connections at low component numbers

As with the other brains we have analysed, components of interest were screened based on signal intensity in cortical grey matter regions of interest (Figure 5.1A), then visualised in both surface and volume space. It has been observed by ourselves (Chapter 3; Hunt et al., 2025) and others (Thompson et al., 2020) that NMF performance varies on a per-tract and a per-brain basis, with different tracts better reconstructed at different component numbers.

In the galago brain, we observed that our NMF procedure fails to differentiate between anterior temporal-frontal and occipitotemporal-frontal connections, at 50 and 60 components (Figure 5.1B-C). At these lower component numbers, the components which correspond to the ventral stream connections we aim to reconstruct exhibit the hook-shaped morphology and fronto-temporal-frontal path characteristic of the uncinate fasciculus, yet include a substantial posterior signal, more characteristic of the inferior fronto-occipital fasciculus. The failure to identify anterior temporal-frontal and occipitotemporal-frontal connections could potentially have been due to a deficiency in our screening procedure. Therefore, to ascertain that these connections could not be identified among any of the remaining NMF components, we visually inspected each component at K = 50 and K = 60, and found

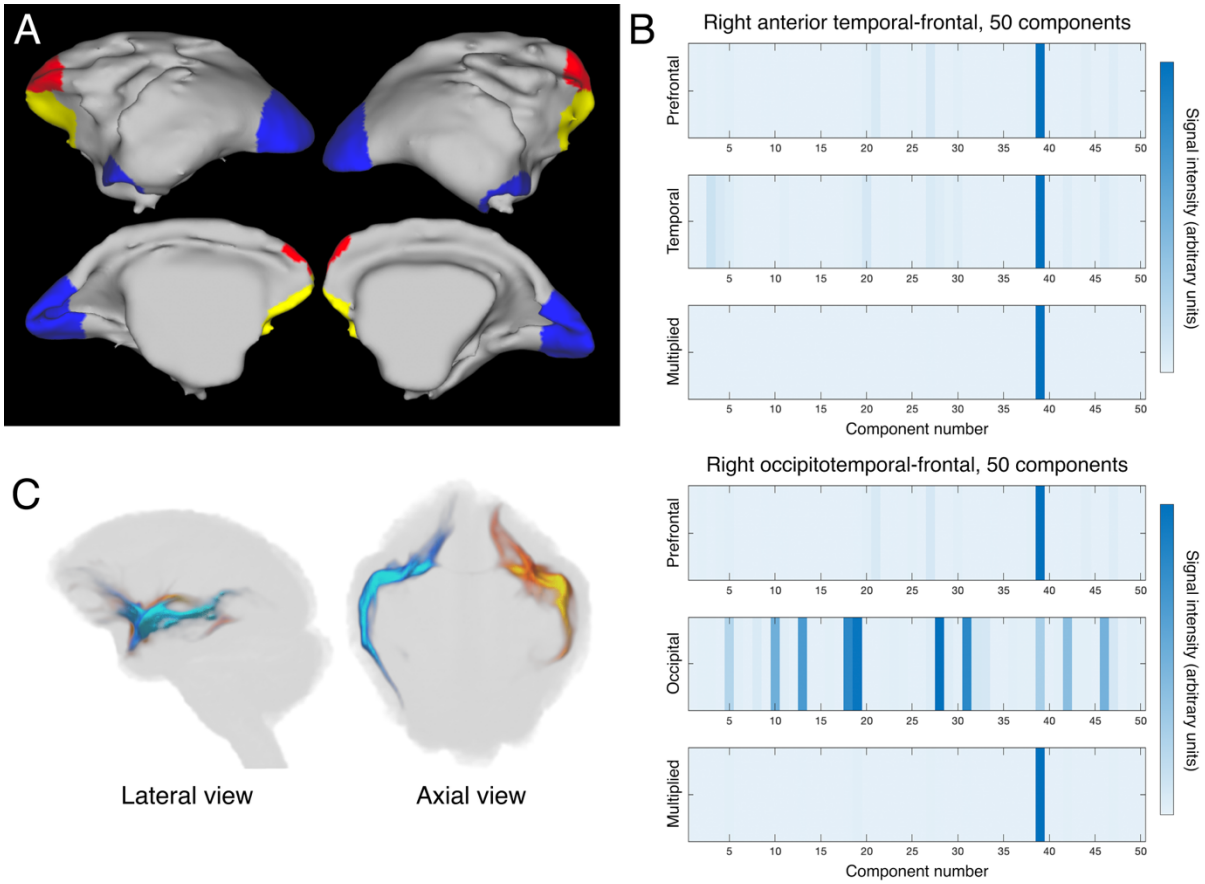


Figure 5.1. Merging of anterior temporal-frontal and occipitotemporal-frontal connections at 50- and 60-component levels. (A) *Galago cortical surface, with regions of interest (ROIs). Blue regions indicate the anterior temporal pole or occipital cortical ROI used in selecting components for further screening. Yellow regions indicate the orbitofrontal cortex. Red indicates the remaining portion of prefrontal cortex. Note that the prefrontal cortical ROI includes all of the orbitofrontal cortex, as well as the remaining regions indicated in red.* ***(B)*** *Representative examples of the white matter connection screening procedure at* K *= 50. A single component (#39) shows high signal intensity in prefrontal, temporal, and occipital regions, with no other candidate components emerging.* ***(C)*** *Anterior temporal-frontal and occipitotemporal-frontal connections are merged into a single component, representative examples at* K *= 50. 3-D volumetric reconstructions show a lateral view of the left hemisphere (left) and an angled view (right), showing slightly more of the dorsal aspect for visualisation purposes. Blue indicates the left hemispheric component; orange indicates the right hemispheric component.*

---

no additional components with a morphology characteristic of either of these connections. Therefore, for parity of comparison with the other species in our study, we decomposed the galago brain at two additional model orders – K = 300 and K = 400 – in addition to the original component numbers of $K = 100$ and $K = 200$ we had

intended. This yielded eight total reconstructions of each connection (two brain hemispheres multiplied by four model orders).

3.2. At higher component numbers, NMF reliably reconstructs and differentiates ventral stream connections in the galago

At higher component numbers (i.e., $K = 100$ and above), NMF produced components corresponding to the anterior temporal-frontal and occipitotemporal-frontal connections we sought to reconstruct from our whole-brain tractography matrix. The anterior temporal-frontal connection and occipitotemporal-frontal connections were both successfully differentiated at higher component numbers (Figure 5.2A-B).

Within these data, we observed the same characteristics of NMF-based white matter decomposition noted in previous chapters. At lower component numbers, connections were more likely to include nonspecific white matter (Figure 5.2B), while at higher component numbers, individual components were more likely to correspond to subdivisions of connections. However, this latter effect was less pronounced in the galago brain. Anterior temporal-frontal connections were not subdivided at any component numbers tested, while occipitotemporal-frontal connections were subdivided among two components only at $K = 300$ and $K = 400$. In contrast, anterior temporal-frontal connections in the macaque, squirrel monkey, and lemur were subdivided across multiple components at $K = 60$, 100, and 200 components in each species, while occipitotemporal-frontal connections were subdivided among

multiple components at $K = 50$, 60, 100, and 200 components in the macaque and squirrel monkey, and at $K = 60$, 100, and 200 components in the lemur.

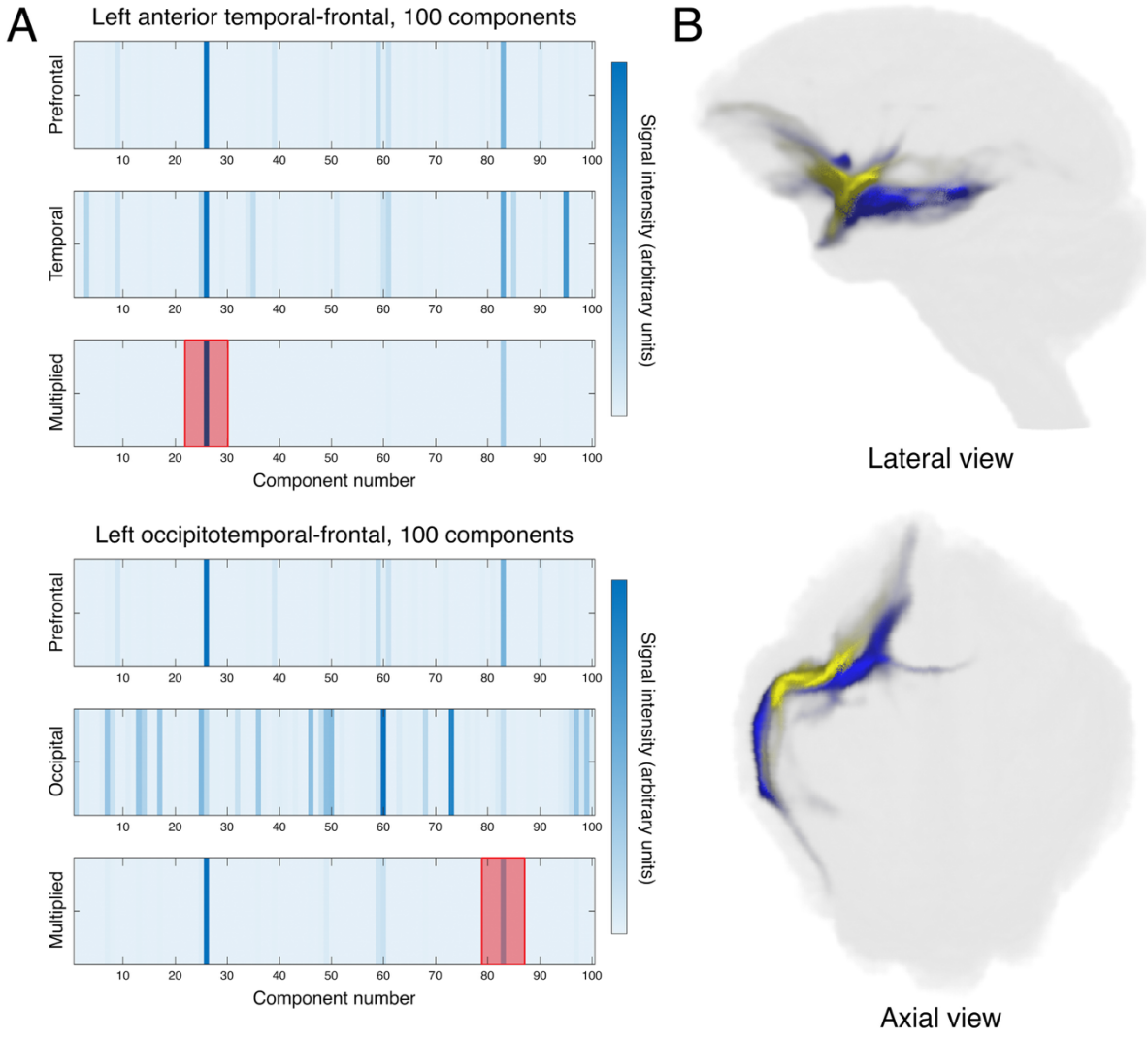


Figure 5.2. NMF-based reconstruction of ventral stream connections in the galago. (A) *Example screening output, showing that different connections of the ventral stream are decomposed into different components, at* K *= 100. Red boxes correspond to the components comprising each connection, visualised in Panel B.* ***(B)*** *Anterior temporal-frontal and occipitotemporal-frontal connections are represented by distinct components in NMF decomposition. 3-D volumetric reconstructions show the ventral stream connections at* K *= 100. Images show a lateral view of the left hemisphere (above) and an axial view (below). Yellow indicates the left anterior temporo-frontal connection; blue indicates the right occipitotemporal-frontal connection. Note the nonspecific volumetric signal on the posterior side of the anterior temporal-frontal connection and the medial side of the occipitotemporal-frontal connection.*

3.3. The galago's ventral visual stream's prefrontal innervation patterns are most similar to those in lemur

Prefrontal cortical termination patterns were quantified using the Non-Orbitofrontal Innervation Bias (NOIB) index introduced in Chapter 4, calculated as follows):

$$NOIB = \frac{Density\ of\ innervation\ in\ PFC\ (less\ OFC)}{Density\ of\ innervation\ in\ OFC}$$

("PFC" stands for "prefrontal cortex" and OFC stands for "orbitofrontal cortex".)

The NOIB values for the galago's ventral stream connections were compared against those in the macaque, squirrel monkey, and lemur, described previously (Chapter 4). To assess the extent to which the galago differs from the three species previously studied, we used observed mean values and a parametric bootstrap technique to simulate distributions which were then used for many-to-one comparisons of the galago NOIB values to the macaque, squirrel monkey, and lemur NOIB values. This parametric bootstrap technique is an alternative to Dunnett's test for many-to-one comparisons, and provides greater robustness against unequal sample sizes and heteroscedasticity (Alver & Zhang, 2024).

The NOIB values of the anterior temporal-frontal connections for each group were as follows, reported as mean ± standard deviation (number of brain hemispheres). Macaque: 0.20 ± 0.06 ($n = 6$); squirrel monkey: 0.39 ± 0.07 ($n = 6$); lemur: 0.10 ± 0.09 ($n = 6$); galago: 0.12 ± 0.08 ($n = 2$). Based on the parametric bootstrap distributions, the mean NOIB for anterior temporal-frontal connections in the galago was significantly different from that in the squirrel monkey (difference

from galago: 0.28, 95% confidence interval: 0.15 – 0.41, $p = 1.6 \times 10^{-3}$), but not from the macaque or lemur (macaque difference from galago: 0.08, 95% confidence interval: -0.02 – 0.19, $p = 0.10$; lemur difference from galago: -0.01, 95% confidence interval: -0.15 – 0.13, $p = 0.98$). Anterior temporal-frontal innervation patterns across both the orbitofrontal cortex and the (non-orbitofrontal) prefrontal cortex are presented for all species in Figure 5.3A.

For occipitotemporal-frontal connections, NOIB values for each group were as follows, reported as mean ± standard deviation (number of brain hemispheres). Macaque: 1.22 ± 1.61 ($n = 6$); squirrel monkey: 0.79 ± 0.38 ($n = 6$); lemur: 0.26 ± 0.31 ($n = 6$); galago: 0.13 ± 0.12 ($n = 2$). The mean NOIB among occipitotemporal-frontal connections in the galago differed from that in the macaque (difference from galago: 1.09, 95% confidence interval: 0.05 – 2.12, $p = 0.04$) and the squirrel monkey (difference from galago: 0.66, 95% confidence interval: 0.41 – 0.91, $p = 4 \times 10^{-4}$), but not from the lemur (difference from galago: 0.13, 95% confidence interval: -0.12 – 0.37, $p = 0.35$). The innervation patterns across both the orbitofrontal cortex and the (non-orbitofrontal) prefrontal cortex are shown for all species' occipitotemporal-frontal connections in Figure 5.3B.

In sum, these data indicate that prefrontal cortical innervation patterns in the galago, measured via the NOIB index, do not statistically differ from those in the lemur. Analysis did not reveal a difference between the macaque and the galago in innervation patterns of the anterior temporal-frontal connections, but did reveal a difference in occipitotemporal-frontal connections. The galago and squirrel monkey differed in NOIB values for both sets of connections.

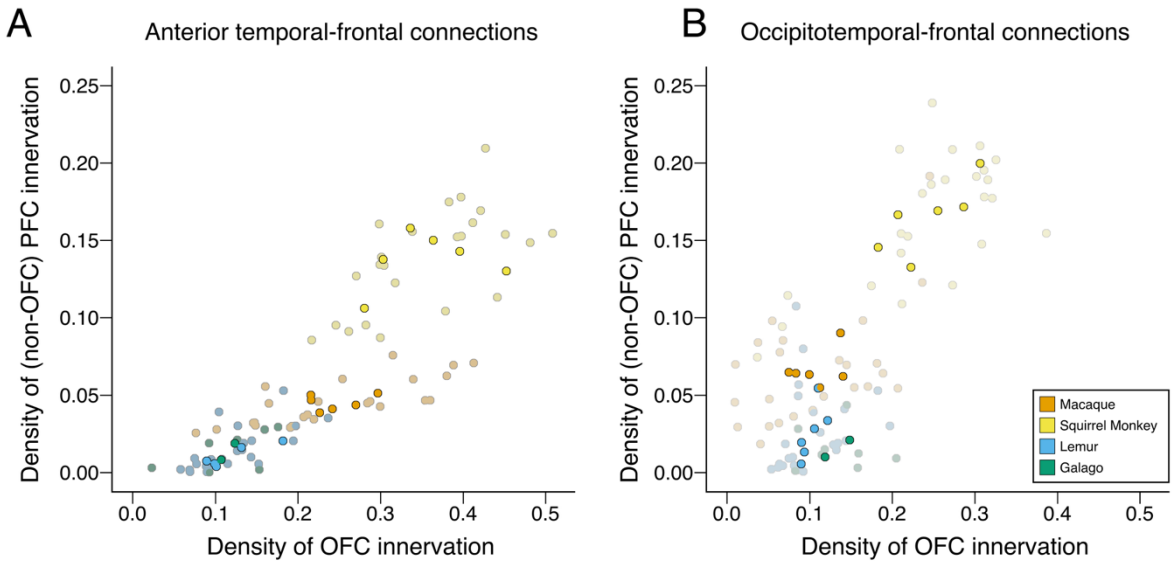


Figure 5.3. Density of prefrontal and orbitofrontal cortical innervation, across all species. *Innervation densities are shown for both* ***(A)*** *anterior temporal-frontal and* ***(B)*** *occipitotemporal-frontal connections in all species. Light markers indicate NMF-based reconstructions of a connection in that species. Dark markers indicate the average among reconstructions on a per-hemisphere basis. All density scales use arbitrary units. Data are colour-coded by species in both panels based on the legend in Panel B. NOIB values presented throughout the text are calculated by dividing the (non-OFC) PFC innervation densities (visualised on the vertical axis) by the OFC innervation densities (visualised on the horizontal axis) for each reconstruction.*

---

4. Discussion

This study has used a data-driven tractography approach based on non-negative matrix factorisation (NMF) to reconstruct two pairs of ventral stream connections in the brain of a Senegal bushbaby (*Galago senegalensis*): the anterior temporal-frontal connections and the occipitotemporal-frontal connections. The anterior temporal-frontal connections bear a resemblance to the uncinate fasciculus, while the occipitotemporal-frontal connections resemble the inferior fronto-occipital fasciculus.

By reconstructing each connection four times with a different number of NMF components each time, we were able to average the results on a per-hemisphere, per-

connection basis for comparison with connections we have reconstructed via the same methodology in three other primate brains: the macaque, the squirrel monkey, and the lemur. Our results demonstrate that compared to the macaque and the squirrel monkey, the density of ventral stream innervation to the orbitofrontal cortex is higher compared to the innervation of the rest of the prefrontal cortex in the galago, for one or both sets of connections. If more data were available, it is possible that a greater sample size for the galago would have yielded a significant difference between the galago and the macaque for both sets of connections, as higher sample sizes yield greater statistical power if the sample's error terms are randomly distributed (Cohen, 1988). Nevertheless, the present data indicate that the galago and lemur have similar orbitofrontal and (non-orbitofrontal) prefrontal cortical innervation densities for both sets of connections, with the macaque and squirrel monkey generally exhibiting divergent patterns of prefrontal cortical innervation densities. Because the galago and the lemur are both strepsirrhines while the macaque and squirrel monkey are both anthropoids, these results reinforce our prior work indicating a divergence of the lemur from the macaque and squirrel monkey. The present work suggests a common pattern of prefrontal cortical innervation across both extant clades of the strepsirrhine lineage.

Strepsirrhines are known to use visual cues to guide decisions in contexts such as predator evasion and foraging (Bearder et al., 2006). However, it has been argued that the anthropoids occupy a more complex foraging niche and utilise more volatile food sources than other primates (Passingham & Wise, 2012). Concomitantly with this behavioural specialisation, fossil evidence suggests that the anthropoids underwent a dramatic expansion of the temporal lobe after their divergence from the

strepsirrhines (Kay et al., 2025). This temporal lobe expansion, paired with the expansion of the reciprocally-connected ventrolateral prefrontal cortex in anthropoids (Eldridge et al., 2021), is believed to be an innovation unique to the anthropoids.

Our work supports and extends this hypothesis, demonstrating that the white matter of the anthropoid ventral stream differs from that of strepsirrhines. While the previous chapter first identified this difference between clades by comparing the lemur against the macaque and the squirrel monkey, this chapter supports that finding with additional data from the other major branch of the strepsirrhines, the lorisoids. With the availability of data from multiple species in each group, we demonstrate that this pattern seems to hold in both the cathemeral lemur and the obligate nocturnal galago.

It is also worth noting, however, that multiple possible confounding explanations exist for our findings. First, it is well-appreciated that brain mass scales with body mass across a wide diversity of species, often with taxon-specific scaling rules (Armstrong, 1983; Burger et al., 2019; Jerison, 1973; Martin, 1981; Pagel & Harvey, 1989; Schoenemann, 2003 and many more). Furthermore, it is known that within the primate lineage, different scaling rules govern changes in areal mass and neuron count, across the visual system (Collins et al., 2013). The primate species examined in this work differ in overall brain mass and body size, and it is possible that the differences in prefrontal cortical innervation patterns described here co-vary with confounding variables which have not been considered. In the absence of additional data from a greater number of species, it is not possible to rule out such an explanation; however, it seems unlikely that such factors would completely confound

an inference of evolutionary adaptive differences in ventral stream evolution, independent of overall brain or body size.

More generally, the present work validates the utility of NMF-based, data-driven tractography across a wider range of species. Our previous work identified that the between-species variability in ventral visual stream connections is much greater than variability arising from NMF parameterisation, and our current work extends this finding by reconstructing ventral visual stream connections in another primate brain. The NMF-based technique we have employed here seems to be sensitive enough to identify cross-species patterns in the scaling of connections to the prefrontal cortex, providing further validation that the technique can produce reliable tract reconstructions across species, with a degree of precision to uncover as-yet undescribed patterns in brain evolution. As high-quality neuroimaging data become available for more species, we believe that NMF will allow us to address additional questions in these previously understudied brains.

References

Alver, S., & Zhang, G. (2022). *pbANOVA: Parametric Bootstrap for ANOVA Models* (Version 0.1.0) [R]. https://CRAN.R-project.org/package=pbANOVA

Alver, S., & Zhang, G. (2024). Multiple comparisons of treatment against control under unequal variances using parametric bootstrap. *Journal of Applied Statistics*, *51*(10), 1861–1877. https://doi.org/10.1080/02664763.2023.2245179

Armstrong, E. (1983). Relative Brain Size and Metabolism in Mammals. *Science*, *220*(4603), 1302–1304. https://doi.org/10.1126/science.6407108

Bearder, S. K., & Martin, R. D. (1980). Acacia gum and its use by bushbabies,Galago senegalensis (Primates: Lorisidae). *International Journal of Primatology*, *1*(2), 103–128. https://doi.org/10.1007/BF02735592

Bearder, S. K., Nekaris, K. a. I., & Curtis, D. J. (2006). A Re-Evaluation of the Role of Vision in the Activity and Communication of Nocturnal Primates. *Folia Primatologica*, *77*(1–2), 50–71. https://doi.org/10.1159/000089695

Behrens, T. E. J., Berg, H. J., Jbabdi, S., Rushworth, M. F. S., & Woolrich, M. W. (2007). Probabilistic diffusion tractography with multiple fibre orientations: What can we gain? *NeuroImage*, *34*(1), 144–155. https://doi.org/10.1016/j.neuroimage.2006.09.018

Benn, R. A., Xu, T., Mars, R. B., Boch, M., Roumazeilles, L., Heuer, K., Toro, R., Margulies, D. S., Manzano-Patron, J. P., Montesinos, P., Galan-Arriola, C., Lopez-Martin, G., Sanchez-Gonzalez, J., Duff, E. P., & Ibañez, B. (2025). *Precon_all: A species-agnostic automated pipeline for non-human cortical surface*

reconstruction (p. 2025.04.16.649072). bioRxiv. https://doi.org/10.1101/2025.04.16.649072

Boutsidis, C., & Gallopoulos, E. (2008). SVD based initialization: A head start for nonnegative matrix factorization. *Pattern Recognition*, *41*(4), 1350–1362. https://doi.org/10.1016/j.patcog.2007.09.010

Bryant, K. L., Ardesch, D. J., Roumazeilles, L., Scholtens, L. H., Khrapitchev, A. A., Tendler, B. C., Wu, W., Miller, K. L., Sallet, J., van den Heuvel, M. P., & Mars, R. B. (2021). Diffusion MRI data, sulcal anatomy, and tractography for eight species from the Primate Brain Bank. *Brain Structure and Function*, *226*(8), 2497–2509. https://doi.org/10.1007/s00429-021-02268-x

Burger, J. R., George, M. A., Jr., Leadbetter, C., & Shaikh, F. (2019). The allometry of brain size in mammals. *Journal of Mammalogy*, *100*(2), 276–283. https://doi.org/10.1093/jmammal/gyz043

Cohen, J. (1988). *Statistical Power Analysis for the Behavioral Sciences* (1st edn). Routledge.

Collins, C. E., Leitch, D. B., Wong, P., Kaas, J. H., & Herculano-Houzel, S. (2013). Faster scaling of visual neurons in cortical areas relative to subcortical structures in non-human primate brains. *Brain Structure & Function*, *218*(3), 805–816. https://doi.org/10.1007/s00429-012-0430-5

Cox, D. T. C., & Gaston, K. J. (2024). Cathemerality: A key temporal niche. *Biological Reviews*, *99*(2), 329–347. https://doi.org/10.1111/brv.13024

Donati, G., Santini, L., Razafindramanana, J., Boitani, L., & Borgognini-Tarli, S. (2013). (Un-)expected nocturnal activity in “Diurnal” Lemur catta supports cathemerality as one of the key adaptations of the lemurid radiation. *American*

Journal of Physical Anthropology, *150*(1), 99–106. https://doi.org/10.1002/ajpa.22180

Dunnett, C. W. (1955). A Multiple Comparison Procedure for Comparing Several Treatments with a Control. *Journal of the American Statistical Association*, *50*(272), 1096–1121. https://doi.org/10.2307/2281208

Eldridge, M. A., Hines, B. E., & Murray, E. A. (2021). The visual prefrontal cortex of anthropoids: Interaction with temporal cortex in decision making and its role in the making of 'visual animals'. *Current Opinion in Behavioral Sciences*, *41*, 22–29. https://doi.org/10.1016/j.cobeha.2021.02.012

Fischl, B. (2012). FreeSurfer. *NeuroImage*, *62*(2), 774–781. https://doi.org/10.1016/j.neuroimage.2012.01.021

Fleagle, J. G., & Seiffert, E. R. (2020). Chapter 20—The Phylogeny of Primates. In J. H. Kaas (Ed.), *Evolutionary Neuroscience (Second Edition)* (pp. 483–518). Academic Press. https://doi.org/10.1016/B978-0-12-820584-6.00020-9

Hilary Simons Morland. (1991). *Social organization and ecology of black and white ruffed femurs (Varecia variegata variegata) in lowland rain forest, Nosy Mangabe, Madagascar* [Ph.D.]. Yale University.

Hunt, J. E., Warrington, S., Roumazeilles, L., Jbabdi, S., Molnár, Z., Sotiropoulos, S. N., & Mars, R. B. (2025). An anthropoid/strepsirrhine divergence in ventral visual stream connectivity. *bioRxiv*, 2025.05.19.653861. https://doi.org/10.1101/2025.05.19.653861

Jenkinson, M., Beckmann, C. F., Behrens, T. E. J., Woolrich, M. W., & Smith, S. M. (2012). FSL. *NeuroImage*, *62*(2), 782–790. https://doi.org/10.1016/j.neuroimage.2011.09.015

Jerison, H. J. (1973). *Evolution of the Brain and Intelligence*. Academic Press.

Kaas, J. H., Gharbawie, O., & Stepniewska, I. (2011). The Organization and Evolution of Dorsal Stream Multisensory Motor Pathways in Primates. *Frontiers in Neuroanatomy*, *5*. https://doi.org/10.3389/fnana.2011.00034

Kay, R. F., Kirk, E. C., Vizcaino, S. F., Bargo, M. S., Allen, K. L., Olson, S., & Morse, P. E. (2025). The Fossil Record of Anthropoid Brain Evolution. *American Journal of Biological Anthropology*, *187*(3), e70081. https://doi.org/10.1002/ajpa.70081

Kirk, E. C. (2006). Eye Morphology in Cathemeral Lemurids and Other Mammals. *Folia Primatologica*, *77*(1–2), 27–49. https://doi.org/10.1159/000089694

LaFleur, M., Sauther, M., Cuozzo, F., Yamashita, N., Jacky Youssouf, I. A., & Bender, R. (2014). Cathemerality in wild ring-tailed lemurs (Lemur catta) in the spiny forest of Tsimanampetsotsa National Park: Camera trap data and preliminary behavioral observations. *Primates*, *55*(2), 207–217. https://doi.org/10.1007/s10329-013-0391-1

Lee, D. D., & Seung, H. S. (1999). Learning the parts of objects by non-negative matrix factorization. *Nature*, *401*(6755), Article 6755. https://doi.org/10.1038/44565

Lee, D. D., & Seung, H. S. (2000). Algorithms for Non-negative Matrix Factorization. *Advances in Neural Information Processing Systems*, *13*. https://proceedings.neurips.cc/paper_files/paper/2000/hash/f9d1152547c0bde01830b7e8bd60024c-Abstract.html

Marcus, D., Harwell, J., Olsen, T., Hodge, M., Glasser, M., Prior, F., Jenkinson, M., Laumann, T., Curtiss, S., & Van Essen, D. (2011). Informatics and Data Mining

Tools and Strategies for the Human Connectome Project. *Frontiers in Neuroinformatics*, *5*. https://doi.org/10.3389/fninf.2011.00004

Mars, R. B., Verhagen, L., Gladwin, T. E., Neubert, F.-X., Sallet, J., & Rushworth, M. F. S. (2016). Comparing brains by matching connectivity profiles. *Neuroscience & Biobehavioral Reviews*, *60*, 90–97. https://doi.org/10.1016/j.neubiorev.2015.10.008

Martin, R. D. (1981). Relative brain size and basal metabolic rate in terrestrial vertebrates. *Nature*, *293*(5827), 57–60. https://doi.org/10.1038/293057a0

Nekaris, A., & Bearder, S. K. (2011). The Lorisiform Primates of Asia and Mainland Africa. In *Primates in Perspective* (2nd edn, pp. 34–54). Oxford University Press.

Pagel, M. D., & Harvey, P. H. (1989). Taxonomic Differences in the Scaling of Brain on Body Weight Among Mammals. *Science*, *244*(4912), 1589–1593. https://doi.org/10.1126/science.2740904

Parga, J. A. (2011). Nocturnal ranging by a diurnal primate: Are ring-tailed lemurs (Lemur catta) cathemeral? *Primates*, *52*(3), 201–205. https://doi.org/10.1007/s10329-011-0257-3

Passingham, R. E., & Wise, S. P. (2012). *The Neurobiology of the Prefrontal Cortex: Anatomy, Evolution, and the Origin of Insight*. OUP Oxford.

Pedregosa, F., Varoquaux, G., Gramfort, A., Michel, V., Thirion, B., Grisel, O., Blondel, M., Prettenhofer, P., Weiss, R., Dubourg, V., Vanderplas, J., Passos, A., Cournapeau, D., Brucher, M., Perrot, M., & Duchesnay, É. (2011). Scikit-learn: Machine Learning in Python. *Journal of Machine Learning Research*, *12*(85), 2825–2830.

Preuss, T. M., & Goldman-Rakic, P. S. (1991). Myelo- and cytoarchitecture of the granular frontal cortex and surrounding regions in the strepsirhine primate Galago and the anthropoid primate Macaca. *Journal of Comparative Neurology*, *310*(4), 429–474. https://doi.org/10.1002/cne.903100402

Richard, A. F., & Dewar, R. E. (1991). Lemur Ecology. *Annual Review of Ecology, Evolution, and Systematics*, *22*(Volume 22,), 145–175. https://doi.org/10.1146/annurev.es.22.110191.001045

Scheun, J., Bennett, N. C., Ganswindt, A., & Nowack, J. (2014). Spicing up the menu: Evidence of fruit feeding in Galago moholi. *Primates*, *55*(3), 359–363. https://doi.org/10.1007/s10329-014-0420-8

Schoenemann, P. T. (2003). Brain Size Scaling and Body Composition in Mammals. *Brain Behavior and Evolution*, *63*(1), 47–60. https://doi.org/10.1159/000073759

Svensson, M. S., Nekaris, K. a. i., Bearder, S. K., Bettridge, C. M., Butynski, T. M., Cheyne, S. M., Das, N., de Jong, Y. A., Luhrs, A. M., Luncz, L. V., Maddock, S. T., Perkin, A., Pimley, E., Poindexter, S. A., Reinhardt, K. D., Spaan, D., Stark, D. J., Starr, C. R., & Nijman, V. (2018). Sleep patterns, daytime predation, and the evolution of diurnal sleep site selection in lorisiforms. *American Journal of Physical Anthropology*, *166*(3), 563–577. https://doi.org/10.1002/ajpa.23450

Tendler, B. C., Hanayik, T., Ansorge, O., Bangerter-Christensen, S., Berns, G. S., Bertelsen, M. F., Bryant, K. L., Foxley, S., van den Heuvel, M. P., Howard, A. F., Huszar, I. N., Khrapitchev, A. A., Leonte, A., Manger, P. R., Menke, R. A., Mollink, J., Mortimer, D., Pallebage-Gamarallage, M., Roumazeilles, L., … Miller, K. L. (2022). The Digital Brain Bank, an open access platform for post-

mortem imaging datasets. *eLife*, *11*, e73153. https://doi.org/10.7554/eLife.73153

Thompson, E., Mohammadi-Nejad, A. R., Robinson, E. C., Andersson, J. L. R., Jbabdi, S., Glasser, M. F., Bastiani, M., & Sotiropoulos, S. N. (2020). Non-negative data-driven mapping of structural connections with application to the neonatal brain. *NeuroImage*, *222*, 117273. https://doi.org/10.1016/j.neuroimage.2020.117273

Chapter 6

General discussion.

Declarations

Contribution statement

JEH drafted all of the text and produced all figures which appear in this chapter. ZM and RBM assisted in editing the manuscript and designing figures.

Acknowledgements

JEH is funded by a Wellcome Trust Doctoral Studentship in Neuroscience (222368/Z/21/Z). RBM is supported by the Biotechnology and Biological Sciences Research Council UK (BB/N019814/1) and the Medical Research Council UK (MR/Y010698/1). The funders had no role in the design or writing of this report, nor in the collection, analysis, and interpretation of data.

1. Summary of findings

This thesis sets out to achieve two goals:

i) To advance scientific understanding of the evolution and diversity of vertebrate visual systems, and

ii) To develop new tools and approaches in the support of comparative neuroscience research.

To do this, I have revisited prior reports on spontaneous retinal waves (Chapter 2), a kind of spontaneous activity in the developing retina. Afterwards, I have developed the use of a data-driven approach for identifying and analysing white matter tracts. I have used this approach to compare the ventral stream's prefrontal cortical innervation patterns across four primate species (Chapters 3-5).

1.1. Neuroethology and retinal waves

In Chapter 2, I review reports on retinal waves across the vertebrate lineage. I identify that retinal waves have been observed in four orders of mammals as well as one bird, one reptile, and one ray-finned fish. However, retinal waves have been reported absent in frogs. This is surprising, given the position of frogs in the vertebrate lineage, relative to amniotes and fishes. I additionally describe a temporal-to-nasal pattern in retinal activation that is common across species in both early development and adulthood. Finally, considering the dynamics of retinal waves in zebrafish and the ecological context in which zebrafish develop, I propose the possibility of a relatively simple ancestral retinal wave which was important for the development of the retina itself, but not its retinofugal projections.

1.2 Developing a data-driven approach to study white matter connections across species

In Chapter 3, I develop the use of a data-driven approach based on non-negative matrix factorisation (NMF) to reconstruct known white matter fibre bundles across multiple species. This approach has previously been applied to the human brain (Thompson et al., 2020), identifying known white matter connections in a sample of 323 subjects. My work extends this approach as I demonstrate that even within a single adult human or macaque brain, NMF can reliably reproduce known white matter tracts. This data-driven approach enables the reconstruction of white matter tracts without the anatomical priors required for the production of the tractographic atlases upon which the gold-standard tractographic approach relies.

1.3. An anthropoid/strepsirrhine divergence in ventral visual stream connectivity

Chapter 4 applies the approach developed in the previous chapter to the study of ventral stream connections in primates. First, I extend the findings of the previous chapter to describe how a higher sample size improves poor NMF-based tract reconstructions in the macaque, but yields negligible improvements for tracts which are already well-reconstructed via NMF. I then use the NMF-based approach to reconstruct ventral stream white matter tracts in the macaque, squirrel monkey, and lemur. I identify that ventral stream prefrontal innervations in the lemur are more restricted to the orbitofrontal cortex than in the macaque or squirrel monkey. I furthermore quantify the different contributors to variance in this data set, concluding

that the variance arising from cross-species differences is far greater than the variance between brain hemispheres or the variance between NMF-based tract reconstructions. To my knowledge, this is the first quantification of various contributions of variance in a cross-species tractographic data set, providing an important validation of earlier studies on between-species differences in connectivity.

1.4. Ventral stream connectivity in the galago

Chapter 5 reconstructs the same ventral stream connections from the previous chapter, in a galago brain. I characterise how the analysis pipeline must be slightly modified to accommodate the small size of the galago brain, and then I quantify the extent of prefrontal innervation by these tracts. Prefrontal innervation is restricted to the orbitofrontal cortex by an even greater extent in the galago than in any species studied in the previous chapter. After controlling for the size of the orbitofrontal cortex, the extent of orbitofrontal restriction is similar to that in lemur, suggesting a scaling of ventral stream orbitofrontal innervation with relative orbitofrontal size in the strepsirrhines. I extend this observation to identify a potential allometry between prefrontal cortical innervation patterns and orbitofrontal cortical size across the primates, with a grade shift between strepsirrhines and anthropoids.

2. Future work: methodological considerations

2.1. Granularity of analysis

For psychologists, neuroscientists, and philosophers alike, the *granularity* of a neuroscientific analysis deserves attention. The granularity of an analysis, study,

phenomenon, explanation, etc., sometimes called its *level*, refers to how coarse- or fine-grained it is. A (very) coarse-grained explanation of how a match works might be "When the match is struck, it will light", while a finer-grained explanation might refer to the physical and chemical interactions of the phosphorus or other materials which constitute the match. Within neuroscience, a coarse-grained explanation of long-term potentiation (LTP) may invoke Hebb's rule, while a fine-grained explanation might refer to the activity of CaMKII and PKC. Several debates in neuroscience and philosophy turn on the granularity of an analysis or concept. This is exemplified best, perhaps, by the controversies surrounding the eliminative materialism position championed by Paul and Patricia Churchland (Ramsey, 2024), which states that the mental states posited by common/folk psychology do not actually exist.

In the present thesis, it bears explicit mention that I have validated the suitability for NMF-based methodologies for identifying coarse differences in comparing white matter connectivity across species. However, it is equally important to note that I have *not* validated the technique's suitability for assessing finer differences, such as inter-individual differences or hemispheric asymmetries. Indeed, in Chapter 4, I present an analysis which suggests that the NMF-based approach I have taken to reconstruct white matter connections may be poorly-suited for assessing these kinds of finer differences – at least, at the low sample sizes used in the present study. In our data set, there is greater variance between NMF-based reconstructions of a connection within a brain hemisphere than between hemispheres of the same species (see Figure 4.4).

It is an open question whether an increased sample size would resolve this issue. If a sample's error terms are randomly distributed, then greater sample sizes

yield greater statistical power (see, e.g., Cohen, 1988). However, if errors are systematically biased, increasing sample sizes may yield minimal or nonexistent benefits. This thesis employs no analysis suitable to assess NMF-based tractography's performance on assessing these sorts of differences.

2.2. Model selection

Stated in broad terms, my thesis work models brains' white matter connectivity based on diffusion MRI data. Using an NMF-based, data-driven approach, I "reconstruct" white matter connections, which is to say I generate models of putative tract paths and innervation patterns based on diffusion-based signals from across the brain. Models are approximations of the real world, and the relevant question in assessing a model is whether it provides useful information (Burnham & Anderson, 2002).

My thesis has shown that there is notable variance in NMF-based reconstructions of a given tract, and indeed there are differences between NMF-based and atlas-based reconstructions of the same tract, within a single brain. These patterns of variance suggest that the NMF-based technique presented here is poorly-suited for assessing the ground-truth of white matter connectivity in a given brain. However, as Burnham and Anderson noted (2002), the question is whether a model provides useful information. NMF-based models have shown robust for detecting large, cross-species differences, even within the same infraorder (e.g., squirrel monkeys and macaques; infraorder: Simiiformes), at sample sizes of 1-3 brains. This is particularly important for comparative neuroscience, where sample sizes are frequently small and neuroimaging provides a non-destructive approach for assessing

white matter connectivity. Although other methodologies such as blunt dissection and viral tracing may be better suited for the assessment of a white matter connection's absolute ground truth, the NMF-based technique I have developed in this thesis has the notable benefits of being non-destructive and requiring minimal sample sizes to draw cross-species inferences. These benefits are particularly important, given the small numbers of species on which primate comparative studies are frequently based. The NMF-based approach presented here overcomes several of the challenges faced by other methodologies for comparative neuroscience, offering a more efficient workflow with which to leverage high-throughput neuroimaging techniques (Mars et al., 2014)

3. Neuroanatomical findings: implications for an evolutionary framework

3.1. White matter expansion in the anthropoid lineage

Having reconstructed the prefrontal cortex-innervating ventral stream connections in two anthropoids and two strepsirrhines, this thesis identifies a clear demarcation between the two groups. The two anthropoids in these studies both show a broader innervation of the prefrontal cortex by ventral visual connections (i.e., a relatively decreased innervation of the orbitofrontal cortex compared to other prefrontal cortical regions). This is consistent with the work of Murray and colleagues (2017), who have proposed that the ventral stream in primates can be understood as providing visual context rather than merely object categorisation. Murray and

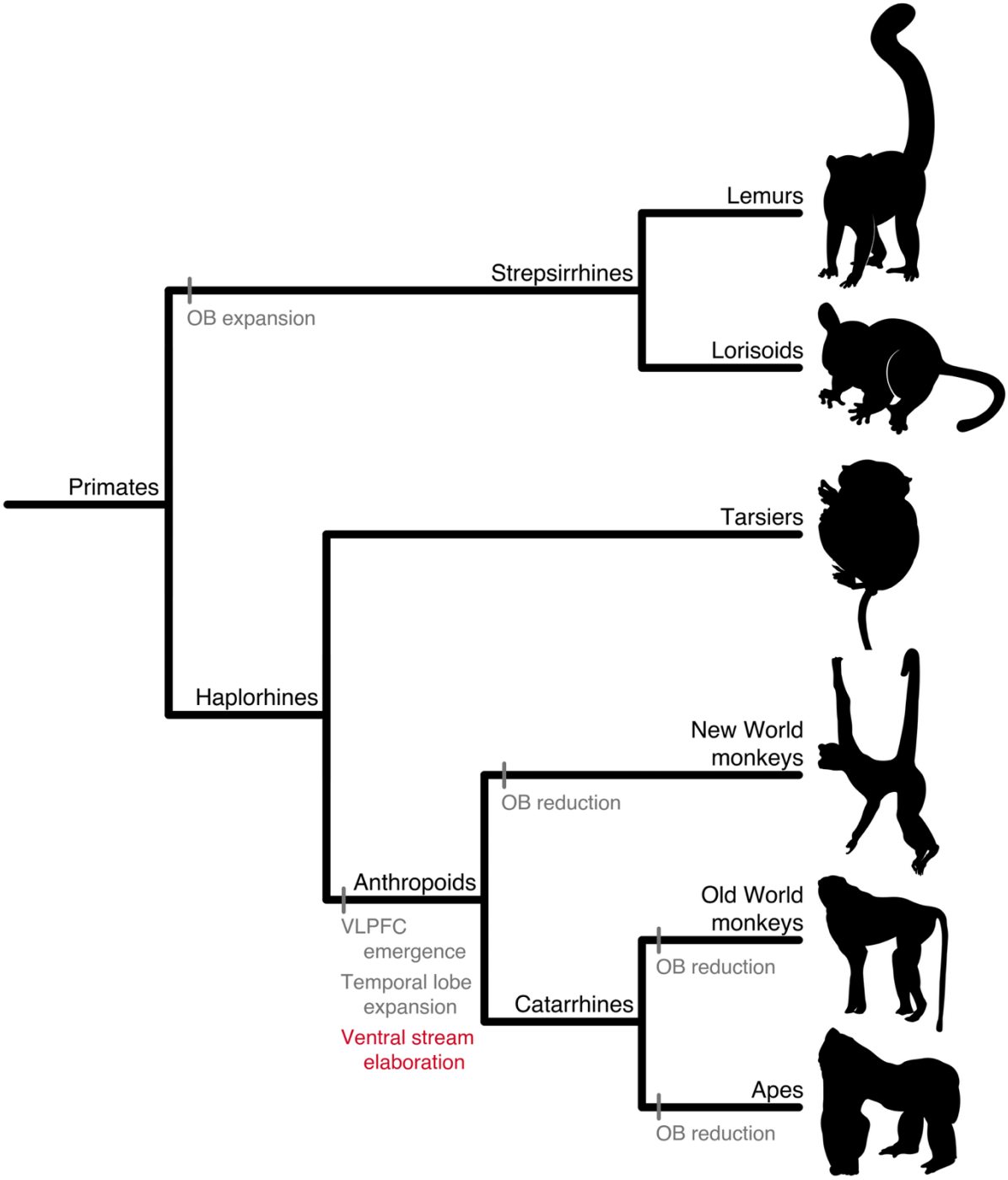


Figure 6.1. Simplified primate cladogram with annotations. *Vertical markings indicate evolutionary changes which occurred at the indicated divisions. Light grey text indicates grey matter changes occurring at the indicated time points. OB expansion in strepsirrhines is based on phylogenetic modelling by Heritage (2014). Parallel OB reductions across the anthropoids are based on fossil endocast data, discussed by Gonzales et al. (2015). Temporal lobe expansion is based on fossil endocast data, discussed by Ni et al. (2019). VLPFC emergence in anthropoids is based on the proposed phylogeny of Eldridge et al. (2021). Red text indicates a likely locus of the white matter changes identified in this thesis. OB: Olfactory bulbs. VLPFC: Ventrolateral prefrontal cortex.*

colleagues have proposed that in anthropoids, the inferior temporal cortex provides information to the ventrolateral prefrontal cortex to guide foraging-relevant decisions (Murray et al., 2017) and the ventrolateral prefrontal cortex is uniquely elaborated in anthropoids (Eldridge et al., 2021). Other authors (Braunsdorf et al., 2021) have also identified an elaboration of the temporal cortex specific to anthropoids, with multiple studies finding temporal cortical specialisations specific to the catarrhine and ape lineages (Braunsdorf et al., 2021; Roumazeilles et al., 2020).

Our work supports these conclusions. While we have not been able to examine ventral prefrontal connectivity in any species of tarsier, due to data availability, we propose that an expansion of the ventral visual stream's connectivity to new prefrontal cortical regions coincided with the expansion of the temporal lobe and the emergence of the ventrolateral prefrontal cortex (VLPFC) in anthropoids after their divergence from tarsiers (Figure 6.1). After all, as Molnár (2021) observes, there is an increasing recognition that complex cognitive functions, such as decision-making, rely on distributed, overlapping networks of interconnected areas. Under this view, the emergence of the VLPFC in anthropoids would be expected to coincide with the expansion of the ventral stream, to incorporate the additional grey matter into networks which support decision-making and other cognitive functions. This interpretation also coheres with the finding that anatomically and functionally connected regions have tended to expand concurrently in both primates and non-primate insectivores (Barton & Harvey, 2000), and the assertions of the mosaic brain hypothesis more generally.

Another possibility which cannot be ruled out by the present work is that the ventral stream underwent independent expansions into prefrontal cortex across

multiple anthropoid lineages. Based primarily on fossil endocast data, a similar proposal has been put forward for olfactory bulb reduction, with multiple parallel reductions across the anthropoid lineage (Eldridge et al., 2021; Gonzales et al., 2015; Figure 6.1). Still a further possibility is that successive elaborations occurred both before and after the divergence of new world monkeys from the catarrhines.

Finally, while our work identifies an expansion of the anterior ventral visual stream in the anthropoids which seems to be absent in the strepsirrhines, we cannot claim that this expansion is unique to the anthropoids. To our knowledge, there have been no studies investigating the possibility of a ventrolateral prefrontal cortex in the other branch of the haplorhines, the tarsiers, and we were unable to investigate white matter connectivity in the tarsiers due to the unavailability of neuroimaging data in tarsiers. As such, the finding we have been describing as an anthropoid/strepsirrhine divergence could suggest a morphology common to all haplorhines.

It is worth noting that while cranial endocasts have been used to estimate grey matter regional expansions and gyrification (Gonzales et al., 2015, among others), similar methodologies do not exist for estimating white matter connectivity from fossil evidence. As such, perhaps the most that can be concluded is that the ventral stream elaboration seems to be a pan-anthropoid phenomenon.

3.2. Implications for the ancestral state

Chapter 2 of this thesis drew inferences about the ancestral state of retinal waves based on the diversity of retinal waves in extant species. Similarly, limited inferences can be drawn about the ancestral primate ventral stream based on the findings in Chapters 4 and 5.

The anterior projections of the ventral stream principally innervate the orbitofrontal cortex in the two strepsirrhine species studied here (see visualisation in Figure 5.3). This is true in both lemurs and galagos, regardless of diel activity pattern (e.g., nocturnality or diurnality). As such, it seems likely that this was the anatomy of the last common ancestor to strepsirrhines, and perhaps of the last common ancestor to all extant primates. After all, it was in a common ancestor to primates and tree shrews that granular orbitofrontal cortex first developed (Eldridge et al., 2021; Wong & Kaas, 2009). The temporal lobe has been argued to be a unique specialisation within the primate order (Bryant & Preuss, 2018), further suggesting that its dense connectivity with the (relatively) nascent granular orbitofrontal cortex may have emerged early on in primate evolution. As such, we posit that the ancestral state for primates was dense connectivity between temporal cortical regions and the orbitofrontal cortex, a state which has been largely retained within the strepsirrhine lineage.

These results can be situated in the broader context of visual specialisation within the primate lineage. The parvocellular layer of the lateral geniculate nucleus is the primary input to the ventral visual stream (Merigan & Maunsell, 1993). Cross-species comparisons within the primate lineage have indicated that parvocellular neuron count scales with both primary visual cortical size and overall neocortical size, whereas magnocellular neurons – the primary inputs to the dorsal visual stream – exhibit no such scaling (Barton, 1998). Of particular note, there are associations between both parvocellular neuron count and parvocellular layer size, and diel activity pattern, frugivory, and social group size, with diurnal, frugivorous, and more

social primates having greater relative parvocellular neuron counts and a relatively larger parvocellular layer (Barton, 1998).

Intriguingly, in contrast to these findings in the lateral geniculate nucleus, our results suggest that diel activity pattern is not associated with differences in the distribution of anterior projections of the ventral visual stream. The cathemeral ring-tailed lemur and the obligate nocturnal galago had the most similar patterns of prefrontal cortical innervation by the ventral visual stream, of the primates studied. This is not entirely unprecedented, however. Other visual adaptations, such as degree of orbital convergence, are not associated with diel activity pattern (Barton, 2004). The complex interplay between visual anatomical specialisations and behavioural ecological factors makes the possibility of extending the present analysis to tarsiers all the more intriguing. Tarsiers are believed to have evolved trichromatic vision despite their nocturnality (Melin et al., 2013), in opposition to the general trend of trichromacy being associated with diurnality among primates. If tarsiers are found to have the anterior ventral stream specialisations identified among the anthropoids in this thesis, it would shed light on the early evolution of the ventral stream. Our view is that ventrolateral prefrontal cortical expansion coincided with an expansion of the prefrontal targets of the ventral visual stream. If the tarsier's ventral visual stream innervates a more extensive area of the prefrontal cortex, like the anthropoids, this would suggest a likely expansion of the ventrolateral prefrontal cortex in tarsiers as well.

4. Conclusions

In sum, this thesis has investigated aspects of the organisation and development of the visual system, using both ethological and phylogenetic information to guide its enquiries. As well as yielding new information about the organisation and evolution of the visual systems of vertebrates – particularly primates – this work has established the suitability of a novel, data-driven technique for reconstructing white matter tracts in less-studied brains. This project has yielded insights into the development of the visual system and the connectivity of the ventral visual stream, including the first identification of anthropoid/strepsirrhine differences in prefrontal innervation by the ventral visual stream. Furthermore, the methodological side of this work has provided a first characterisation of the magnitude of within-species versus cross-species differences in white matter connectivity. It is my hope that the methods and methodological findings presented here should prove fruitful for future cross-species comparisons of brain development and organisation.

References

Barton, R. A. (1998). Visual specialization and brain evolution in primates. *Proceedings of the Royal Society of London. Series B: Biological Sciences*, *265*(1409), 1933–1937. https://doi.org/10.1098/rspb.1998.0523

Barton, R. A. (2004). Binocularity and brain evolution in primates. *Proceedings of the National Academy of Sciences*, *101*(27), 10113–10115. https://doi.org/10.1073/pnas.0401955101

Barton, R. A., & Harvey, P. H. (2000). Mosaic evolution of brain structure in mammals. *Nature*, *405*(6790), 1055–1058. https://doi.org/10.1038/35016580

Braunsdorf, M., Blazquez Freches, G., Roumazeilles, L., Eichert, N., Schurz, M., Uithol, S., Bryant, K. L., & Mars, R. B. (2021). Does the temporal cortex make us human? A review of structural and functional diversity of the primate temporal lobe. *Neuroscience & Biobehavioral Reviews*, *131*, 400–410. https://doi.org/10.1016/j.neubiorev.2021.08.032

Bryant, K. L., & Preuss, T. M. (2018). A Comparative Perspective on the Human Temporal Lobe. In E. Bruner, N. Ogihara, & H. C. Tanabe (Eds), *Digital Endocasts: From Skulls to Brains* (pp. 239–258). Springer Japan. https://doi.org/10.1007/978-4-431-56582-6_16

Burnham, K. P., & Anderson, D. R. (2002). *Model Selection and Multimodel Inference: A Practical Information-Theoretic Approach*. Springer Science & Business Media. https://link.springer.com/book/10.1007/b97636

Cohen, J. (1988). *Statistical Power Analysis for the Behavioral Sciences* (1st edn). Routledge.

Eldridge, M. A., Hines, B. E., & Murray, E. A. (2021). The visual prefrontal cortex of anthropoids: Interaction with temporal cortex in decision making and its role in the making of 'visual animals'. *Current Opinion in Behavioral Sciences*, *41*, 22–29. https://doi.org/10.1016/j.cobeha.2021.02.012

Gonzales, L. A., Benefit, B. R., McCrossin, M. L., & Spoor, F. (2015). Cerebral complexity preceded enlarged brain size and reduced olfactory bulbs in Old World monkeys. *Nature Communications*, *6*(1), 7580. https://doi.org/10.1038/ncomms8580

Heritage, S. (2014). Modeling Olfactory Bulb Evolution through Primate Phylogeny. *PLOS ONE*, *9*(11), e113904. https://doi.org/10.1371/journal.pone.0113904

Mars, R. B., Neubert, F.-X., Verhagen, L., Sallet, J., Miller, K. L., Dunbar, R. I. M., & Barton, R. A. (2014). Primate comparative neuroscience using magnetic resonance imaging: Promises and challenges. *Frontiers in Neuroscience*, *8*. https://doi.org/10.3389/fnins.2014.00298

Melin, A. D., Matsushita, Y., Moritz, G. L., Dominy, N. J., & Kawamura, S. (2013). Inferred L/M cone opsin polymorphism of ancestral tarsiers sheds dim light on the origin of anthropoid primates. *Proceedings of the Royal Society B: Biological Sciences*, *280*(1759), 20130189. https://doi.org/10.1098/rspb.2013.0189

Merigan, W. H., & Maunsell, J. H. R. (1993). How Parallel are the Primate Visual Pathways? *Annual Review of Neuroscience*, *16*(Volume 16, 1993), 369–402. https://doi.org/10.1146/annurev.ne.16.030193.002101

Molnár, Z. (2021). Zoltán Molnár: The developing brain. In T. L. Horváth, J. Hirsch, & Z. Molnár (Eds), *Body, Brain, Behavior: Three Views and a Conversation* (1st

edn, pp. 1–66). Academic Press. https://doi.org/10.1016/B978-0-12-818093-8.00005-7

Murray, E. A., Wise, S. P., & Graham, K. S. (2017). *The Evolution of Memory Systems: Ancestors, Anatomy, and Adaptations*. Oxford University Press.

Ni, X., Flynn, J. J., Wyss, A. R., & Zhang, C. (2019). Cranial endocast of a stem platyrrhine primate and ancestral brain conditions in anthropoids. *Science Advances*, *5*(8), eaav7913. https://doi.org/10.1126/sciadv.aav7913

Ramsey, W. (2024). Eliminative Materialism. In *The Stanford Encyclopedia of Philosophy* (Winter 2024). Metaphysics Research Lab, Stanford University. https://plato.stanford.edu/archives/win2024/entries/materialism-eliminative/

Roumazeilles, L., Eichert, N., Bryant, K. L., Folloni, D., Sallet, J., Vijayakumar, S., Foxley, S., Tendler, B. C., Jbabdi, S., Reveley, C., Verhagen, L., Dershowitz, L. B., Guthrie, M., Flach, E., Miller, K. L., & Mars, R. B. (2020). Longitudinal connections and the organization of the temporal cortex in macaques, great apes, and humans. *PLOS Biology*, *18*(7), e3000810. https://doi.org/10.1371/journal.pbio.3000810

Thompson, E., Mohammadi-Nejad, A. R., Robinson, E. C., Andersson, J. L. R., Jbabdi, S., Glasser, M. F., Bastiani, M., & Sotiropoulos, S. N. (2020). Non-negative data-driven mapping of structural connections with application to the neonatal brain. *NeuroImage*, *222*, 117273. https://doi.org/10.1016/j.neuroimage.2020.117273

Wong, P., & Kaas, J. H. (2009). Architectonic Subdivisions of Neocortex in the Tree Shrew (Tupaia belangeri). *The Anatomical Record*, *292*(7), 994–1027. https://doi.org/10.1002/ar.20916